# Optimisation of Well Trajectory and Hydraulic Fracture Design in a Poor Formation Quality Gas-Condensate Reservoir

**André Carlo Torres de Carvalho Tipping**

Thesis to obtain the Master of Science Degree in

## Petroleum Engineering

Thesis Supervisors:

Mr. David Edward Tipping

Prof. Maria João Correia Colunas Pereira

## Examination Committee

Chairperson: Prof. Amílcar de Oliveira Soares

Supervisor: Mr. David Edward Tipping

Members of the Committee: Prof. Leonardo Azevedo Guerra Raposo Pereira

February 2017

# Dedication

To my family

## Abstract

The main aim of this project is to determine the optimal well trajectory and hydraulic fracture design that give the maximum sustainable production rates and recovery from a low-quality gas-condensate reservoir in North Africa. Specifically, this will mean quantifying recovery and production potential of the reservoir with different well types: vertical or high angle (horizontal). The backbone of the methodology consisted of constructing high resolution 3-dimensional numerical models followed by evaluation of recovery with a commercial reservoir simulator

This document first describes the nature of the reservoir, the characterisation of the formation, and analysis of the reservoir fluid in question. Next it outlines the inputs into building the model.

The reservoir fluid analysis and the model grid geometry, properties, permeability and porosity values were provided by PetroCeltic International plc, the operator of the field.

Potential well and hydraulic fracture scenarios were simulated with their respective recovery factors compared. A financial model was then constructed to evaluate the commercial value of each option and, hence allow recommending options for implementation. The financial selection criterion is Net Present Value (NPV). This study concludes that the optimal well design, for when there is no high permeability zone and an optimal kv/kh ratio of 1, is a hydraulically fractured 2km horizontal well: NPV = 142,247,066 USD, recovery = 2,071,570,000 $sm^3$.

**Keywords:** Gas-condensate, poor-quality formation, hydraulic fracture design, well trajectory

## Acknowledgements

First and foremost, I would like to thank Petroceltic International plc for providing me with the opportunity to pursue this project.

I would especially like to thank my supervisor, David Tipping, for the guidance, support, and patience shown during the length of the project, and Prof. Maria João Pereira for her constructive feedback.

My thanks also go out to Prof. Leonardo Azevedo for helping to set me up in CERENA when I needed it.

Not forgetting my colleagues and friends from the 2014/15 cohort, who ensured that my time abroad was not just spent working hard. Special mention to Gonçalo Simões, who's generosity is greatly appreciated.

Finally, I would like to acknowledge and thank my family for the love and support given, in every sense, without which I would never have made it to this point.

## Abbreviations

| | | |
|---|---|---|
| BHP | - | Bottomhole Pressure |
| bbl | - | Barrel |
| CAPEX | - | Capital expenditure |
| CGR | - | Condensate Gas Ratio |
| FGPR | - | Field Gas Production Rate |
| FGPT | - | Field Gas Production Total |
| HF | - | Hydraulic Fracture |
| J | - | Joule |
| k | - | permeability |
| $k_v/k_h$ | - | Vertical permeability / horizontal permeability |
| MMBTU | - | One Million British Thermal Units |
| MW | - | Molecular Weight |
| OilSat | - | Condensate Saturation |
| OPEX | - | Operational expenditure |
| PermX | - | Permeability X direction |
| PermY | - | Permeability Y direction |
| PermZ | - | Permeability Z direction |
| PVT | - | Pressure Vapour and Temperature |
| RF | - | Recovery Factor |
| RGPR | - | Region Gas Production Rate |
| RGPT | - | Region Gas Production Total |
| API | - | American Petroleum Institute |
| IFT | - | Interfacial tension |
| $sm^3$ | - | standard cubic meters |
| SPE | - | Society of Petroleum Engineers |
| WOGR | - | Well Condensate - Gas Ratio |

## List of Figures

## List of Tables

# 1. Introduction

## 1.1. Motivation

This thesis is a summary of a project undertaken during my internship with PetroCeltic International plc, a company developing a poor formation quality gas-condensate reservoir in North Africa. The reservoir is at the appraisal stage. At the present time the company is considering a development plan consisting of 2km vertical wells with a 2km spacing designed to penetrate the upper 50m of the reservoir column. However, further analysis is needed to determine if this is the optimal plan. This provided an opportunity to build a multi-phase flow simulation model, optimised through calibration of model to measurements, and then simulate development options to suit the unique characteristics of this reservoir.

## 1.2. Objectives

The overall objective of this project is to determine the optimal well trajectory and hydraulic fracture design for a low-quality gas-condensate reservoir that give sustainable high production rates that, in turn, give maximum commercial value. This will entail predicting and comparing recovery factors, well types, trajectories, and well spacing with a simulation model.

Specifically, this will mean quantifying recovery and production potential of the reservoir with different well types: vertical or high angle (horizontal). Due to the generally very poor formation matrix quality, except for a high permeability layer (0 - 8 m) in the appraisal area, plus the inclusion of natural fractures, hydraulic fracturing will be essential to attain commercial production rates – whose impact will in turn be analysed.

The appraisal well tests show that well productivity is low and therefore hydraulic fracturing is needed.

Primary questions to answer: What is the best well trajectory and HF design to give sustainable production rates and high recovery factors?

The main uncertainties in the reservoir are the

- Thickness of a high permeability layer at the top of the reservoir. The appraisal wells show that this layer varies from 0 to 8 m
- Vertical Transmissibility determined by the ratio of the vertical to the horizontal permeability.

The $k_v/k_h$ is not known until it is tested with recordings of pressure build-up. Which leads to a secondary question: Should pressures be recorded to establish $k_v/k_h$?

## 1.3. Structure of the thesis

This project is divided into six parts:

1. Definition of the key questions to evaluate. Introduction, where the key questions are identified, and the theoretical concepts necessary to approach them are presented

2. Reservoir description alongside the characterisation of the formation, and analysis of the reservoir fluid
3. Characteristics of the predictive dynamic model.
4. Dynamic simulation of well and reservoir scenarios
5. Financial analysis to determine best options
6. Comparison and analysis of results

# 2. Literature Review

## 2.1. Gas-Condensate Reservoir Behaviour

A gas condensate fluid at initial reservoir conditions exists as gas. As the reservoir temperature is higher than the critical temperature of the fluid, at the initial state in-situ, the reservoir fluid is in the state of a single phase – gas, rather than oil. During the production phase, reservoir pressure will decline. When the pressure reaches saturation pressure, a liquid phase, consisting of heavier hydrocarbon components will condense in the formation and as can be interpreted from Figure 1, once the pressure drops below the dew-point, a liquid phase will drop out (condense) containing highly valued, heavier hydrocarbon components containing principally heptane and higher components.

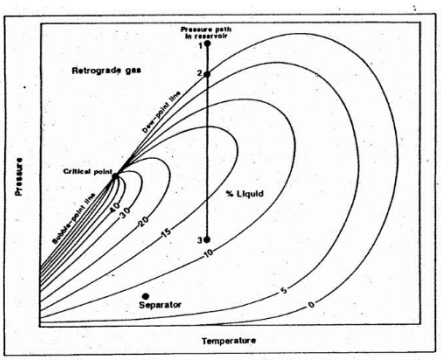


*Figure 1 Gas Condensate reservoir phase envelopes*

Without pressure maintenance, this will occur in the reservoir and valuable condensate will be lost as it becomes immobile below critical condensate saturation irrespective of fluid flow. Condensate accumulates not only in the formation but also forms in the wellbore and the surface as the produced gas reaches the well head. This occurs because of the decrease in pressure and temperature. Regardless of whether the reservoir pressure drops below the dewpoint, production will result in condensate at surface conditions, both temperature and pressure, as both are below that point as indicated by the location of the separator on the graph.

In the formation, the immobile condensate builds up resulting in heterogeneities within the wellbore region and further in the reservoir as the radius of condensate ring expands which can lead to well productivity and loss of valuable condensed liquid as the condensate content in the formation increases. The graph below is an example from the Arun reservoir in Indonesia (*Henderson et al. 1998*) which illustrates this phenomenon - a substantial reduction in well productivity occurs as the average reservoir pressure in the wellbore region declines below the dewpoint.

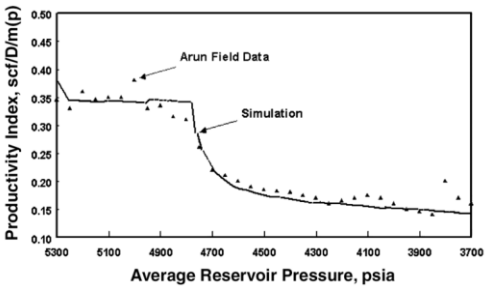


*Figure 2 Reduction in well productivity caused by condensate buildup, Arun field, Indonesia. (http://petrowiki.org/Formation_damage_from_condensate_banking)*

The most direct method of reducing condensate build-up is to reduce the drawdown so that the bottomhole pressure remains above the dewpoint. In cases when this is not desirable, the impact of condensate formation can be reduced by increasing the inflow area and achieving linear flow rather than radial flow into the wellbore. This minimizes the impact of the reduced gas permeability in the near-wellbore region. Both benefits can be achieved by hydraulic fracturing.

## 2.2. Hydraulic fracture

Hydraulic fracture (HF) stimulation is a common method used to remedy condensate build-up problems. The creation of a fracture results in a significant decrease in the drawdown needed to produce the well. In addition, build-up of a liquid hydrocarbon phase on the faces of the fracture does not affect well productivity as significantly as in radial flow around the wellbore. Hydraulic fractures are modelled in the reservoir simulation as discrete blocks of high permeability. However, these blocks are often significantly wider than the actual width of the fracture itself by one or two orders of magnitude. A hydraulic fracture has a fracture conductivity, $C_f$, which is the product of the average propped width and the proppant permeability:-

$$C_f = w\, k_f \qquad (1)$$

where w = average propped width

$k_f$ = proppant (fracture) permeability

The fracture conductivity is a measure of the ease with which fluid flows through the fracture. From Darcy's Law, flow rate is proportional to the permeability and width. Therefore, by altering the fracture permeability within the model, the fracture conductivity can be changed.

## 2.3. Capillary Pressure

In a poor-quality formation, capillary effects can be significant. They can lead to a thick transition zone of movable water and gas, and a variable gas-water contact. To assess their impact, capillary pressure measurements are made on representative core samples in the laboratory. They give the expected change in vertical gas saturation for the given core sample. With the capillary pressure and FWL known, the water saturation at any point in the reservoir can be calculated.

Capillary pressure is the difference in pressure across the interface between two phases. Specifically, it is defined as the pressure differential between two immiscible fluid phases occupying the same pores caused by interfacial tension

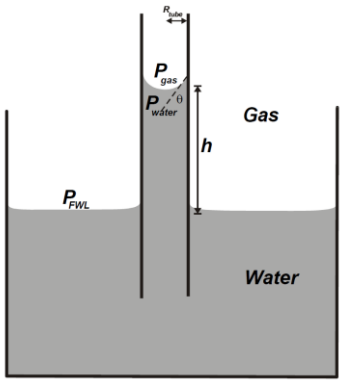


*Figure 3 Capillary pressure in gas/water system (Glover, 2000)*

The free water level is the height of the interface when the radius of the capillary tube tends to infinity (i.e., the capillary pressure is zero and h=0). The interface at the free water level may exist at any given absolute pressure $P_{FWL}$. Capillary forces exist inside the restricted capillary tubing that result in the rise of the water to a height h above the free water level. The pressure in the gas phase above the meniscus in the capillary tube is

$$P_{gas} = P_{FWL} - \rho_{gas}\, g\, h \qquad (2)$$

The pressure in the water phase below the meniscus in the capillary tube is

$$P_{water} = P_{FWL} - \rho_{water}\, g\, h \qquad (3)$$

Hence the capillary pressure is

$$P_{cap} = P_{gas} - P_{water} = (\rho_{water} - \rho_{gas})\, g\, h \qquad (4)$$

The capillary pressure depends most critically upon the interfacial tension and the wetting angle. These parameters change with pressure and temperature for any given system.

Real rocks contain an array of pores of different sizes connected by pore throats of differing size. Each pore or pore throat size can be considered heuristically to be a portion of a capillary tube.

A capillary tube or a rock that contains 100% saturation of a gas (non-wetting fluid) then has water (wetting fluid) introduced at one end, the capillary pressure will draw the water into the tube or the pores of the rock, this is known as spontaneous imbibition. If the tube is horizontal this process can continue if there is more tube or rock for the wetting fluid to fill. If the pathway is vertical, the process will continue until the capillary force pulling the fluid into the tube or rock pores is balanced by the gravitational force acting on the suspended column of fluid.

By completely saturating a sample of rock in the laboratory with a wetting fluid, the size, number and volume of pores together with their respective displacement pressures can be recorded to then plot a capillary pressure curve.

The Gas Water Contact (GWC) is the pressure level required for gas to displace water, and is above the Free Water Level (FWL) by a height related to the size of the displacement pressure and controlled by the largest pore openings in the rock. If the rock was composed of 100% of pores of equal size, this would be the level above which there would be 100% gas saturation and below which there would be 100% water saturation. However, the rock also contains smaller pores, with higher displacement pressures. Thus, there will be a partial water saturation above the 100% water level occupying the smaller pores, and this water saturation will reduce and become confined to smaller and smaller sized pores as one progresses to higher levels above the 100% water level. Water will only be displaced from

a given pore size if there is a sufficiently large force to overcome the capillary force for that size of pore. The force driving the gas into the reservoir rock is insufficient to overcome the capillary forces associated with the smallest pores. Hence, the smallest pores in a gas zone remain saturated with water, resulting in an irreducible water saturation ($S_{wi}$) in the reservoir.

## 2.4. Post-fracture Well Behaviour

Figure 4 is a procedure to determine the fracture length and fracture conductivity required to achieve a certain fold of increase in a well's productivity index (ratio of production rate to pressure drop).

The graph shows that for low-permeability reservoirs, fracture length is more important than fracture conductivity.

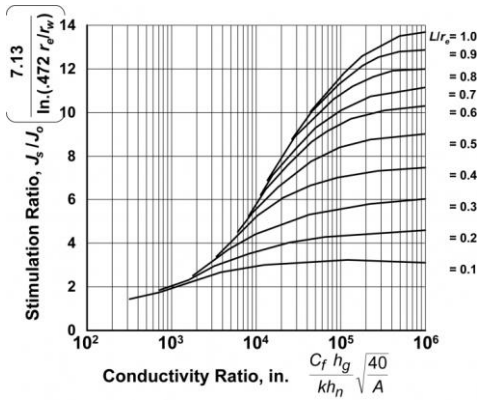


*Figure 4 McGuire and Sikora graph showing the increase in productivity from fracturing*

In his paper, Prats shows that, hypothetically, the case of a vertical well with several distinct vertical fractures, would only improve the productivity index of the same well with a single fracture by a small amount; suggesting that one long vertical fracture may be preferable to several shorter ones, and provided it is sufficiently conductive, it will act to extend the wellbore. Therefore, putting emphasis on the half-length of a hydraulic fracture to have an impact on a well's productivity.

Hydraulic fracturing is expected to increase the productivity index of a well; and, under certain circumstances, also increase the ultimate recovery. Without fracture treatment, most low-permeability wells will flow at low rates and recover only modest volumes of oil and gas before reaching their economic limit. A low-permeability well will not be economic unless a successful fracture treatment is both designed and pumped into the formation. A successful stimulation treatment will increase the flow rate, the ultimate recovery, and extend the producing life.

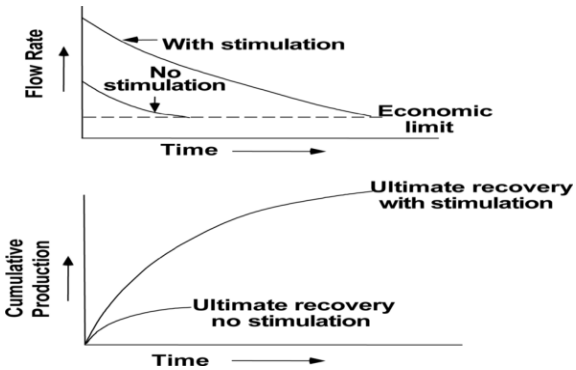


*Figure 5 Expected Production behaviour in a low-permeability formation (http://petrowiki.org/Post-fracture_well_behavior)*

## 2.5. Net Present Value (NPV)

"Net present value is the present value of the cash flows at the required rate of return of your project compared to your initial investment," *Berman et al.* (2013) cited by Gallo (2014). In other words, it is a method of calculating one's return on investment for a project, thereby determining its value. A project

adds value, if its NPV is positive. The greater the NPV, the greater the value. Hence NPV allows comparing different projects.

The NPV is calculated by summing the present value of cash flows for each year associated with the investment, discounted so that it is expressed in today's money, equation (5).

$$\text{Net Present Value} = \sum \frac{\text{Year n Total Cash Flow}}{(1 + \text{Discount Rate})^n} \tag{5}$$

Where *n* is the year whose cash flow is being discounted.

## 3. Methodology

This project involved creation of a high-resolution dynamic model to simulate recovery under different reservoir conditions. The dynamic model was built using reservoir conditions of a gas-condensate field located in North Africa under development by PetroCeltic International plc.

A numerical model was used due to the limitations of the conventional volumetric balance method:

- Homogeneous reservoir - fluid properties and formation characteristics are represented by single values, meaning that spatial variations in properties are not considered.
- Gradient effects on the fluid are not accounted for. This can be significant as the reservoir pressure falls below saturation pressure. The liquid in reality would tend to flow downwards. Hence, condensate would tend to accumulate near the base of the accumulation. Volumetric balance modelling does not consider this.
- The impacts of variations in reservoir properties on well productivity cannot be assessed. Hence, volumetric modelling does not allow comparing different design options.

A numerical model can accurately represent multiphase flow, capillary and gravity forces, spatial variations of rock properties, fluid properties, and relative permeability characteristics, though it is computationally more intensive and slower.

The high-resolution dynamic model was constructed from a geological static model provided by PetroCeltic. The following elements provided the data to simulate in-situ flow behaviour:

- Measurements on core samples. In particular, air-brine capillary pressure and relative permeability data.
- Compositional analysis measured from gas chromatography, and fluid expansion tests (Constant Composition Expansion) of the reservoir fluid samples.
- Test results of the appraisal wells – wireline logs when the well is opened through a separator on an adjustable choke, providing data on flow rates, CGR, WHP, BHP, and temperatures.

A commercial 3-D flow simulator (ECLIPSE100 ®) enabled modelling recovery under different potential reservoir description scenarios and well designs. The model was calibrated to the appraisal well test

data. Initially, this project assessed the recovery potential of PetroCeltic's proposed plan. This case was considered a starting point. The objective was to determine the commercial feasibility of the proposed plan – drill shallow (50m) hydraulically fractured vertical wells.

Then alternative design options were considered by analysing the impact had on production, while also considering the recovery's sensitivity to the possible range of reservoir factors expected to have an impact on recovery. These factors were identified due to their uncertainties, and whose impacts on recovery may point to the need for more tests.

- The impact a high permeability zone has on productivity
- The sensitivity of recovery to vertical transmissibility
- The impact fracture conductivity, height and length have on productivity
- The effect drilling deeper has
- The case for horizontal wells (inclined or not) of 0.5-2km in length
- Determination of the optimal well spacing between two identical hydraulically fractured shallow vertical wells.

As the hydraulic fractures have their own permeability, porosity, and capillary pressures values, they were modelled by creating unique cells for the fractures. In reality, fractures have dimensions of millimetres, however this was not possible to model, therefore the relationship from equation 1 was used – the width of the cell of the fracture was fixed, and from the data, the average fracture conductivity was used to calculate the permeability. This resulted in convergence problems due to having cells of greatly different permeabilities next to each other, however, through calibration these were limited.

A financial model (1)a)i)(1)(a)(i)Appendix B ) was also created to calculate the NPV of the results of each simulation model run, to determine the optimal well design.

When referring to hydraulic fractures (HF), I have used the following shorthand to easily describe the design of said HF: Height/Length/Width. For example, a hydraulic fracture 20m high, 70m long, and 0.5m width would be described in shorthand as 20/70/0.5.

# 4. Reservoir Description

## 4.1. Structure

The reservoir was formed during the Ordovician period by the deposition of sands transported by a glacier cutting through a valley, Figure 6. The gas-condensate field is a large, low-relief, four-way dip closure, approximately 80 x 50 km in area, with a hydrocarbon column in excess of 100 m. The reservoir

sequence comprises the Upper Ordovician (Ashgill) glacial to glaciomarine Unit IV sandstones, Appendix A (*English et al. 2016*). The flow of sediments is turbulent; hence formation properties can vary widely.

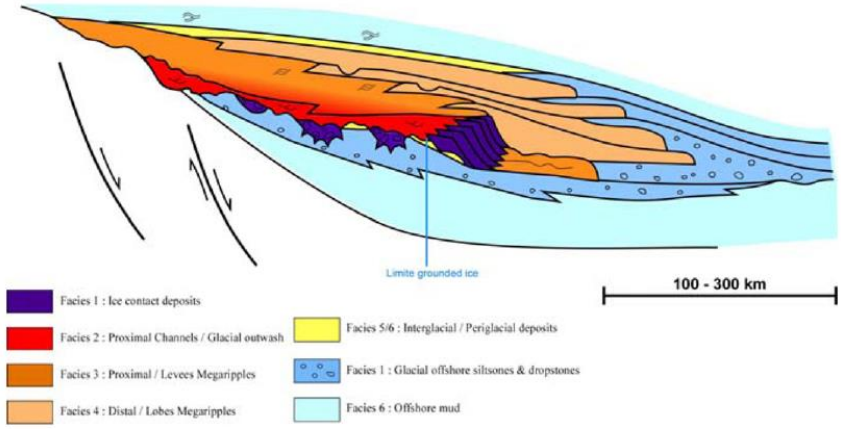


*Figure 6 Facies partitioning in glacial sequences*

Core samples taken from the appraisal wells show the presence of a high permeability layer of 2 to 8 m in the north-eastern sector of the reservoir. This high permeability is key to a successful development since the lower permeability zones, although predicted to contain sizable quantities of gas, will require enhanced recovery techniques, such as multiple hydraulic fractures in long horizontal wells.

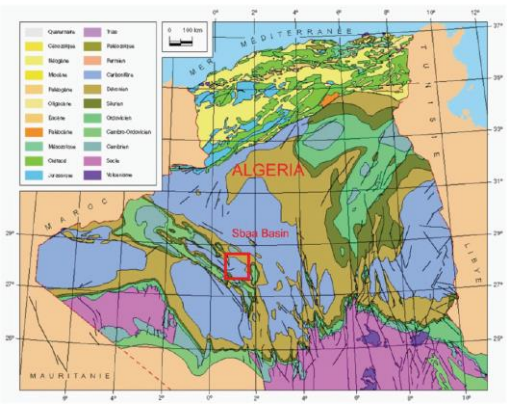


*Figure 7 Geological map of Algeria (Panien, 2010)*

It is believed the high permeability was formed by chemical dissolution (diagenesis) of the cemented sandstones. (*English et al. 2016*).

This project focuses on evaluating the reservoir properties and well designs that influence recovery.

### 4.1.1. Sedimentology

The deposition of sediments was turbulent resulting in grains of various sizes and hence variable formation quality. Mineralisation led to the formation of quartz and barite cement which has severrely restricted permeability.

It is believed the high permeability layer was formed by chemical dissolution of the cemented sandstones freeing up pore space of varying sizes. (*English et al. 2016*). The variation in pore size across the reservoir, can be compared to a collection of capillary tubes with different radii (Dake, 1991), meaning that different sections will have different capillary characteristics.

### 4.1.2. Petrophysics

From facies and wireline electrofacies identification for each well, five glacial units have been defined, correlated, and mapped, showing a complex infill of valley-like network:

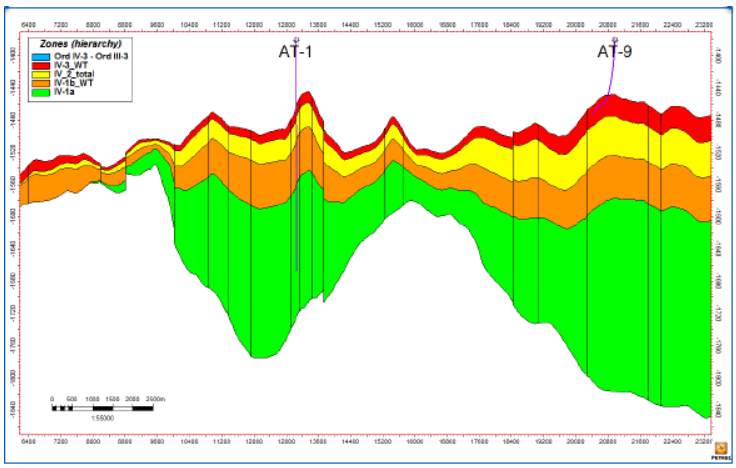


*Figure 8 Stacking pattern and geometry of glacial zones*

The lithofacies define the petrofacies for the petrophysical properties. The porosity-permeability trends for each facies are obtained from core, supplied by PetroCeltic.

The porosity values were calculated from density log interpretation calibrated to core porosity data.

Though at the wells, the reservoir permeability was calculated from porosity-permeability relationships applicable for each petrofacies from core data. These properties were then mapped in a geological program using Sequential Gaussian Simulation (SGS). The reference permeability data are core plug air permeability measurements made at a 131bar overburden or data corrected to 131bar overburden.

Table 1 gives the poro-perm relationships:

*Table 1 – Porosity - permeability facies link*

| Lithology facies | Relations perm -porosity (k-Φ) |
|---|---|
| IV-3 high-k | $k = -3.2845 + 85.4673\Phi - 276.707\Phi^2$ |
| IV-3 | $\log(k) = 42.9822\Phi - 3.68109$ |
| IV-2b | $\log(k) = 15.8518\Phi - 4.37461$ |
| IV-2a | $\log(k) = 28.6008\Phi - 4.13167$ |
| IV-2a (low quality) | $\log(k) = 15.8518\Phi - 4.37461$ |
| IV-1b high-k | $k = -3.2845 + 85.4673\Phi - 276.707\Phi^2$ |
| IV-1b | $\log(k) = 39.9358\Phi - 4.43498$ |
| IV-1a | $\log(k) = 39.9358\Phi - 4.43498$ |

The appraisal well programme reveals very poor reservoir quality in general observed by core data, Figure 9, show that the bulk of the formation has a permeability inferior to 0.1 mD.

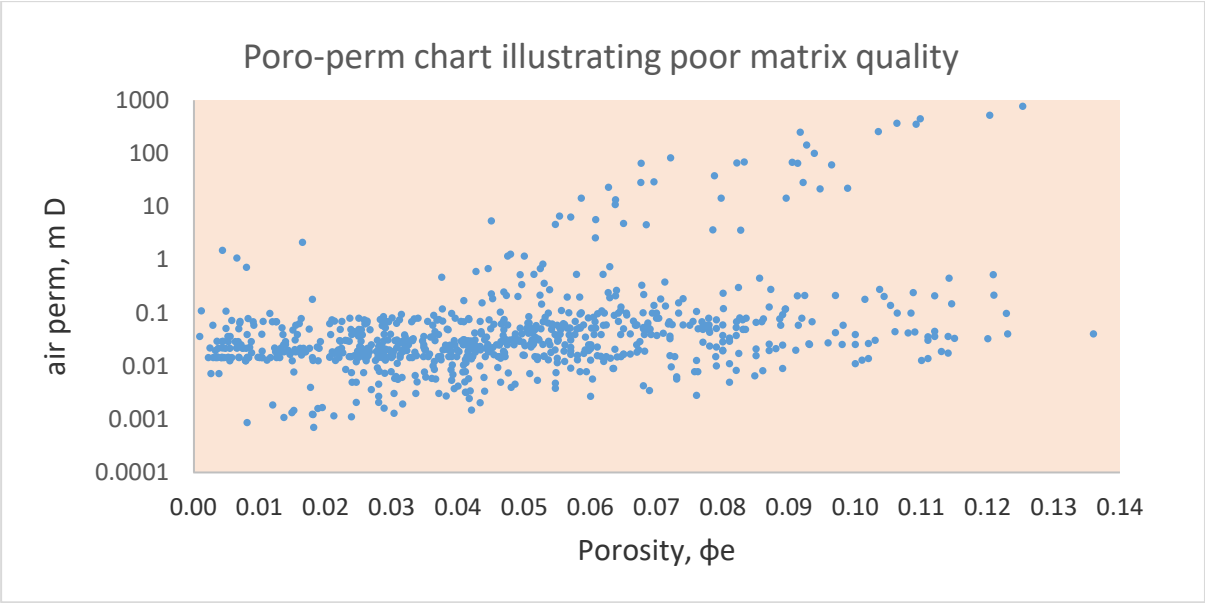


*Figure 9 Relationship of permeability to porosity*

A distribution of the high-k in one of the IV-3 layers is displayed in red, Figure 10. High k – facies were confirmed in IV-1b also.

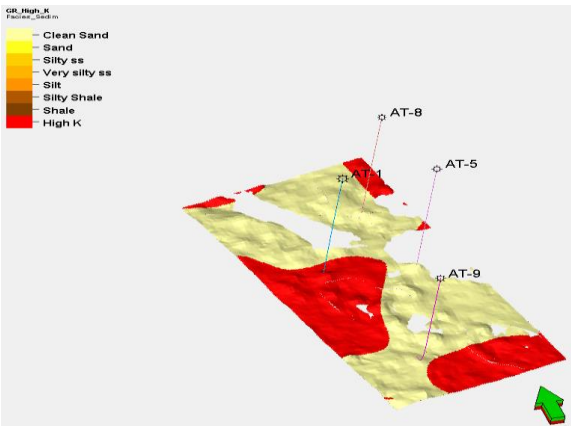


*Figure 10 IV-3 high permeability layer*

### 4.2. Formation Characterisation for reservoir model

Capillary pressures recorded on core samples show irreducible gas saturations and the transition zone thickness are very sensitive to permeability. For example, in the best quality sandstone parts, gas saturations can be expected to exceed 94%. In poor quality regions, the gas saturation can be less than 50%. To determine the gas saturation and, hence the gas volumes through the reservoir, the saturation must be determined from the available data, namely wireline logs and core measurements.

Furthermore, in the dynamic model the fluid distribution is not the same everywhere. It is necessary to classify the formation into categories where each category has a representative saturation model.

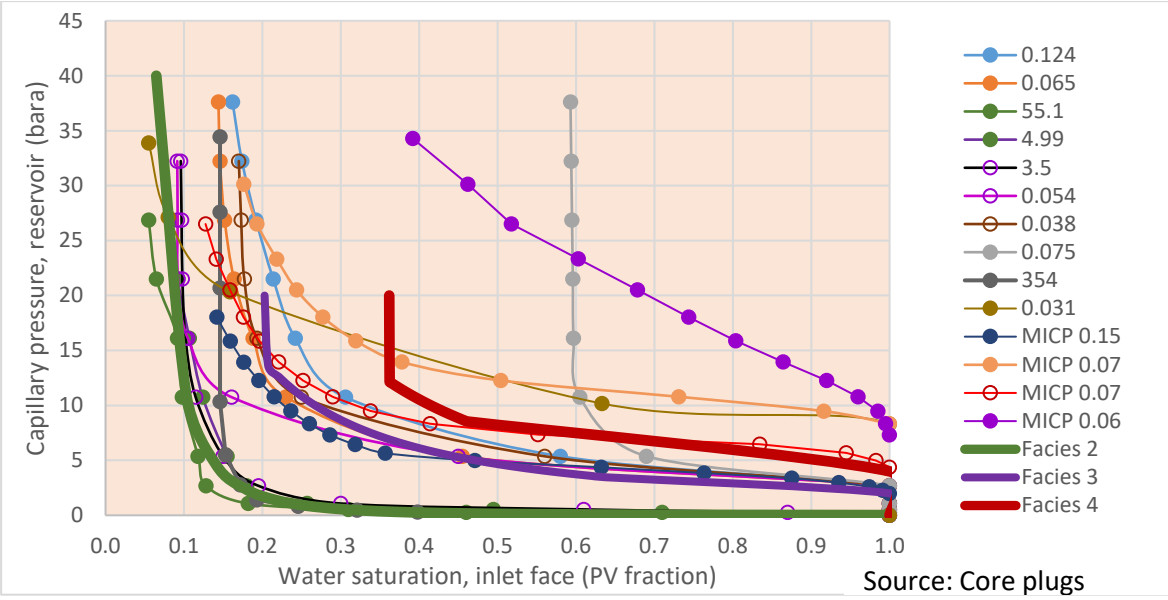


*Figure 11 Capillary Pressure Curves – each curve is the capillary pressure curve of a different core*

The fluid property tables, and the saturation tables for the in-situ flow modelling were provided. These tables were derived from an Equation of State calibrated to the well fluid data, and were obtained from a recombination of separator oil and gas samples at a reservoir ratio.

The distribution of fluid phases and relative permeabilities for the simulation were determined from special core analysis (SCAL): capillary pressures and relative permeabilities. These analyses showed a wide variation of values. It meant characterising the formation in petrofacies so that each petrofacies could be described by a capillary pressure function (gas saturation distribution) and relative permeability curves. Analysis of the data shows that permeability gives a reasonable classification. The saturation tables give:

- The in-situ gas saturation at initial conditions
- The relative permeability tables of the gas, condensate and water.

The Petrofacies were based on Flow Zone Indicator (FZI). The relative permeability tables were provided. The tables were calculated using FZI which were based on permeability range as shown in Figure 12. The saturation table regions (SATNUM) are defined based on Petrofacies as shown in Table 2. The relative permeability for gas and water were used in the dynamic simulation.

*Table 2 Saturation regions in simulation model*

| **Category (criterion permeability)** | | **K range, mD** | |
|---|---|---|---|
| **Petrofacies** | **Description** | **min** | **max** |
| 1 | Fractures | 200 | 2000 |
| 2 | Best quality | 1 | 200 |
| 3 | Mid quality | 0.015 | 1 |
| 4 | Poor quality | 0.00001 | 0.015 |

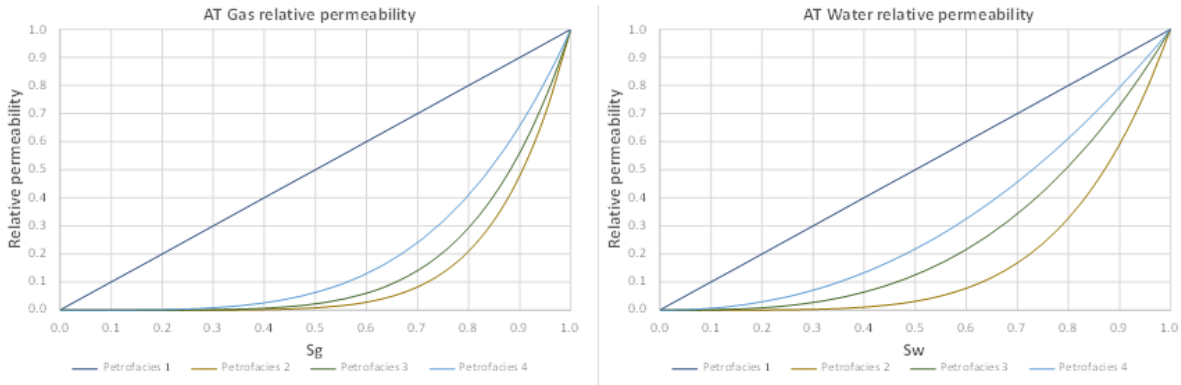


*Figure 12 Gas and water relative permeability curves of the petrofacies*

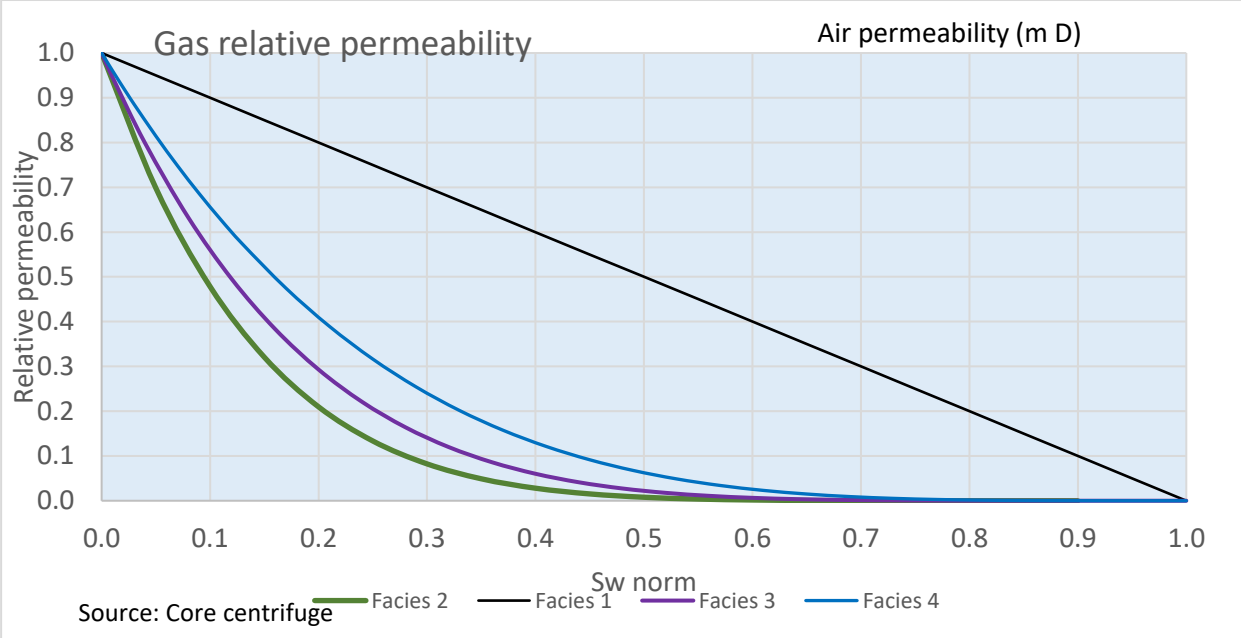


*Figure 13 Gas relative permeability against water saturation curve*

Capillary pressure measurements were made in the lab and then converted to reservoir conditions using Table 3 (Firoozabadi & Ramey, 1988)

*Table 3 Capillary pressure conversion value from lab to reservoir conditions*

| System | IFT | Angle contact | T | Tc | Density water | Density gas |
|---|---|---|---|---|---|---|
| | m N/m | deg | °C | K | g/cm$^3$ | g/cm$^3$ |
| mercury-air | 480 | 140 | | | | |
| Air-brine, lab | 72.0 | 0 | 25 | 132.7 | 1.11 | 0.0012 |
| Gas-water, reservoir | 56.1 | 0 | 96 | 226 | 1.11 | 0.176 |

## 4.3. Reservoir Fluid

The reservoir fluid is gas-condensate, meaning that at initial conditions the fluid is gas. Figure 15 shows that once the pressure drops to the dewpoint 191.9 bar (2783 psia), Table 4, condensate starts to form.

| | Pressure (bar) | Temperature (° |
|---|---|---|
| Standard | 1.01 | 15.56 |
| Initial conditions | 202.5 | 96 |

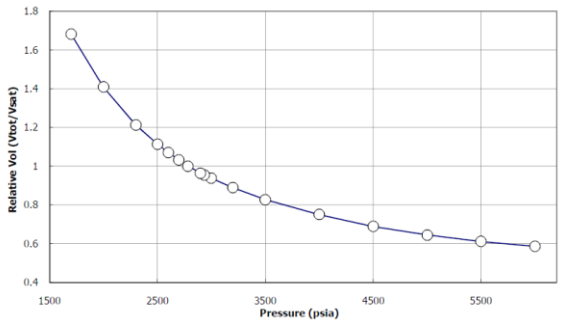


*Figure 14 Relative volume versus pressure of recombined samples*

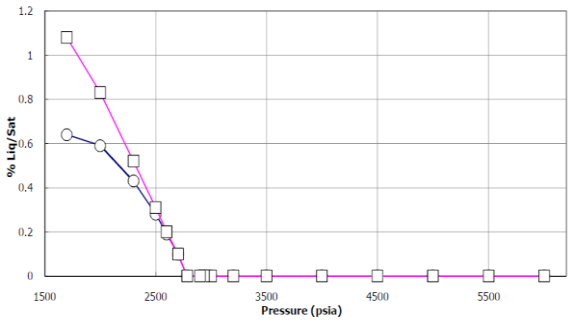


*Figure 15 Ratio of molar of saturated fluid and total fluid volume (purple curve) or saturation point volume (black curve), versus pressure of recombined samples*

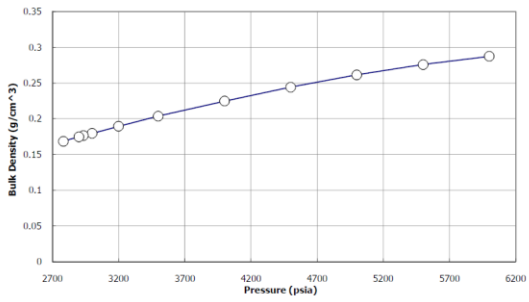


*Figure 16 Bulk density versus pressure of recombined samples*

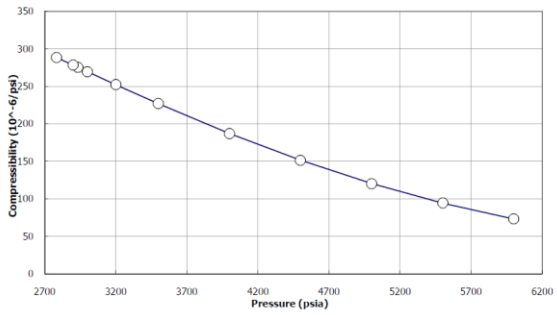


*Figure 17 Compressibility versus pressure of recombined samples*

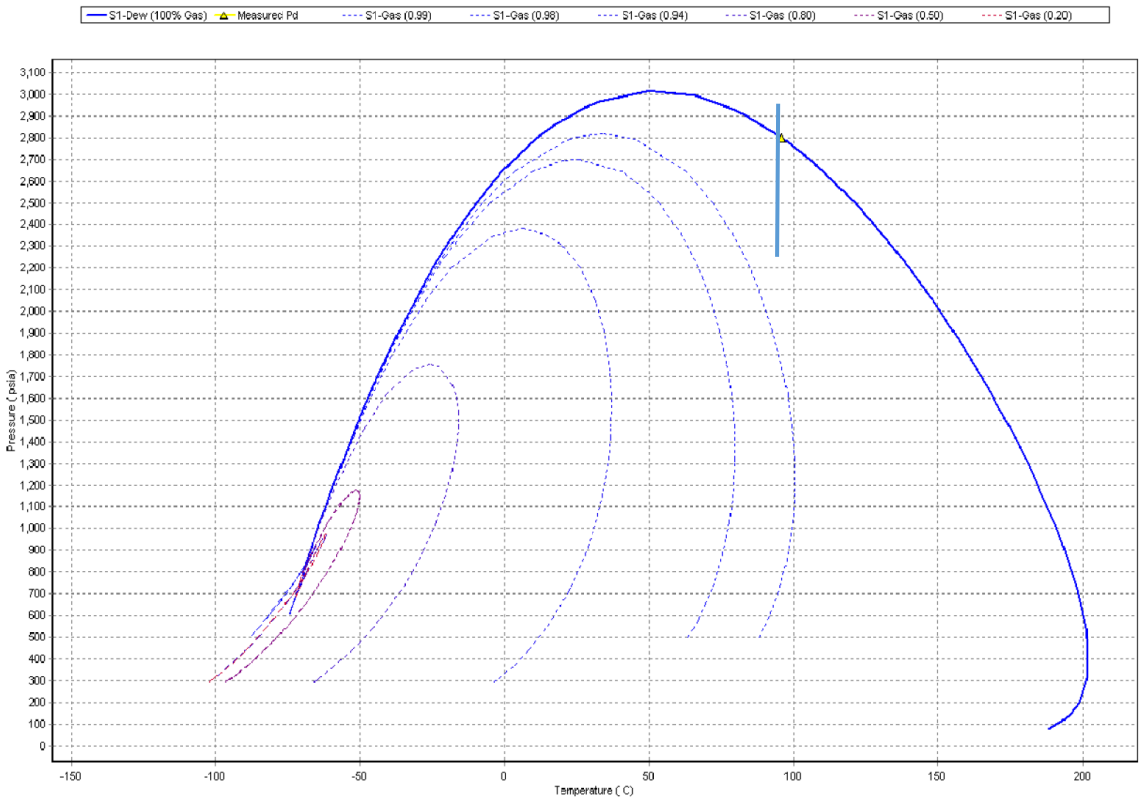


*Figure 18 Phase envelope for recombined samples*

The PVT report provided the following properties at reservoir conditions determined from Constant Composition Expansion (CCE) test.

*Table 4 CCE summary of fluid properties at reservoir conditions*

| Test ID : | **CCE at 96.0 °C** | |
|---|---|---|
| Test Temperature | 96.0 | °C |
| Dew Point Pressure | 2783 | psia |
| Compressibility at Pres | 275.4 | 10^-6/psi |
| Compressibility at Psat | 288.6 | 10^-6/psi |
| Res. Fluid Density at Pres | 0.176 | g/cc |
| Res. Fluid Density at Psat | 0.168 | g/cc |

There are 3 phases present in the formation: gas, water, and condensate.

From the literature, we know that condensate takes up pore space, thereby reducing gas permeability and impacting upon gas productivity. From Figure 13, the relative permeability curves show that the reservoir would have to reach 70% condensate saturation for gas to stop flowing. However, anything between 30 and 40% will heavily impede gas flow.

The initial appraisal well was drilled to a depth of 50m, showing a 'light' gas assuming single phase. However, it was only after the 2nd well appraisal where a sample was taken at a greater depth showing that the gas-condensate was 'heavier' i.e. that it contained more heavy ends.

What can be seen from Figure 19 is how the composition of the gas differs depending on its location in the reservoir. Therefore, there is a need to analyse production from the lower regions of the reservoir.

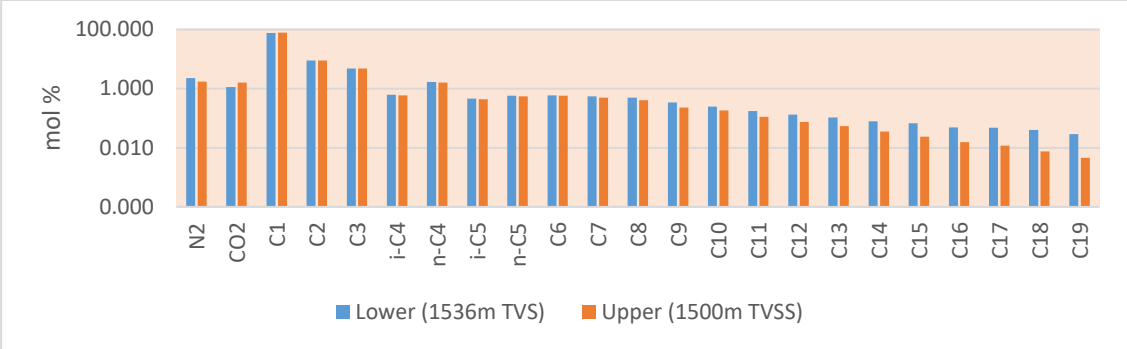


*Figure 19 Fluid composition of samples taken from the upper & lower zone of the reservoir*

This phenomenon can be seen in Figure 20, where, as the reservoir pressure falls the amount of condensate dropping out of the gas increases, as demonstrated by the rising Condensate-Gas Ratio (CGR), resulting in a gas of lower calorific value.

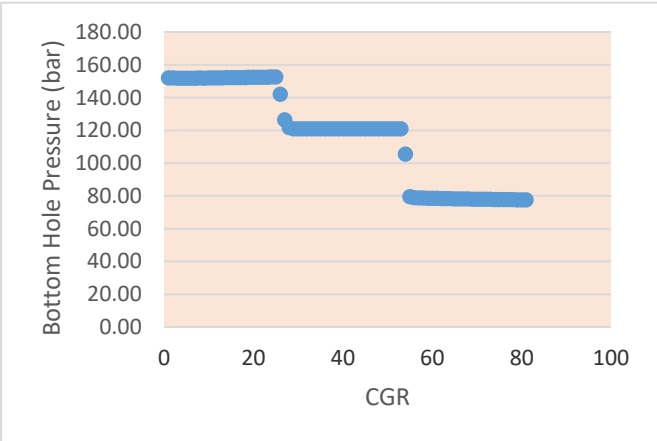


*Figure 20 CGR at different bottomhole pressures*

Figure 21 shows the gas flow rate of the appraisal wells before and after being hydraulically fractured. It can be seen that the gas flow rate increases greatly after hydraulic fracturing.

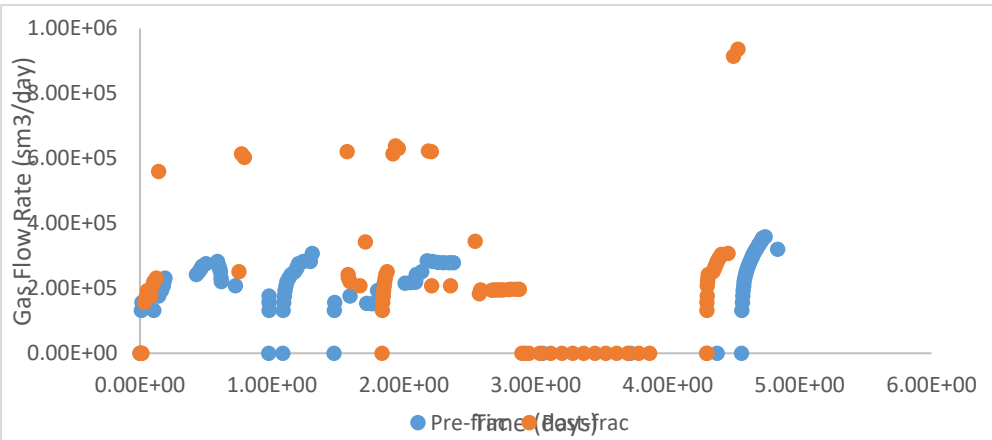


*Figure 21 Production rate of appraisal well before and after hydraulic fracturing*

## 4.4. Reservoir Model description

Figure 22 shows the dimensions of the section of the reservoir looked at in this project.

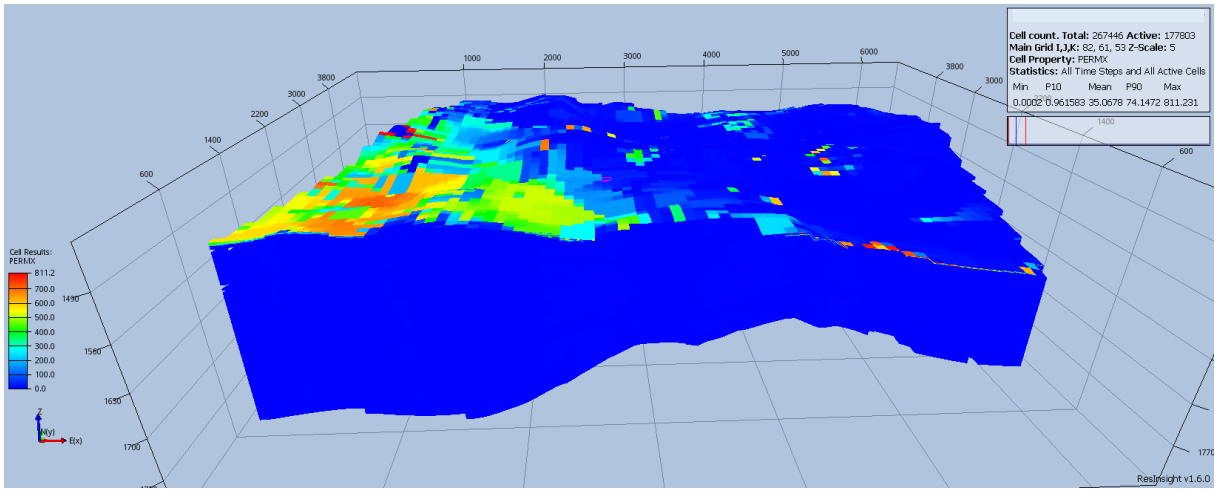


*Figure 22 Reservoir section*

The section covers 6.1 x 4.5 km with a thickness of about 350M. There are 270,041 grid cells in the model. The cell size is a nominal 75 x 75m to capture the geology in sufficient detail.

The model must be high-resolution to reproduce flow behaviour in the high permeability zones and give accurate distributions of the pressure gradients important to assess impacts of condensate banking, and to also allow important small-scale processes to be simulated, such as modelling flow, noting permeability variations, characterising natural fractures and modelling hydraulic fractures, facies characterisation for gas-saturation distribution and flow behaviour (relative permeabilities).

## 4.5. Simulation Model File Structure

The commercial simulator Eclipse 100 was used to model flow behaviour.

### 4.5.1. Grid Section

The grid geometry, properties, permeability and porosity values were generated within Petrel and their .GRDECL files were provided by PetroCeltic.

Using the OPERATE keyword, the permeability in the x-direction was set to a minimum of 0.0001. A variable 'WORK1' is defined by taking the natural log of the permeability, which would be later used in the Properties section.

When necessary, a high permeability zone was applied to the model by using a multiplier.

To perform appropriate modelling of the hydraulic fractures, relevant local grid refinements (LGR) were constructed around each well. The cell in which the well penetrates the reservoir model is divided in an appropriate number of sub-cells which have a logarithmic pattern. It is imperative that the innermost cell will have dimensions that allow fluid flow to happen without too much numerical instability. In the

case of this project the innermost cell is circa 0.5m wide. The same construct is repeated in all the cells that are expected to be in the area covered by the fracture half-length.

The porosity and permeability values of the hydraulic fracture could then be assigned by multiplying the appropriate value those blocks covered by the fracture; then using the REFINE keyword within the Regions section, to additionally apply a saturation table.

### 4.5.2. Edit Section

Due to the large size of the reservoir sector and so as to simplify the simulation and quicken the run-time, the cells outside a select area of interest, a more manageable size of 9737 blocks– 750x750x303.8m, Figure 23, were inactivated using a multiplier.

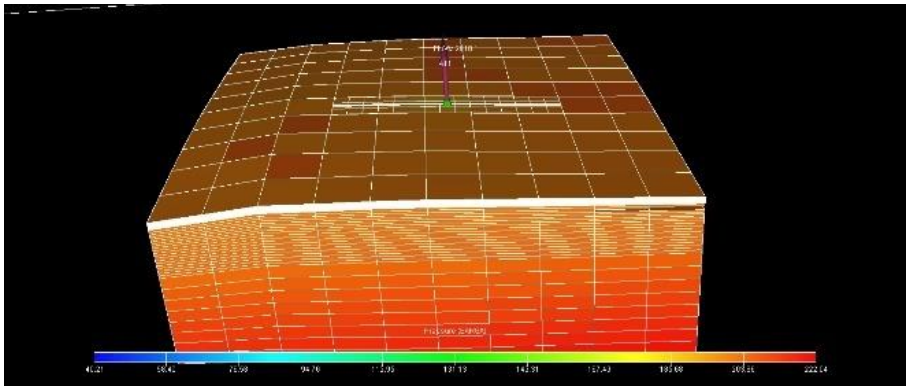

*Figure 23 Active cells of the reservoir sector when simulating a shallow vertical well*

### 4.5.3. Properties Section

The saturation tables which were determined from the capillary curves were placed in this section, and then using the OPERATE keyword once again the endpoints of the saturation tables and corresponding relative permeabilities were calculated.

### 4.5.4. Regions Section

Two regions were defined, Figure 24, so as to better compare zones of high and low permeability.

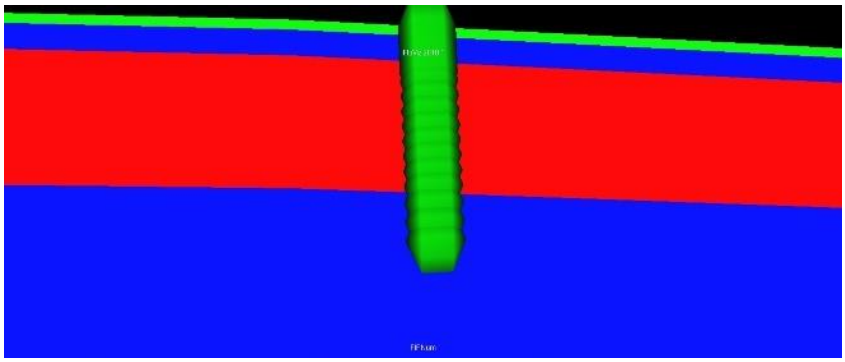

*Figure 24 Defined regions within reservoir sector*

Region 1 [green layer] (28 34 25 34 2 18) 8m height

Region 2 [red layer] (28 34 25 34 20 33) 30m height

### 4.5.5. Schedule Section

The well was defined using the WELSPECL and COMPDATL keywords, assigning its location within the LGR and depth drilled.

The models were simulated from 01 JAN 2020 01:00:00 (T0) to 01 APR 2023 (T20). The time step was one day up to the 8 JAN 2020, when it then jumped to the first of every third month up to T20. The wells were controlled using WCONPROD with gas as target rate and bottom hole pressure (BHP) as secondary target.

# 5. Simulation modelling

## 5.1. Impact of High Permeability Layer

The results of the appraisal well tests suggest that productivity is very sensitive to the presence of the high permeability zone. This part evaluation assesses the impact of the high permeability zone on well productivity and total recovery. To match the development plan, an uncased vertical well was drilled to a depth of 1510m, 50m below top of the reservoir column. Log and core data show the exploration well penetrated a 4m high permeability layer. In the model this is incorporated in Region 1.

From that, three cases were looked at to determine the effect of a high permeability layer to recovery – the exclusion of a high permeability layer, and the inclusion of one of varying size, height 2 and 8m.

| Case | Region 1 height |
|---|---|
| 1 | 0 |
| 2 | 2 |
| 3 | 8 |

The three cases of high permeability zone were added by using the multiplier function in the model, multiplying the permeability in all three directions by 40. Case 2 for example:

```
MULTIPLY

PERMX  40 28 34 25 34 2 6 /

PERMY  40 28 34 25 34 2 6 /

PERMZ  40 28 34 25 34 2 6 /

/
```

The principal observation from the following results is that a high permeability zone does have an impact, increasing recovery, and the larger the zone, the greater the increase.

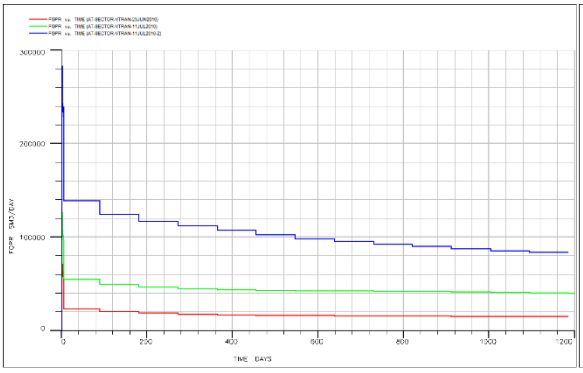

*Figure 25 Sector gas production rates comparison of vertical well passing through a high perm zone of 0m height (red curve), 2m height (green), and 8m height (blue)*

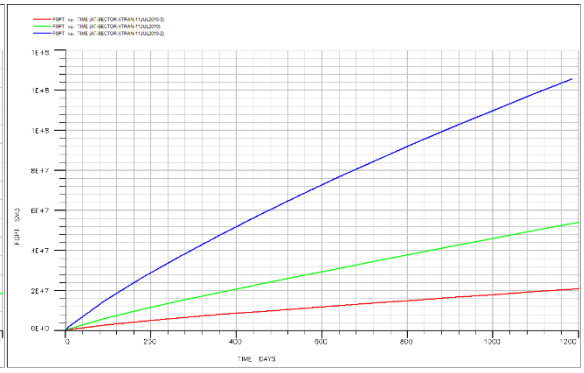

*Figure 26 Sector cumulative gas production comparison of vertical well passing through a high perm zone of 0m height (red curve), 2m height (green), and 8m height (blue)*

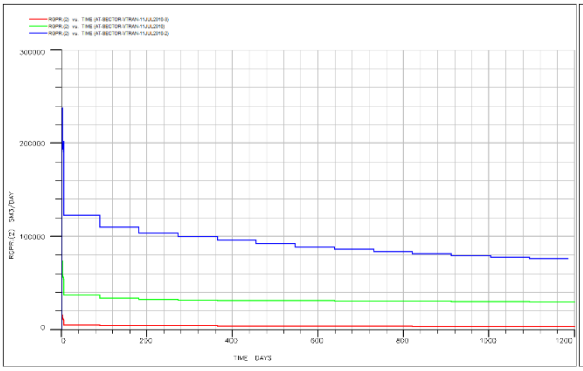

*Figure 27 gas production rates of region 1 comparison of vertical well passing through a high perm zone of 0m (red curve), 2m zone (green), and 8m zone (blue)*

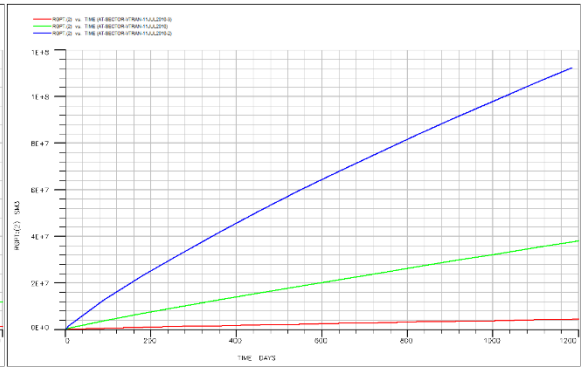

*Figure 28 cumulative gas production of region 1 comparison of vertical well passing through a high perm zone of 0m (red curve), 2m zone (green), and 8m zone (blue)*

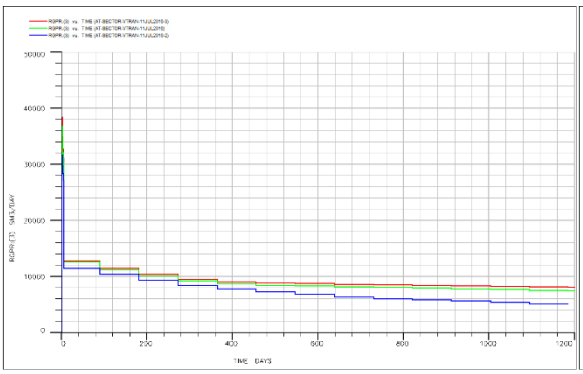

*Figure 29 gas production rates of region 2 comparison of vertical well passing through a high perm zone of 0m (red curve), 2m zone (green), and 8m zone (blue)*

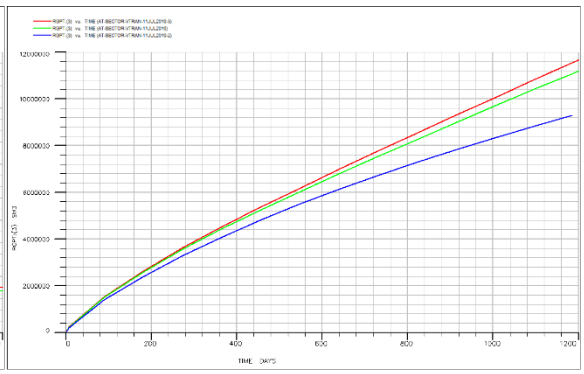

*Figure 30 cumulative gas production of region 2 comparison of vertical well passing through a high perm zone of 0m (red curve), 2m zone (green), and 8m zone (blue)*

Figure 31 shows how the productivity index increases with the increasing size of the high permeability zone, and despite the greater fall in pressure registered, does not affect the index.

It can be seen in Figure 32 that when there is no high permeability region, that the condensate-gas ratio (CGR) remains relatively constant. However, once a high permeability region is defined, a small increase is seen in the initial CGR value. However, after less than 100 days, the ratio starts to drop implying that it is at this point that the reservoir pressure drops below the dewpoint and condensate begins to deposit in the formation. With a larger high permeability zone, 8m, the CGR falls more sharply, indicating a greater deposition of condensate. This can be seen in the condensate saturation map, Figure 48, where there is a greater accumulation of condensate in region 1 around the well compared to when there is a smaller high permeability zone or none at all.

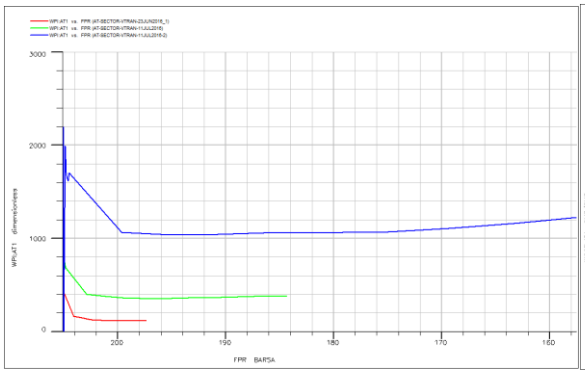


*Figure 31 Dimensionless productivity index compared to average reservoir pressure of vertical well passing through a high perm zone of 0m (red curve), 2m zone (green), and 8m zone (blue)*

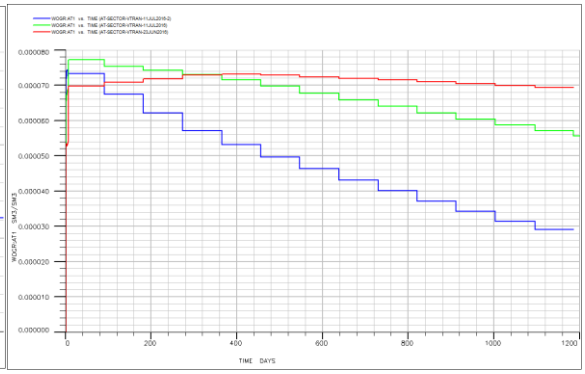


*Figure 32 CGR comparison of vertical well passing through a high perm zone of 0m (red curve), 2m zone (green), and 8m zone (blue)*

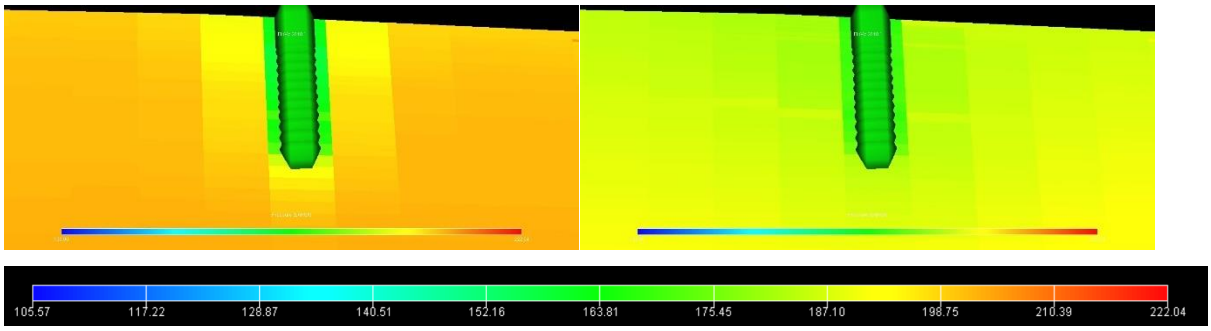


*Figure 33 Pressure distribution 0m high permeability zone at T1*

*Figure 34 Pressure distribution 0m high permeability zone at T20*

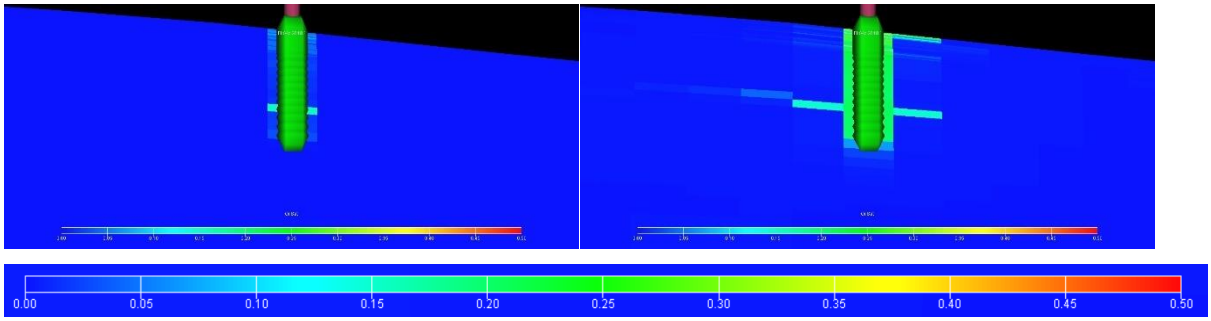


*Figure 35 Condensate Saturation distribution 0m high permeability zone at T1*

*Figure 36 Condensate Saturation distribution 0m high permeability zone at T20*

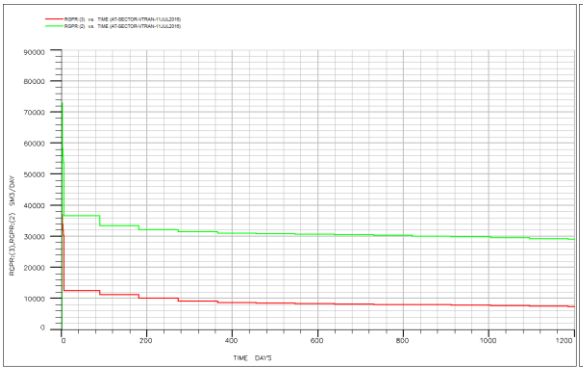


*Figure 37 sector gas production rates comparison of region 1 (green curve) and 2 (red curve) of vertical well passing through a high perm zone of 2m*

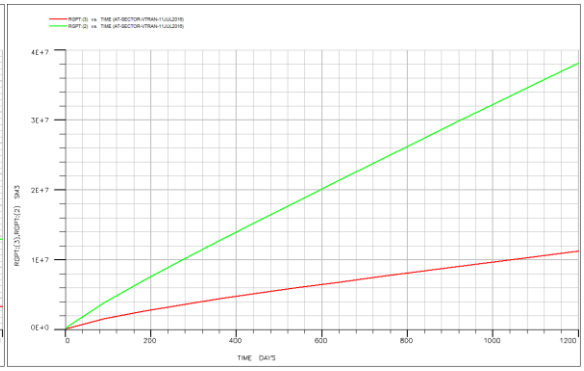


*Figure 38 sector cumulative gas production comparison of region 1 (green curve) and 2 (red curve) of vertical well passing through a high perm zone of 2m*

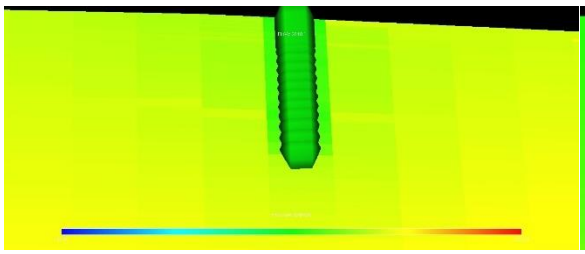

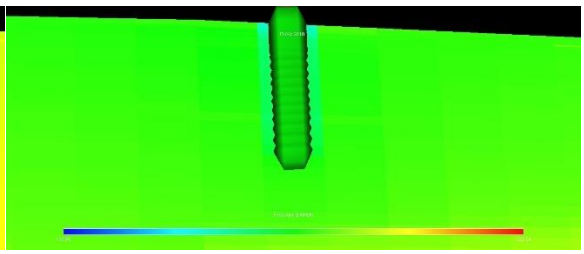

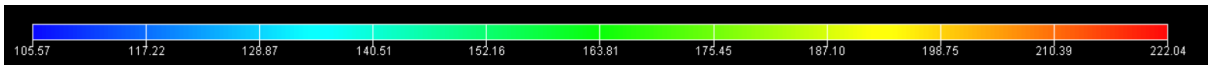


*Figure 39 Pressure distribution 0m high permeability zone at T20*

*Figure 40 Pressure distribution 2m high permeability zone at T20*

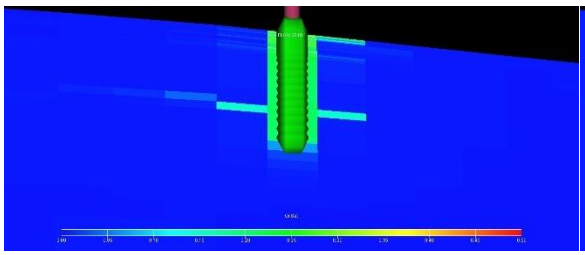

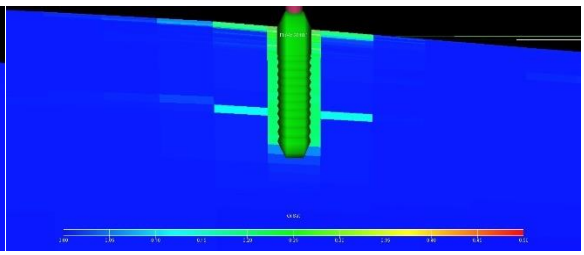

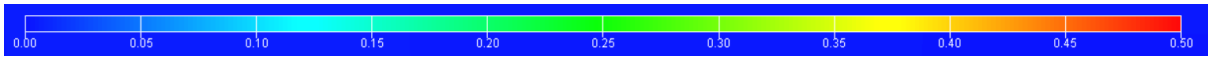


*Figure 41 Condensate Saturation distribution 0m high permeability zone at T20*

*Figure 42 Condensate Saturation distribution 2m high permeability zone at T20*

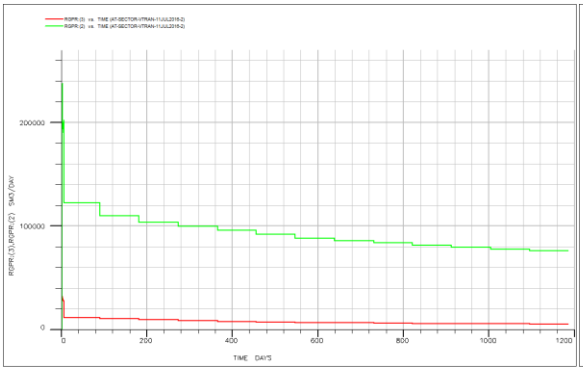


*Figure 43 sector gas production rates comparison of region 1 (green curve) and 2 (red curve) of vertical well passing through a high perm zone of 8m*

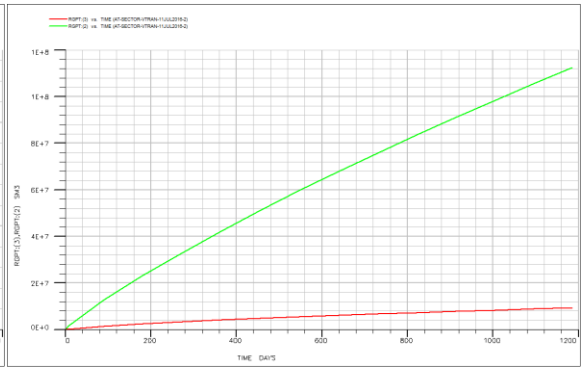


*Figure 44 sector cumulative gas production comparison of region 1 (green curve) and 2 (red curve) of vertical well passing through a high perm zone of 8m*

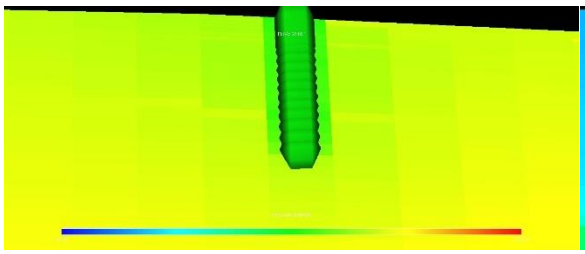

*Figure 45 Pressure distribution 0m high permeability zone at T20*

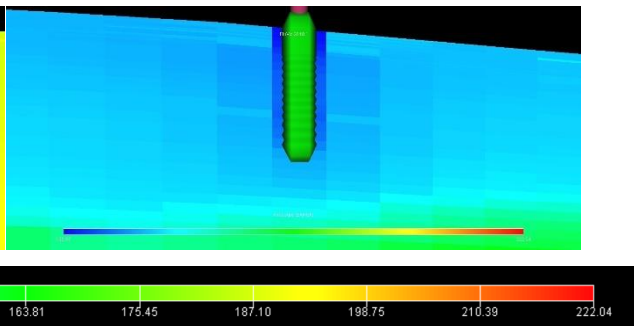


*Figure 46 Pressure distribution 8m high permeability zone at T20*

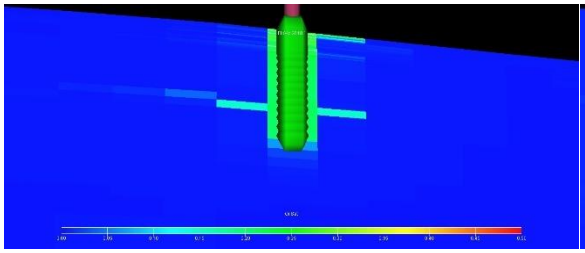

*Figure 47 Condensate Saturation distribution 0m high permeability zone at T20*

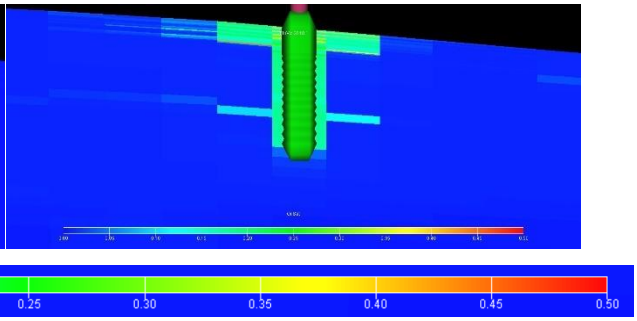


*Figure 48 Condensate Saturation distribution 8m high permeability zone at T20*

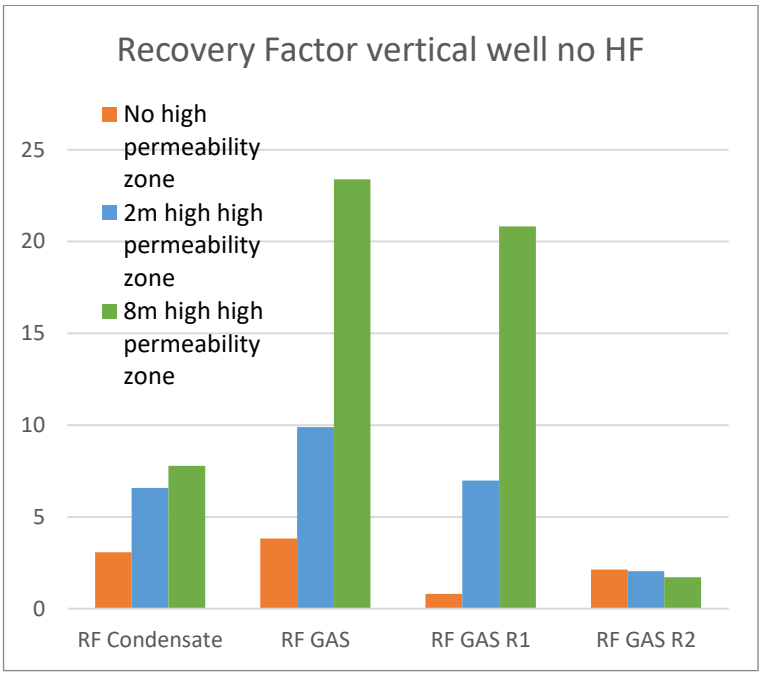


*Figure 49 Shallow vertical well recovery factor of the condensate (RF CONDENSATE), and gas from the sector (RF GAS), gas recovered from region 1 through the sector (RF GAS R1), and region 2 (RF GAS R1)*

Figure 49 shows recovery is highly sensitive to the presence of a high permeability zone. A 2m high zone increases the sector's gas recovery by more than 100%, whilst an 8m high zone produces 6 times more compared to the no high permeability zone case. This can also be seen in Figure 25 & Figure 26 showing the cumulative gas production and rate, where the production is much greater with the presence of a high permeability zone.

The high permeability zone also greatly increases production from that particular region. The bar graph (Figure 49) above shows that no high perm zone in the sector results in a recovery factor for that particular region (defined as 2m in height) of less than 1%; yet when the permeability in this region is multiplied by 40, the recovery factor jumps to 6.5%, and more than 20% when the size of the region is increased to 8m in height. There is also an increase in the recovery of condensate where it increases from 3 to 6.5% (2m) and then 7.8% for the 8m zone. Figure 49 also shows how most of the recovery comes from the high permeability zone ie. region 1.

There is a minor decline of 0.09% in the production rate in the second region when there is a high perm zone present. With an 8m high perm zone, the rate increasingly drops further by around 20,000 $m^3$/day. However, Figure 39 & Figure 40 (2m) and Figure 45 & Figure 46 (8m) show that while the pressure around the well is dropping as the size of the high permeability zone increases, it is also dropping uniformly. This indicates fluid flows from Region 2 to Region 1.

It should be noted that these values are very low and would not be commercially viable.

## 5.2. Impact of Hydraulic Fracturing

A hydraulic fracture of 20m height, 70m half length, 0.5m width, and fracture conductivity of 1000mD.m was added to the previous well to determine the effect it has, along with a high permeability layer, on recovery. The reservoir conditions are identical to those of the previous scenarios.

The principal observation from the following results is that a high permeability zone continues to have an impact on recovery, but the effect is smaller with most of the registered increase coming from the region containing the high permeability zone.

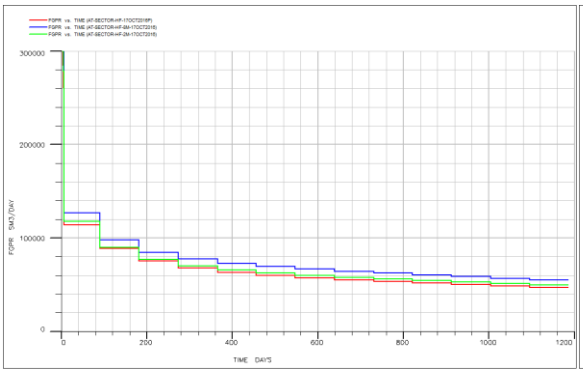


*Figure 50 sector gas production rates comparison of vertical well with HF of 20/70/0.5m passing through a high perm zone of 0m (red curve), 2m zone (green), and 8m zone (blue)*

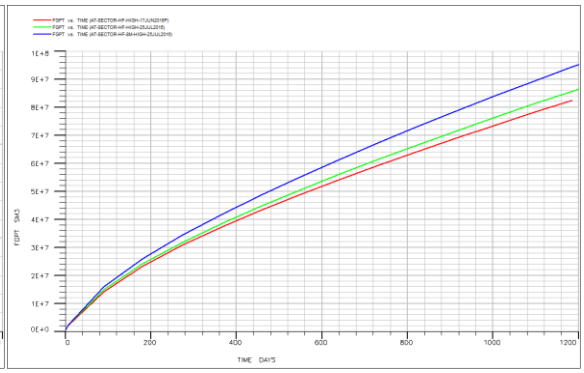


*Figure 51 sector cumulative gas production comparison of vertical well with HF of 20/70/0.5m passing through a high perm zone of 0m (red curve), 2m zone (green), and 8m zone (blue)*

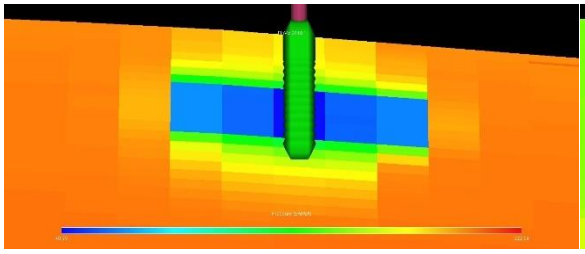

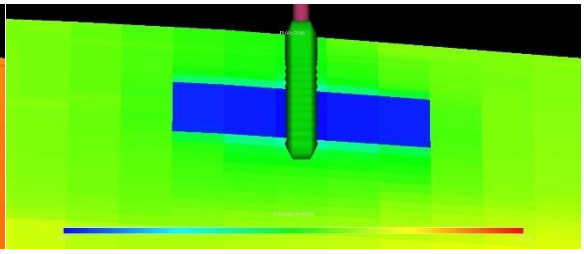


*Figure 52 Pressure distribution 0m high permeability zone at T1*

*Figure 53 Pressure distribution 0m high permeability zone at T20*

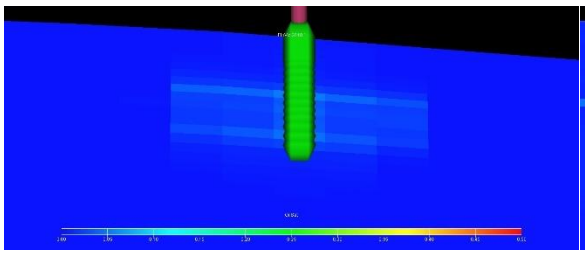

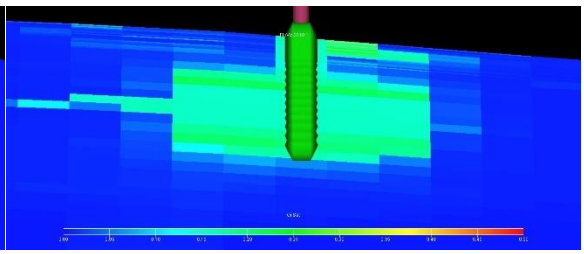

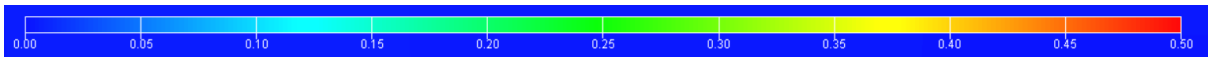


*Figure 54 Condensate Saturation distribution 0m high permeability zone at T1*

*Figure 55 Condensate Saturation distribution 0m high permeability zone at T20*

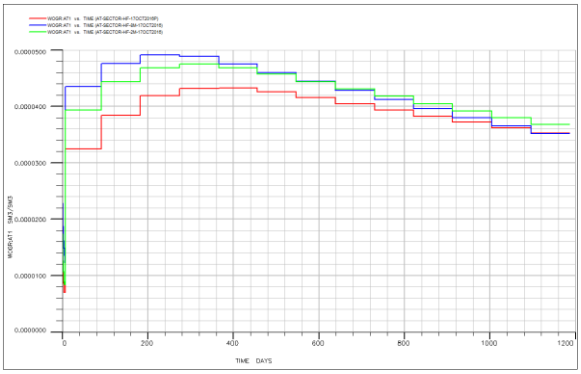

*Figure 56 CGR comparison of vertical well with a hydraulic fracture passing through a high perm zone of 0m (red curve), 2m zone (green), and 8m zone (blue)*

Figure 56 shows that in all three cases of high permeability region size, the presence of hydraulic fracture has the same effect on the behaviour of the CGR. The difference is in the initial CGR, which is lower and the max value reached (and when) by each case. The larger the high permeability region, the higher the initial CGR and max values, and the quicker the max value is reached. Additionally, after reaching their max values the CGR of the three cases falls to roughly the same value after 1200 days. This can be seen in the condensate saturation map, Figure 63, Figure 64, & Figure 70, which show that the most of the accumulation occurs around the hydraulic fracture in region 2 and remains relatively unchanged with the addition of a high permeability zone; the difference being the change in saturation in region 1.

### *No high permeability zone*

Figure 57 shows the difference between the gas production rate confined to region 1 (red curve) of the well hydraulically fractured, compared to the rate from region 2 (green curve) when there is no high permeability zone; while Figure 58 shows the difference between the cumulative production totals. As the hydraulic fracture is located within region 2, there is a disproportionate amount of the recovery coming from that region.

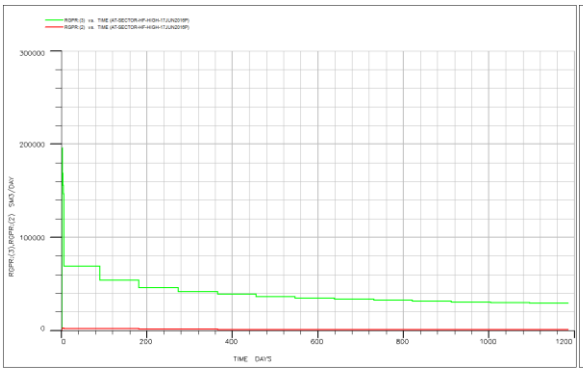

*Figure 57 sector gas production rates comparison of region 1 (red curve) and 2 (green curve) of vertical well with HF of 20/70/0.5m*

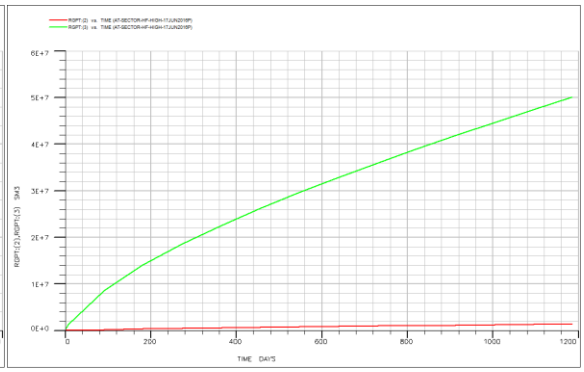

*Figure 58 sector cumulative gas production comparison of region 1 (red curve) and 2 (green curve) of vertical well with HF of 20/70/0.5m*

### 5.2.1. 2m high permeability zone

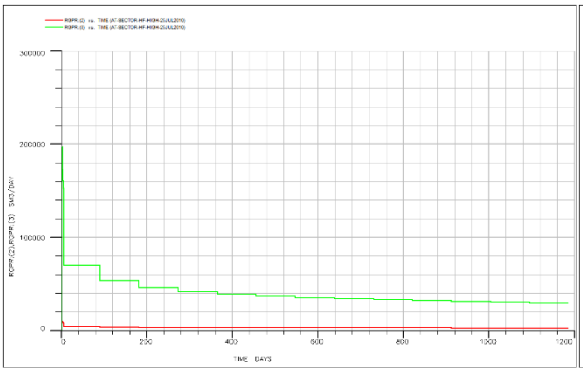


*Figure 59 sector gas production rates comparison of region 1 (red curve) and 2 (green curve) of vertical well with HF of 20/70/0.5m passing through a high perm zone of 2m*

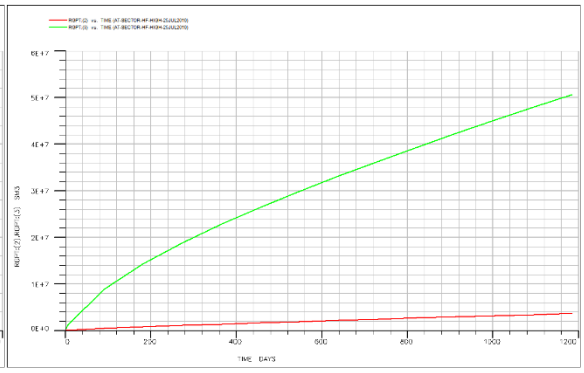


*Figure 60 sector cumulative gas production comparison of region 1 (red curve) and 2 (green curve) of vertical well with HF of 20/70/0.5m passing through a high perm zone of 2m*

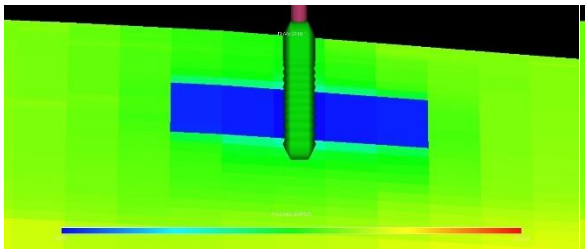

*Figure 61 Pressure distribution 0m high permeability zone at T20*

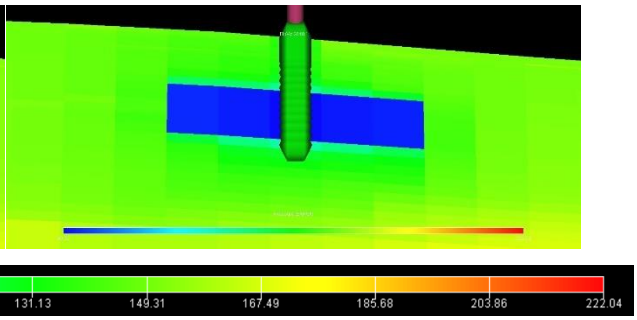


*Figure 62 Pressure distribution 2m high permeability zone at T20*

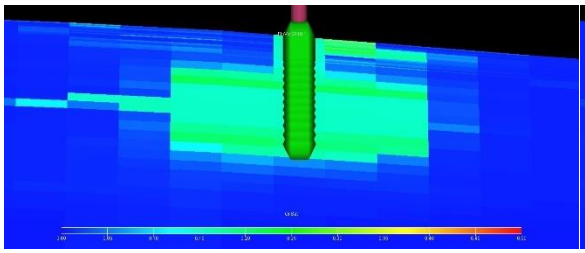

*Figure 63 Condensate Saturation distribution 0m high permeability zone at T20*

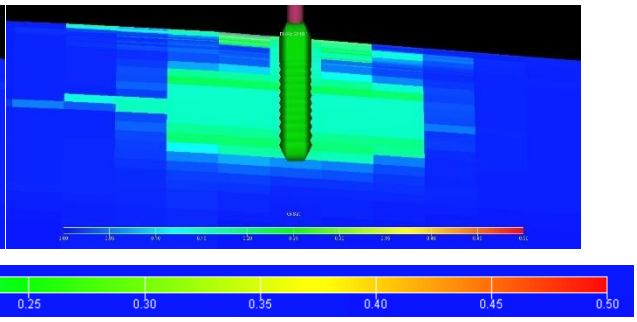


*Figure 64 Condensate Saturation distribution 2m high permeability zone at T20*

### 5.2.1.1. 8m high permeability zone

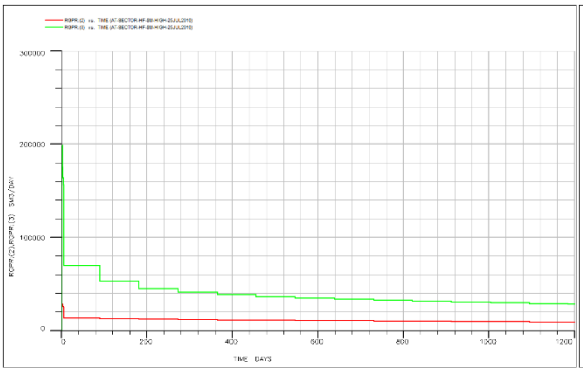


*Figure 65 sector gas production rates comparison of region 1 (red curve) and 2 (green curve) of vertical well with HF of 20/70/0.5m passing through a high perm zone of 8m*

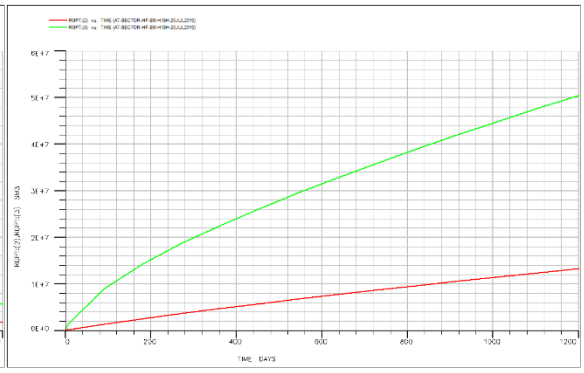


*Figure 66 cumulative gas production comparison region 1 (red curve) and 2 (green curve) of vertical well with HF of 20/70/0.5m passing through a high perm zone of 8m*

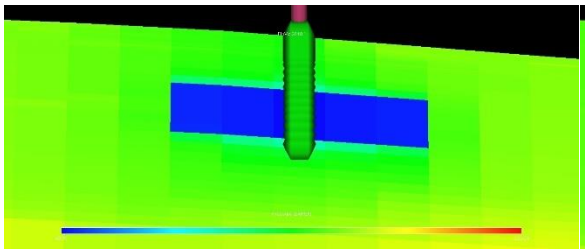

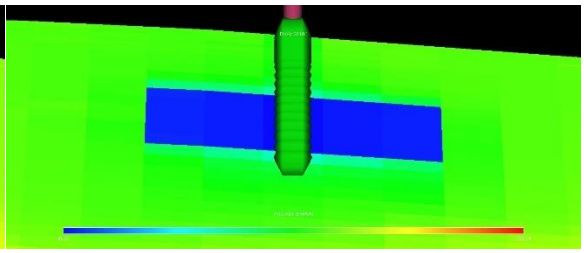


*Figure 67 Pressure distribution 0m high permeability zone at T20*

*Figure 68 Pressure distribution 8m high permeability zone at T20*

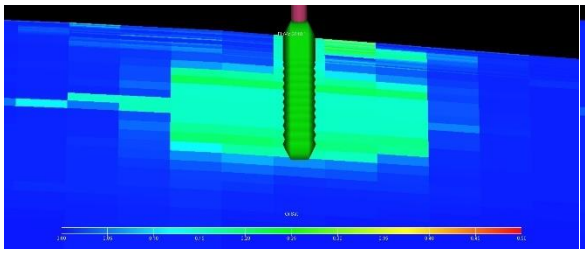

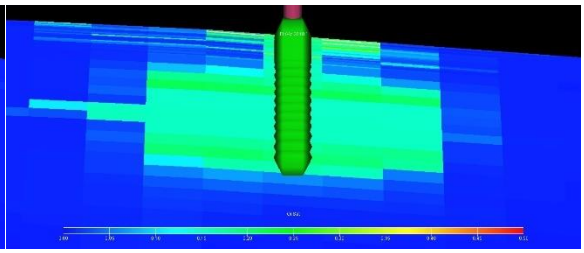

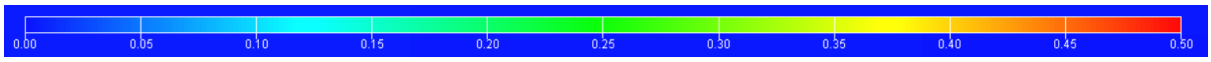


*Figure 69 Condensate Saturation distribution 0m high permeability zone at T20*

*Figure 70 Condensate Saturation distribution 8m high permeability zone at T20*

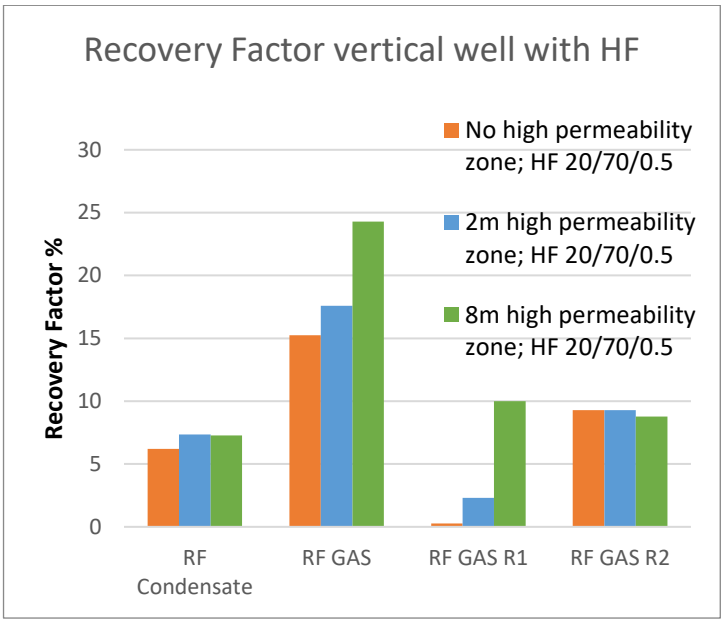


*Figure 71 Shallow vertical well with HF recovery factor of the condensate (RF CONDENSATE), and gas from the sector (RF GAS), gas recovered from region 1 through the sector (RF GAS R1), and region 2 (RF GAS R1)*

Figure 71 shows that with the addition of a hydraulic fracture, a high permeability zone still affects recovery however is much less sensitive to it compared to when there is no HF.

Unlike when there was no HF, here the majority of recovery comes from region 2 as opposed to region 1. This is where the HF is located, and as can be seen in the above pressure maps, the pressure remains constant in all scenarios. This results in very little change to the recovery in region 2 with the inclusion of a high permeability zone.

The high permeability zone affects the production of region 1 where it is located. Without it, recovery is negligible, indicating that fluid is flowing down to the higher permeability of the hydraulic fracture. With its inclusion, production in the region increases, contributing to the general increase across the sector.

Figure 71 also shows that while a hydraulic fracture has the effect of increasing the recovery factor across the reservoir sector, in the case of an 8m high permeability zone, the increase is small, 1%. However, the increase is much more marked when there is a smaller high permeability zone or none at all, 8 and 12% respectively. Therefore, regardless of the uncertainty of the size of the high permeability zone, it appears that hydraulic fracturing is necessary.

### 5.2.2. Comparison of hydraulic fractured well production

The graphs below show the effect that a hydraulic fracture has on production when there is no high permeability zone, compared to the case without hydraulic fracturing. The principal observation from the following results is that hydraulic fracturing has a significant impact on recovery.

Figure 72 & Figure 73 show how a hydraulic fracture increases the recovery total from 20M $m^3$ to more than 80M $m^3$, compared to the case without.

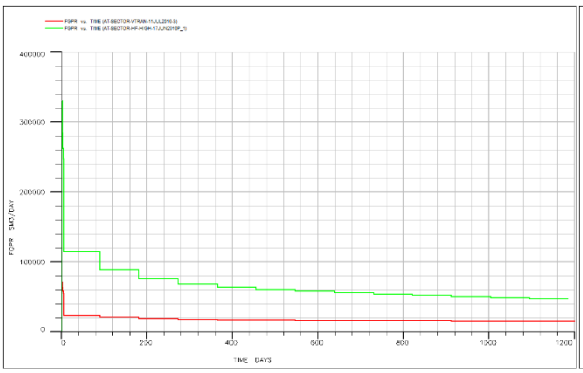

*Figure 72 sector gas production rates comparison of a vertical well with HF of 20/70/0.5m (green curve) and without HF (red curve)*

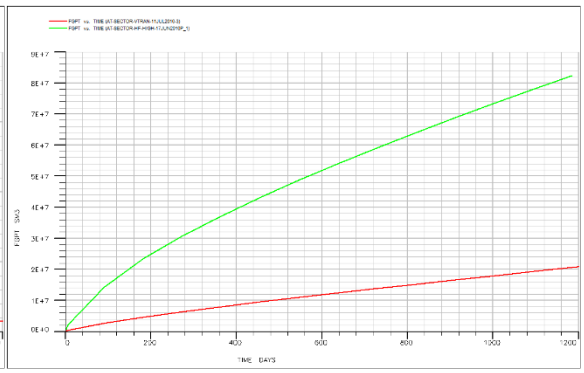

*Figure 73 cumulative gas production comparison of a vertical well with HF of 20/70/0.5m (green curve) and without HF (red curve)*

Figure 74 to Figure 77 indicate that most of the production is coming from region 2 when the well is hydraulically fractured.

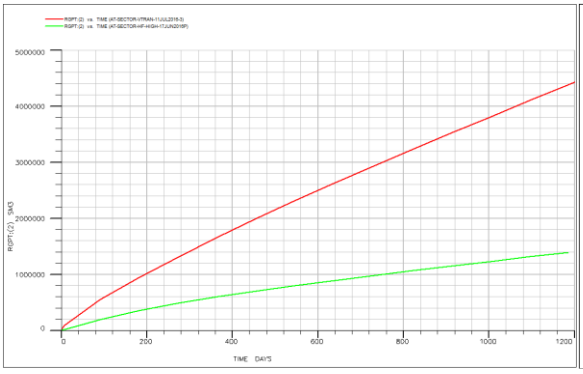

*Figure 74 cumulative gas production from region 1 comparison of a vertical well with HF of 20/70/0.5m (green curve) and without HF (red curve)*

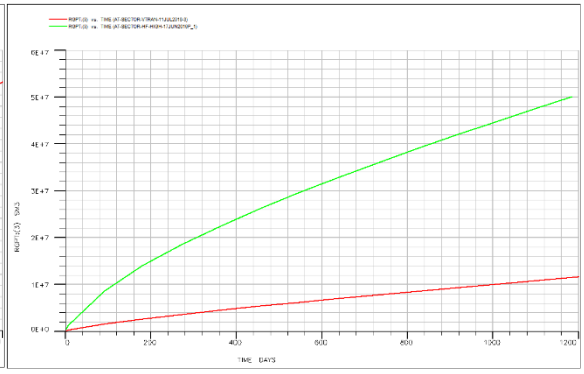

*Figure 75 cumulative gas production from region 2 comparison of a vertical well with HF of 20/70/0.5m (green curve) and without HF (red curve)*

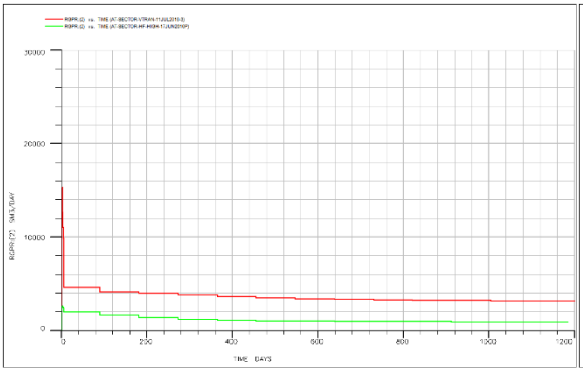

*Figure 76 gas production rates from region 1 comparison of a vertical well with HF of 20/70/0.5m (green curve) and without HF (red curve)*

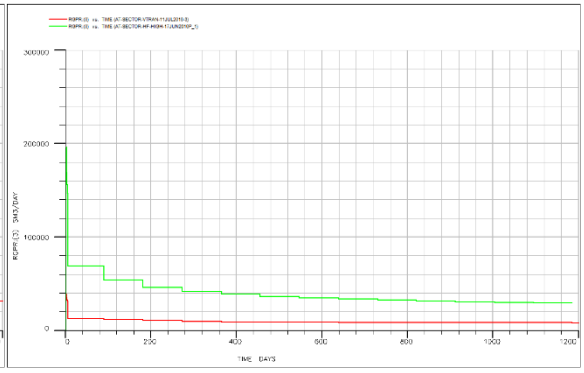

*Figure 77 gas production rates from region 2 comparison of a vertical well with HF of 20/70/0.5m (green curve) and without HF (red curve)*

Figure 78 shows that the hydraulic fracture increases the recovery factor of the gas from 3.8 to 15%, while also increasing that of the condensate from 3 to 6.2%.

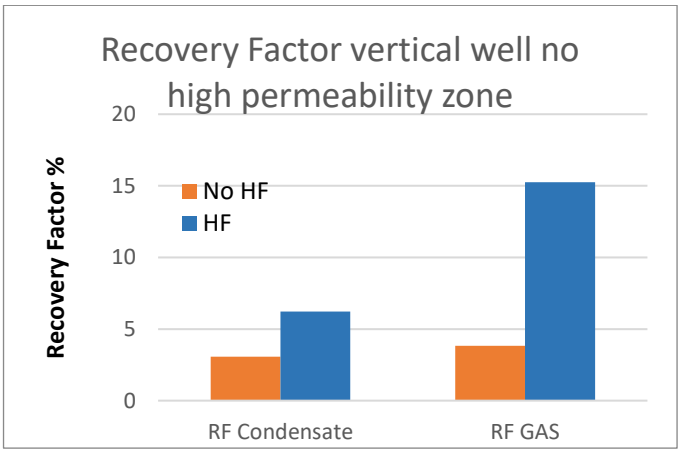


*Figure 78 Recovery factor of shallow vertical wells with HF and without*

Figure 79 to Figure 84 show the effect that a hydraulic fracture has on production when there is a 2m high permeability zone present. While the recovery does increase when the formation hydraulically fractured, the difference between the two states is not as pronounced as it was when the high permeability zone was smaller. The difference in the cumulative gas production totals has dropped to 34M $m^3$ from 60M $m^3$. Though the behaviour remains the same, the region registering the greater pressure drop, be it the hydraulic fracture or the high permeability zone when there is no HF, results in that region attaining the highest recovery.

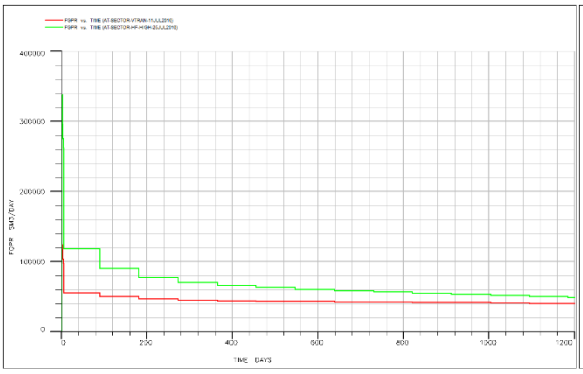

*Figure 79 gas production rates comparison of a vertical well with 2m high permeability zone present with HF of 20/70/0.5m (green curve) and without HF (red curve)*

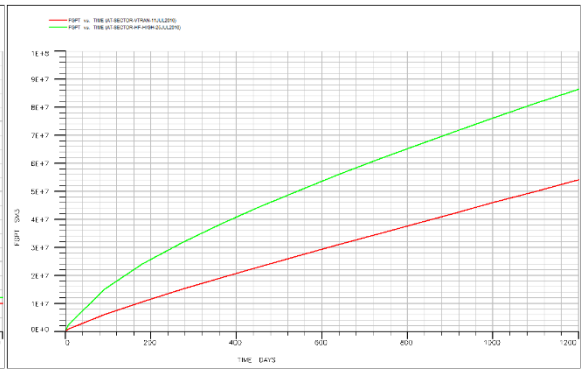

*Figure 80 cumulative gas production comparison of a vertical well with 2m high permeability zone present with HF of 20/70/0.5m (green curve) and without HF (red curve)*

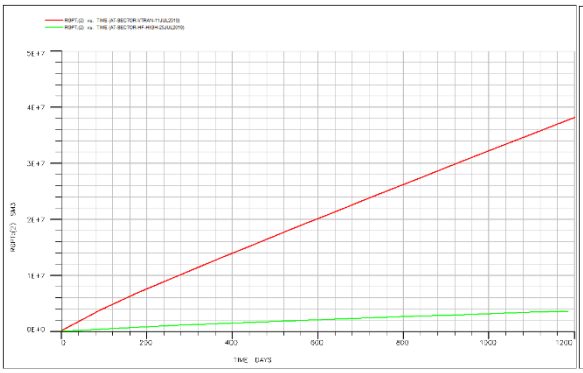

*Figure 81 cumulative gas production from region 1 comparison of vertical well with 2m high permeability zone present with HF of 20/70/0.5m (green curve) and without HF (red curve)*

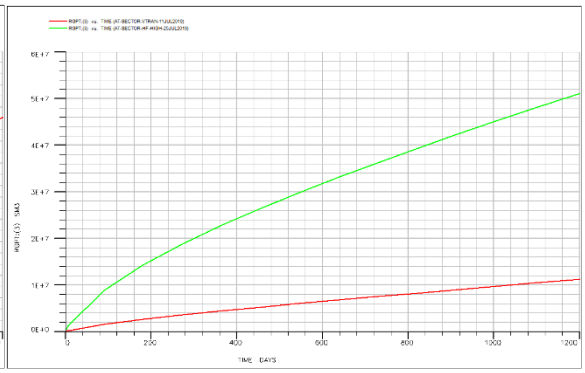

*Figure 824 cumulative gas production from region 2 comparison of vertical well with 2m high permeability zone present with HF of 20/70/0.5m (green curve) and without HF (red curve)*

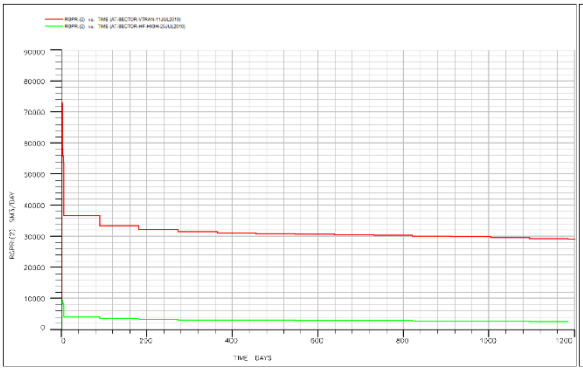

*Figure 83 gas production rates from region 1 comparison of vertical well with 2m high permeability zone present with HF of 20/70/0.5m (green curve) and without HF (red curve)*

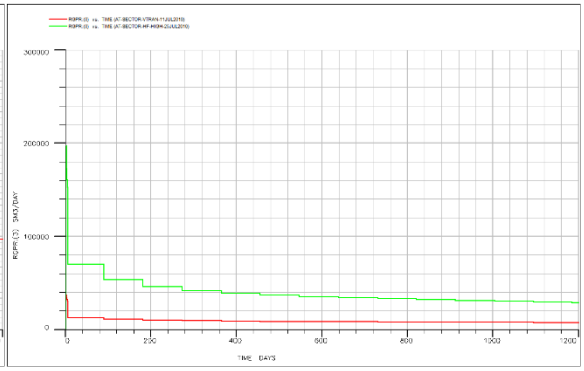

*Figure 84 gas production rates from region 2 comparison of vertical well with 2m high permeability zone present with HF of 20/70/0.5m (green curve) and without HF (red curve)*

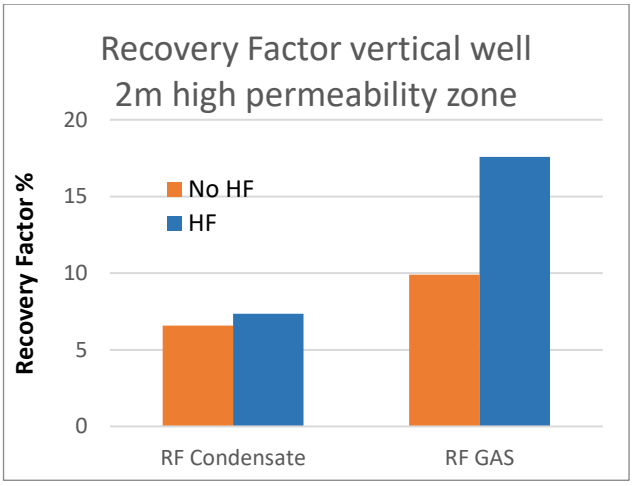


*Figure 85 Recovery factor of shallow vertical wells with HF and without passing through a 2m high permeability zone*

Figure 85 shows that with a high permeability zone present, the hydraulic fracture increases the recovery factor of the gas from 10 to 17.6%, while there is a more modest increase for the condensate from 6.6 to 7.3%.

### 5.2.3. Target Depth of Hydraulic Fracture

This next section involved realigning the depth of the 20/70/0.5m hydraulic fracture so that it penetrates the high permeability zone as seen in Figure 87. This was done by readjusting the porosity and permeability values, of the affected cells, within the grid section of the model.

The principal observation from the following results is that a hydraulic fracture penetrating a high permeability zone sees an increase in recovery compared to penetrating a low permeability zone.

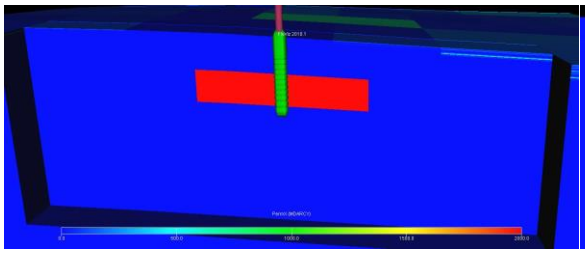

*Figure 86 Hydraulic fracture location 1*

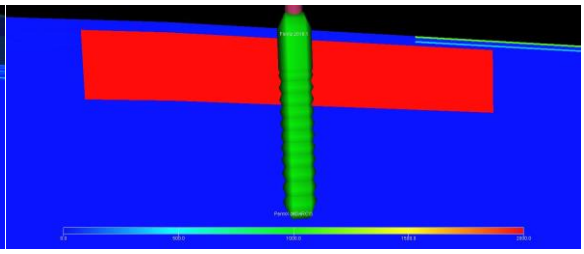

*Figure 87 Hydraulic fracture penetrating region 1*

The simulations were first run without a high permeability zone to determine the effect changing the depth of the hydraulic fracture, the results of which can be seen in Figure 88 & Figure 89. The deeper hydraulic fracture (green curve) has a slightly higher gas production rate of 10000 $sm^3$/day within the first 200 days, however they soon converge leaving the deeper well with only an extra 2M $sm^3$ recovered after 1200 days.

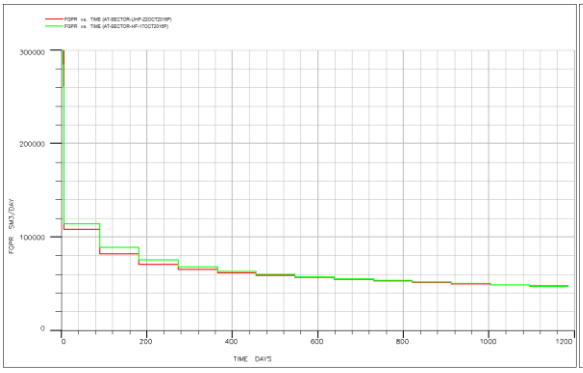


*Figure 88 sector gas production rates comparison of a vertical well with HF of 20/70/0.5m penetrating region 1(red curve) and not penetrating (green curve)*

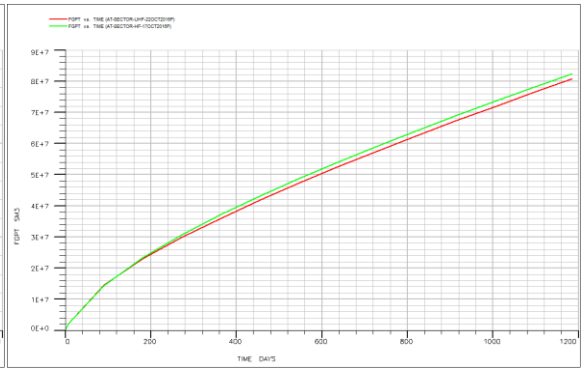


*Figure 89 sector cumulative gas production comparison of a vertical well with HF of 20/70/0.5m penetrating region 1(red curve) and not penetrating (green curve)*

A high permeability zone is introduced and the model with the hydraulic fracture penetrating said zone (red curve) maintains a higher production rate and therefore sees the cumulative recovery rising against the model with no hydraulic fracture, Figure 90 & Figure 91

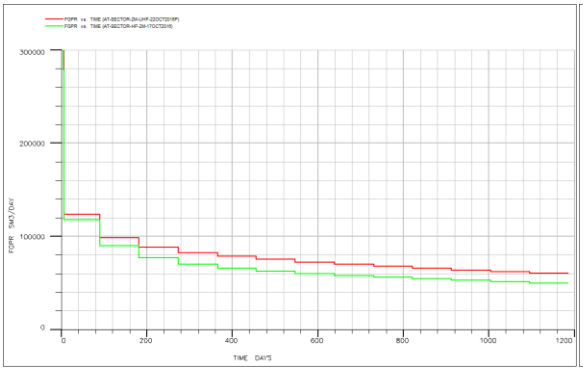


*Figure 90 sector gas production rates comparison of a vertical well with HF of 20/70/0.5m penetrating a 2m high permeability zone (red curve) and not penetrating (green curve)*

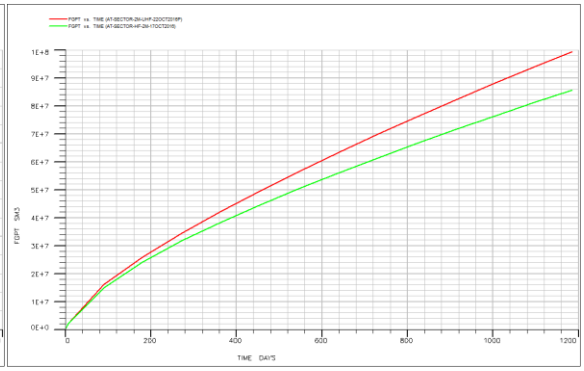


*Figure 91 sector cumulative gas production comparison of a vertical well with HF of 20/70/0.5m penetrating a 2m high permeability zone (red curve) and not penetrating (green curve)*

By increasing the size of the high permeability zone to 8m, it can be seen in Figure 92 & Figure 93 that there is an even greater increase in the recovery of the model with the hydraulic fracture penetrating region 1.

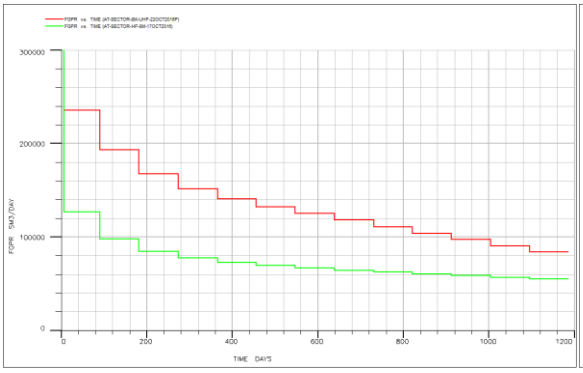


*Figure 92 sector gas production rates comparison of a vertical well with HF of 20/70/0.5m penetrating an 8m high permeability zone (red curve) and not penetrating (green curve)*

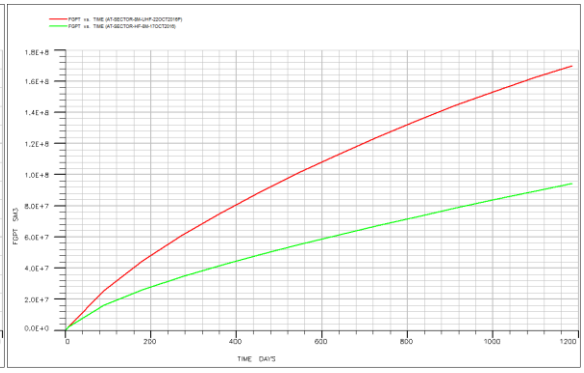


*Figure 93 sector cumulative gas production comparison of a vertical well with HF of 20/70/0.5m penetrating an 8m high permeability zone (red curve) and not penetrating (green curve)*

These results imply that provided there is a high permeability region in the reservoir, it is beneficial to hydraulically fracture the region so as to increase recovery.

## 5.3. $k_v/k_h$ Sensitivity

This part of the project assesses the impact the ratio of vertical against horizontal permeability $k_v/k_h$ has on well productivity and total recovery. Four cases were evaluated ranging from optimal (1), realistic (2) to very pessimistic (4):

| Case | $k_v/k_h$ |
|---|---|
| 1 | 1 |
| 2 | 0.8 |
| 3 | 0.15 |
| 4 | 0.02 |

Additionally, the above were simulated with and without the inclusion of a zone of high permeability, and the uncased vertical wells were not hydraulically fractured.

The reservoir conditions are identical to those of the previous scenarios, initially without a hydraulic fracture.

The principal observation from the following results is that vertical transmissibility only has an impact on recovery when a high permeability zone is present in the reservoir.

### 5.3.1. The Case with No Hydraulic Fracture

#### *5.3.1.1. No high permeability zone*

Figure 94 & Figure 95, which are the recovery rate and cumulative total of a vertical well drilled down to a depth of 1500m without a region of high permeability, and no hydraulic fracture, show that vertical transmissibility has very little effect on recovery, as for commercial purposes there is negligible difference to the four curves.

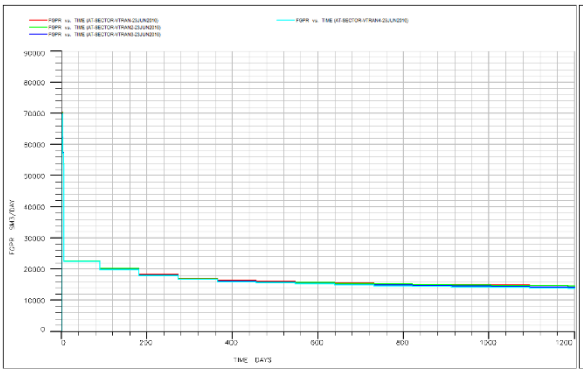

*Figure 94 sector gas production rates comparison of vertical well with a $k_v/k_h$ ratio of 1 (red curve), 0.8 (green), 0.15 (blue) and 0.02 (cyan)*

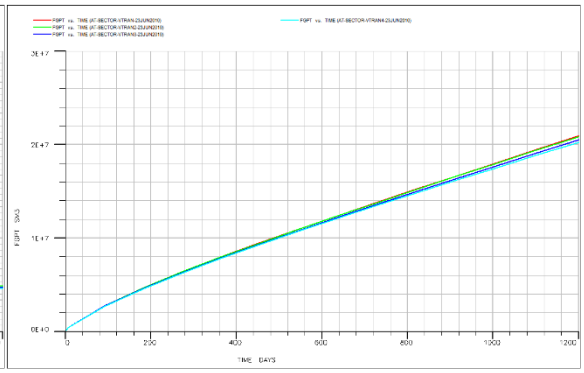

*Figure 95 sector cumulative gas production comparison of vertical well with a $k_v/k_h$ ratio of 1 (red curve), 0.8 (green), 0.15 (blue) and 0.02 (cyan)*

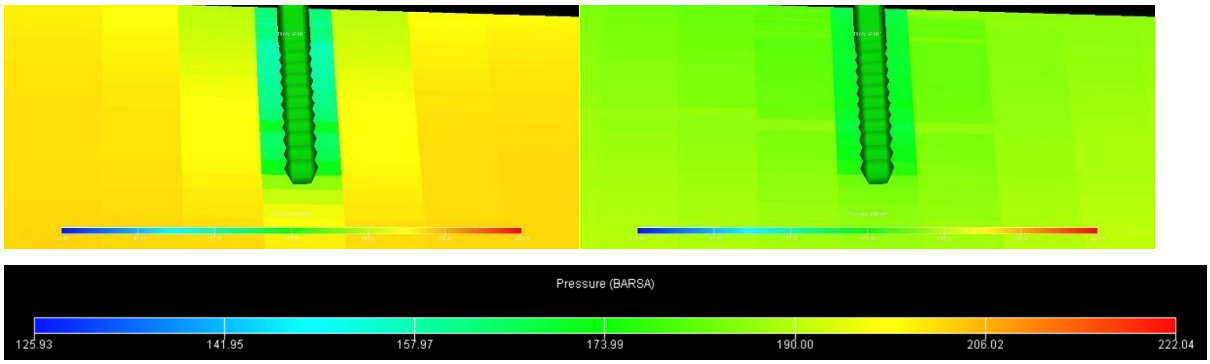


*Figure 96 Pressure distribution of $k_v/k_h$ ratio 1 at T1*

*Figure 97 Pressure distribution of $k_v/k_h$ ratio 1 at T20*

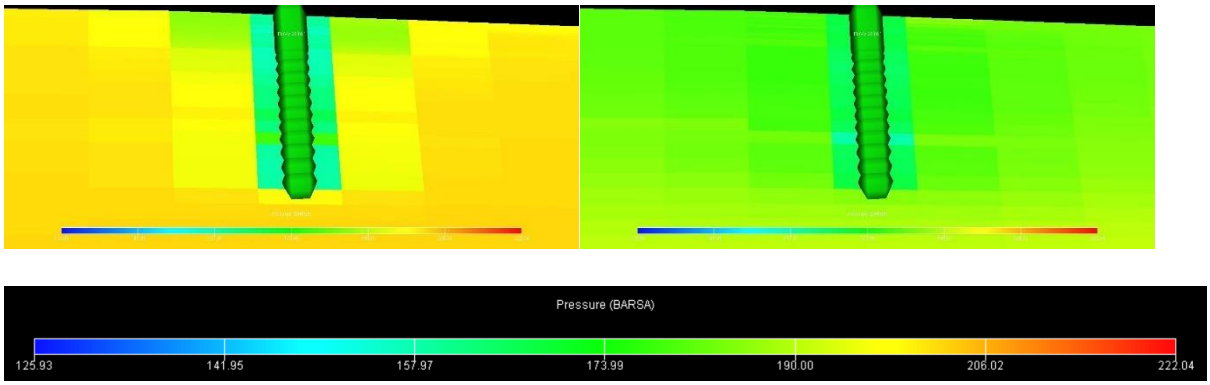


*Figure 98 Pressure distribution of $k_v/k_h$ ratio 0.02 at T1*

*Figure 99 Pressure distribution of $k_v/k_h$ ratio 0.02 at T20*

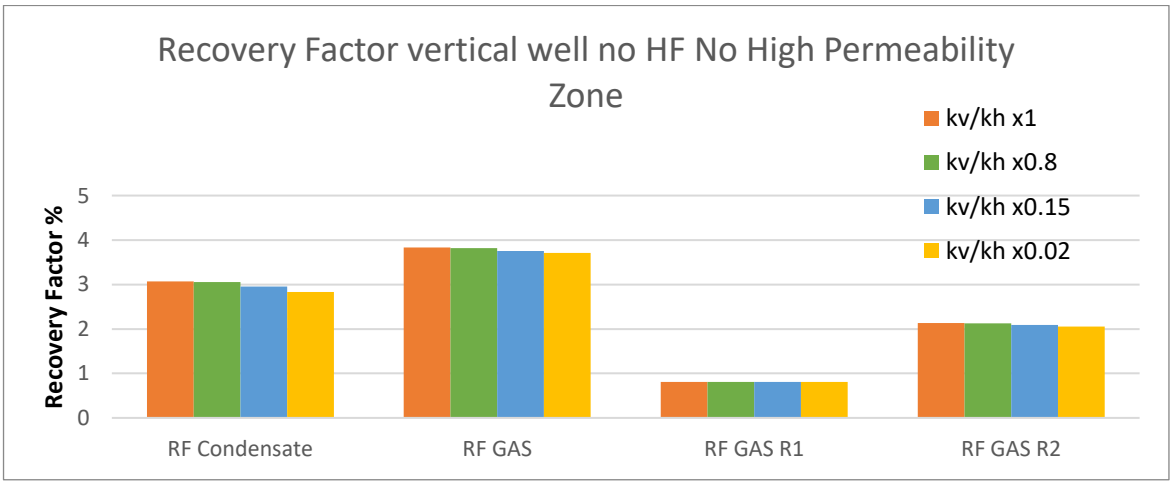


*Figure 100 Shallow vertical well recovery factor of the condensate (RF CONDENSATE), and gas from the sector (RF GAS), gas recovered from region 1 through the sector (RF GAS R1), and region 2 (RF GAS R1) comparison of $k_v/k_h$ ratios*

Permeability anisotropy: Figure 100 shows that by reducing the $k_v/k_h$ ratio, the gas and condensate recovery for the whole sector falls; while region 1, which here does not have a high permeability zone, the gas recovery remains the same. There is a 0.1% difference in the recovery from the perfect case of x1 to the pessimistic case of x0.02. This appears to be happening mainly in the larger region 2.

#### *5.3.1.2. 2m high permeability zone*

A region (525x750x2m) of high permeability was added to the model in region 1. This addition has a noticible effect on the recovery rate and cumulative total of an uncased vertical well, shown in Figure 101 & Figure 102. This effect is quantified in Figure 109, which shows that not only does the introduction of a high permeability zone increase the gas recovery by more than 100%, from 3.8 to 9.9% in the best case scenario, but it also increases the sensitivity of recovery to the vertical transmissibility. The difference in the gas recovery of the whole sector from the perfect case of x1 to the pessimistic case of x0.02, now stands at 1%, up from 0.1% previously. Condensate recovery is also increased from 3 to 6.5%.

Figure 109 also points to a change in the influence the two regions have on the overall recovery of the sector. The gas recovery of region 1 has not only increased by x7 fold but also now displays sensitivity to the changing kv/kh ratio; while region 2 is now displaying insensitivity. This can also be seen in Figure 105 & Figure 106which shows the gas recovery rate and cumulative total of region 1 and whose behaviour more closely resemble the overall sector's shown in Figure 101 & Figure 102 than region 2's Figure 107 & Figure 108.

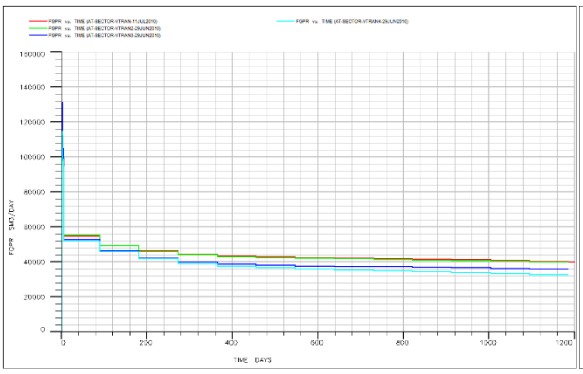

*Figure 101 sector gas production rates comparison of vertical well passing through a 2m high perm layer with a $k_v/k_h$ ratio of 1 (red curve), 0.8 (green), 0.15 (blue) and 0.02 (cyan)*

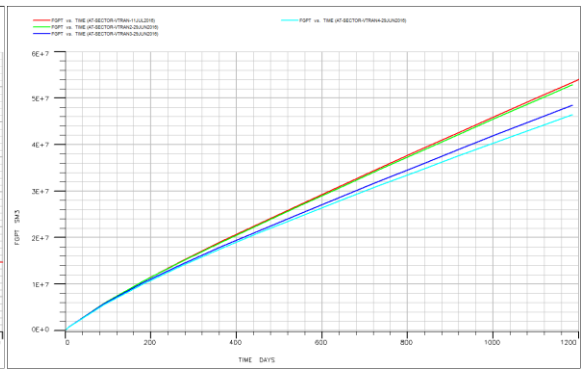

*Figure 102 sector cumulative gas production comparison of vertical well passing through a 2m high perm layer with a $k_v/k_h$ ratio of 1 (red curve), 0.8 (green), 0.15 (blue) and 0.02 (cyan)*

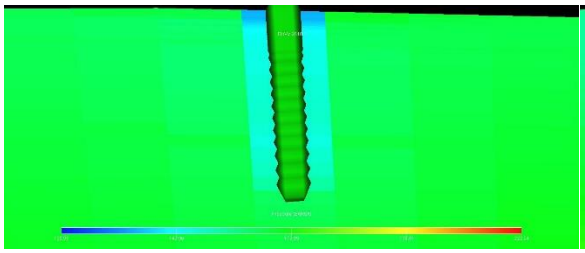

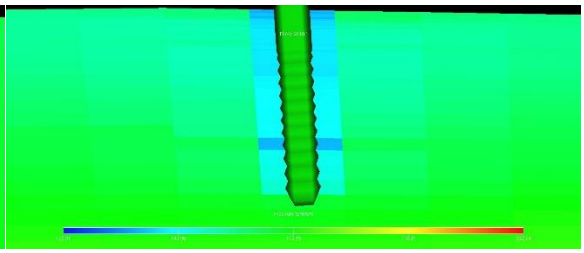

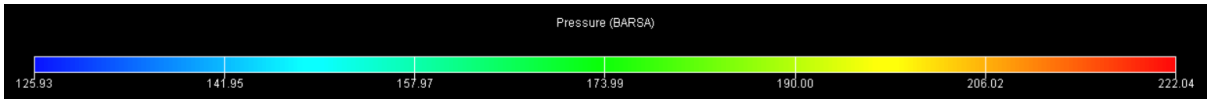


*Figure 103 Pressure distribution of $k_v/k_h$ ratio 1 at T20*

*Figure 104 Pressure distribution of $k_v/k_h$ ratio 0.02 at T20*

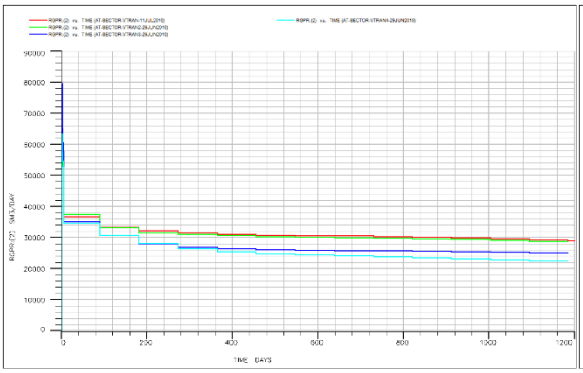

*Figure 105 gas production rates of region 1 comparison of vertical well passing through a 2m high perm layer with a $k_v/k_h$ ratio of 1 (red curve), 0.8 (green), 0.15 (blue) and 0.02 (cyan)*

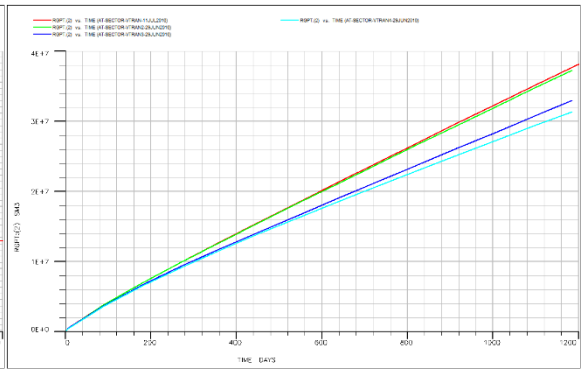

*Figure 106 sector cumulative gas production of region 1 comparison of vertical well passing through a 2m high perm layer with a $k_v/k_h$ ratio of 1 (red curve), 0.8 (green), 0.15 (blue) and 0.02 (cyan)*

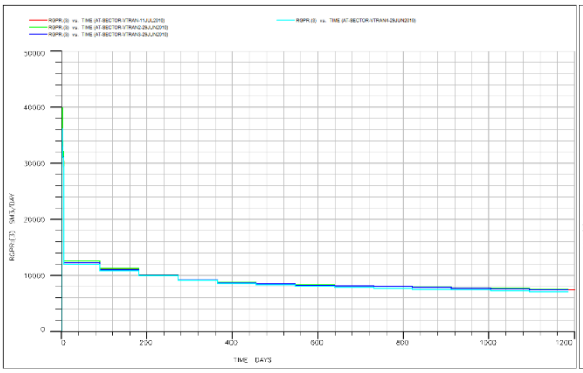

*Figure 107 gas production rates of region 2 comparison of vertical well passing through a 2m high perm layer with a $k_v/k_h$ ratio of 1 (red curve), 0.8 (green), 0.15 (blue) and 0.02 (cyan)*

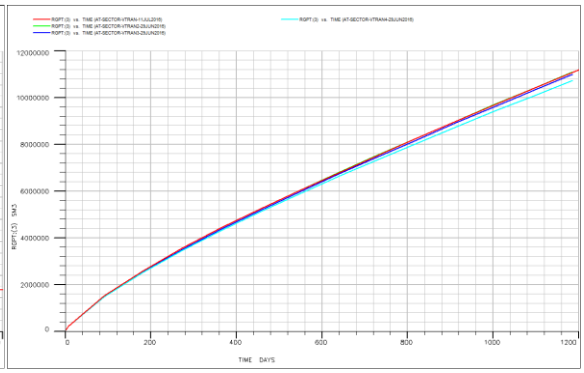

*Figure 108 sector cumulative gas production of region 2 comparison of vertical well passing through a 2m high perm layer with a $k_v/k_h$ ratio of 1 (red curve), 0.8 (green), 0.15 (blue) and 0.02 (cyan)*

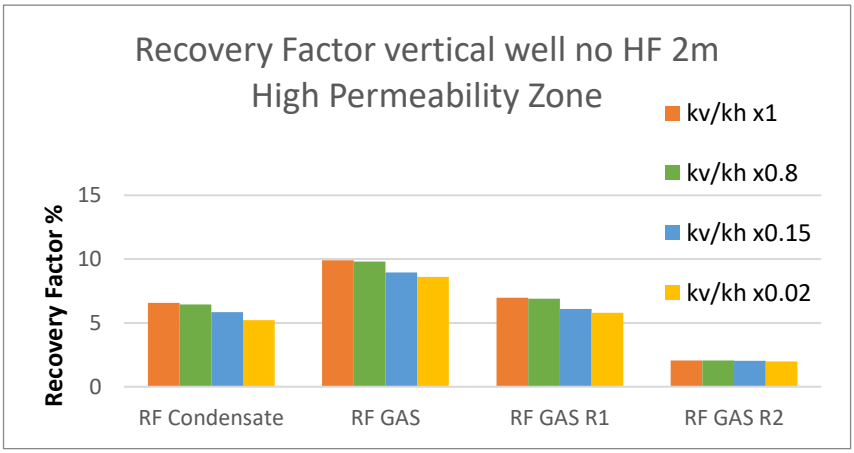


*Figure 109 Shallow vertical well passing through 2m high permeability zone recovery factor of the condensate (RF CONDENSATE), and gas from the sector (RF GAS), gas recovered from region 1 through the sector (RF GAS R1), and region 2 (RF GAS R1) comparison of $k_v/k_h$ ratios*

#### *5.3.1.3. 8m high permeability zone*

The size of the region of high permeability was increased by an additional 6m in its height (525x750x8m). This increase has an even greater effect on the recovery of the uncased vertical well. This effect is quantified in Figure 118, which shows that the increase in the size of a high permeability zone by 6m, increases the gas recovery by more than double, from 9.9 to 23.4% in the best case scenario. Condensate recovery also sees an increase, however not by the same disparity as compared to when there is no high permeability zone, from 6.5 to 7.8%. The sensitivity of recovery to vertical transmissibility also increases - the difference in the gas recovery of the whole sector from the perfect case of x1 to the pessimistic case of x0.02, now stands at 3%, up from 1% previously.

Figure 118 also shows that while region 2 appears to remains insensitive to the changing vertical transmissibility, there is a small decrease in its recovery from 2 to 1.7%.

Figure 116 & Figure 117 are cross sections of the reservoir sector cutting the wellbore along the x-axis, displaying the pressure in the blocks around the well after 1186 days (T20). For the perfect case of kv/kh x1, Figure 116 shows that apart from the blocks immediately surrounding the well, the pressure is generally homogenous across the sector at around 20bar; while for the pessimistic case of kv/kh x0.02, Figure 116 shows a pressure gradient between the upper and lower layers of the reservoir sector in terms of pressure. The high permeability zone is commanding pressure values of 90bar and the deeper the block ie. the further away from region 1 in a vertical sense, the higher the pressure. This implies that in the case of poor kv/kh, fluid is not flowing vertically and therefore more fluid is flowing towards the wellbore horizontally, depleting that region at a faster rate as indicated by the lower pressure values in the upper region, compared to the case when the vertical transmissibility is more favourable.

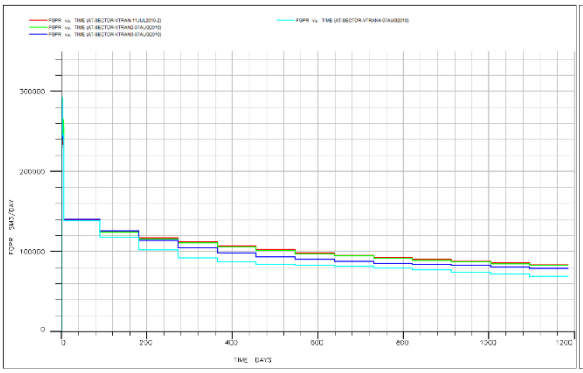


*Figure 110 sector gas production rates comparison of vertical well passing through an 8m high perm layer with a $k_v/k_h$ ratio of 1 (red curve), 0.8 (green), 0.15 (blue) and 0.02 (cyan)*

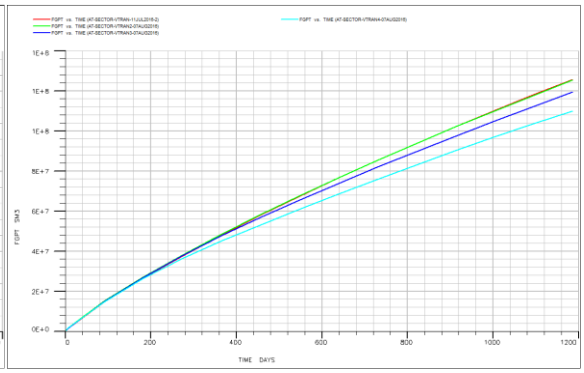


*Figure 111 sector cumulative gas production comparison of vertical well passing through an 8m high perm layer with a $k_v/k_h$ ratio of 1 (red curve), 0.8 (green), 0.15 (blue) and 0.02 (cyan)*

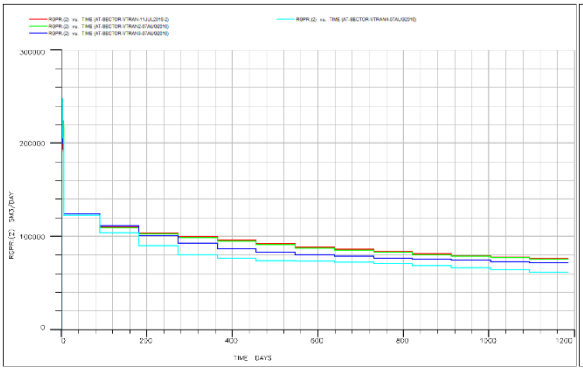

*Figure 112 gas production rates of region 1 comparison of vertical well passing through an 8m high perm layer with a $k_v/k_h$ ratio of 1 (red curve), 0.8 (green), 0.15 (blue) and 0.02 (cyan)*

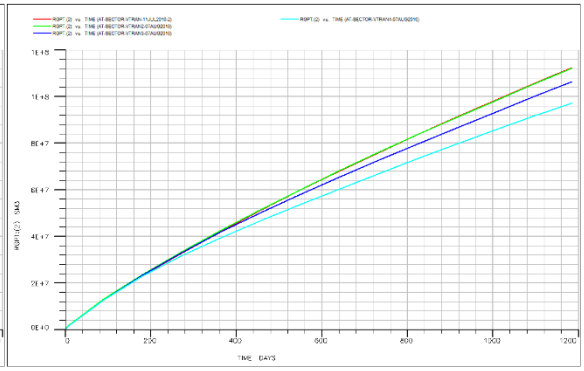

*Figure 113 sector cumulative gas production of region 1 comparison of vertical well passing through an 8m high perm layer with a $k_v/k_h$ ratio of 1 (red curve), 0.8 (green), 0.15 (blue) and 0.02 (cyan)*

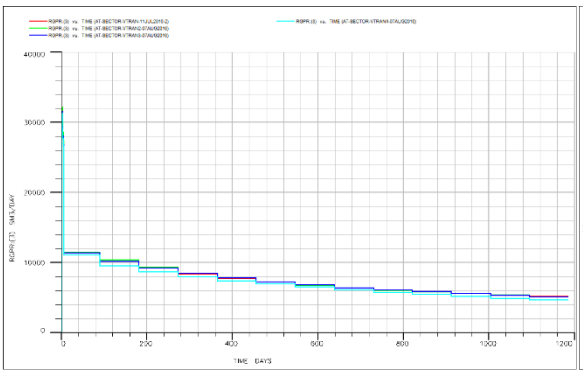

*Figure 114 gas production rates of region 2 comparison of vertical well passing through an 8m high perm layer with a $k_v/k_h$ ratio of 1 (red curve), 0.8 (green), 0.15 (blue) and 0.02 (cyan)*

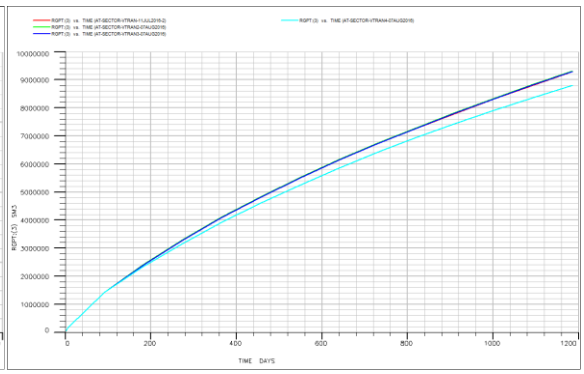

*Figure 115 sector cumulative gas production of region 2 comparison of vertical well passing through an 8m high perm layer with a $k_v/k_h$ ratio of 1 (red curve), 0.8 (green), 0.15 (blue) and 0.02 (cyan)*

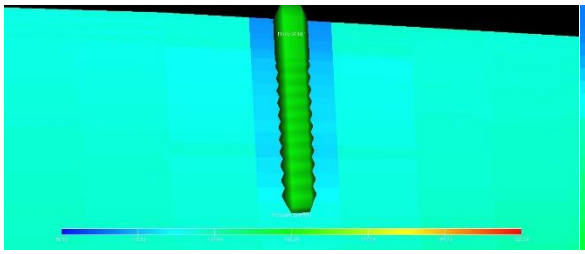

*Figure 116 Pressure distribution of $k_v/k_h$ ratio 1 at T20*

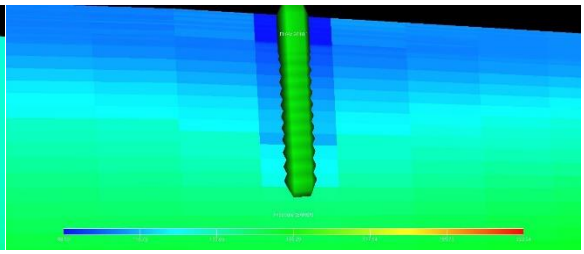


*Figure 117 Pressure distribution of $k_v/k_h$ ratio 0.02 at T20*

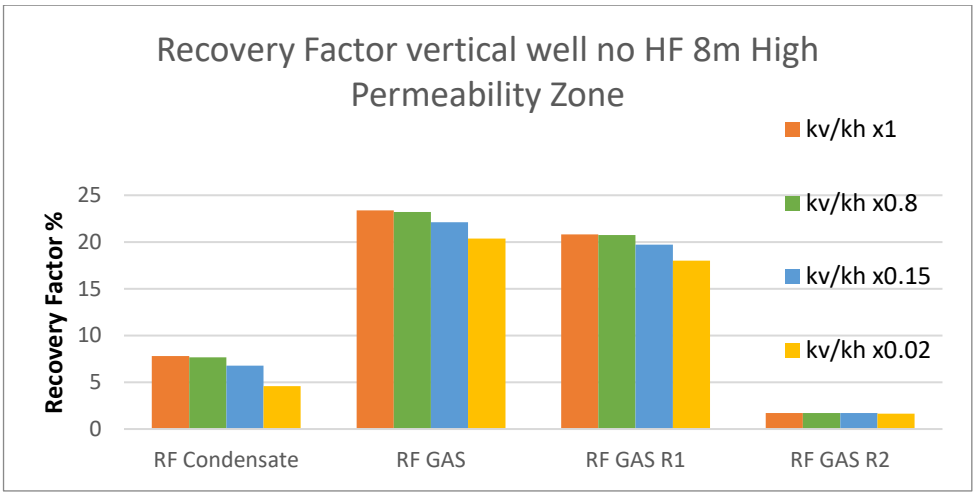


*Figure 118 shallow vertical well passing through 8m high permeability zone recovery factor of the condensate (RF CONDENSATE), and gas from the sector (RF GAS), gas recovered from region 1 through the sector (RF GAS R1), and region 2 (RF GAS R1) comparison of $k_v/k_h$ ratios*

### 5.3.2. The Case with Hydraulic fracturing

A hydraulic fracture of 20m height, 70m half length, 0.5m width, and fracture conductivity of 1000mD was added to the previous well to also determine the effect it has on the $k_v/k_h$ ratio. The reservoir conditions are identical to those of the previous scenarios.

The production was simulated, setting the maximum rate at 300 000 sm3/day, as for the previous scenario. The well stops producing when the WHP falls to 40 bara.

The principal observation from the following results is that vertical transmissibility has a much greater impact on recovery when the well is hydraulically fractured, though the presence of a region of high permeability does not further increase the sensitivity.

#### *5.3.2.1. 20/70/0.5m HF + No High Permeability Zone*

Initially the model with the hydraulic fracture was simulated without a region of high permeability.

Figure 123 shows the effect adding a hydraulic fracture to the model has on the recovery factor. Compared to the previous results from Figure 118, gas recovery increases from 3.8 to 15.2% in the best case scenario, while its sensitivity to the vertical transmissibility also increases. The difference in the gas recovery of the whole sector from the perfect case of x1 to the pessimistic case of x0.02, is 5.4%, up from 0.1%.

Figure 123 also shows there is negligible recovery coming from region 1, > 0.3%. Most of the recovery is coming from region 2, where the hydraulic fracture is located. Figure 121 & Figure 122 are cross sections of the reservoir sector cutting the wellbore along the x-axis, displaying the pressure in the blocks around the well after 1 day (T1) and 1186 days (T20), showing the pressure sink caused by the hydraulic fracture, which is acting as a high permeability zone. When there is good vertical

transmissibility, the recovery from region 2, and in turn the whole sector, increases, as there is more fluid flowing from the depths of the reservoir.

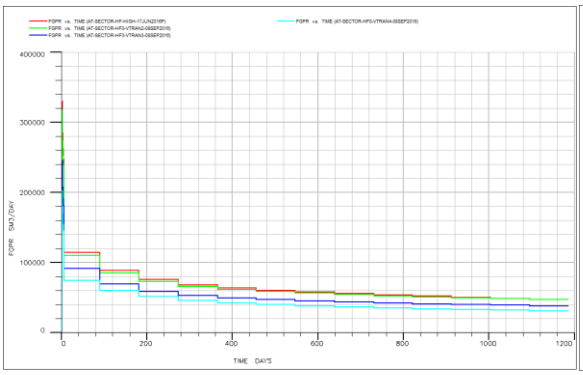

*Figure 119 sector gas production rates comparison of vertical well, with a hydraulic fracture, with a $k_v/k_h$ ratio of 1 (red curve), 0.8 (green), 0.15 (blue) and 0.02 (cyan)*

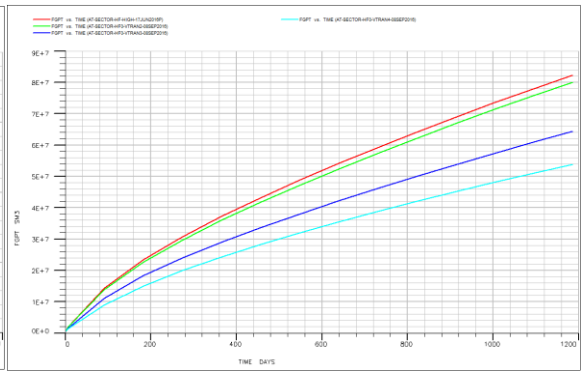

*Figure 120 sector cumulative gas production comparison of vertical well, with a hydraulic fracture, with a $k_v/k_h$ ratio of 1 (red curve), 0.8 (green), 0.15 (blue) and 0.02 (cyan)*

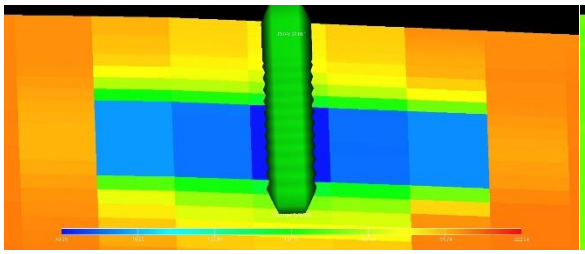

*Figure 121 Pressure distribution of $k_v/k_h$ ratio 1 at T1*

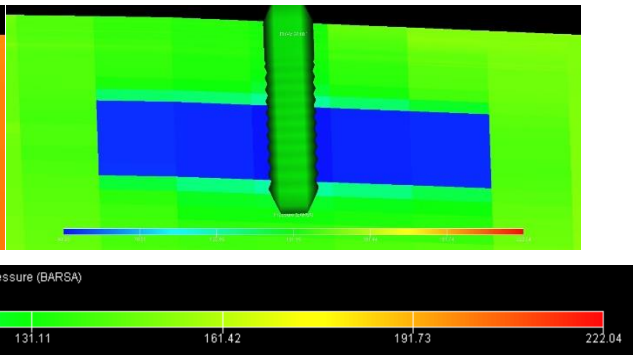


*Figure 122 Pressure distribution of $k_v/k_h$ ratio 1 at T20*

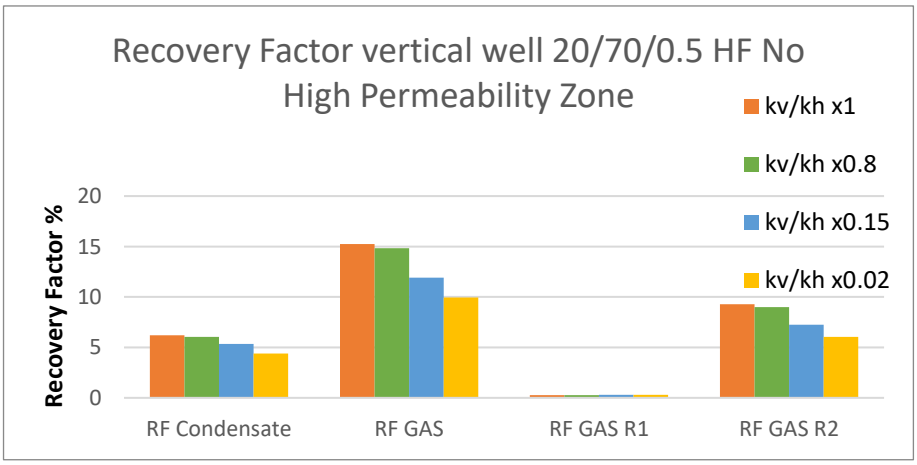


*Figure 123 Shallow vertical well with a hydraulic fracture recovery factor of the condensate (RF CONDENSATE), and gas from the sector (RF GAS), gas recovered from region 1 through the sector (RF GAS R1), and region 2 (RF GAS R1) comparison of $k_v/k_h$ ratios*

#### *5.3.2.2. 20/70/0.5m HF + 2m High Permeability Zone*

A region (525x750x2m) of high permeability was added to the model in region 1. This addition has a noticible effect on the gas and condensate recovery as shown in Figure 132, which shows a modest increase in gas recovery, from 15.3 to 17.6% in the best case scenario of vertical transmissibility. Condensate recovery is also increased from 6.2 to 7.3%. Unlike the case when there was no hydraulic fracture, the presence of a region of high permeability does not increase the sensitivity of recovery to vertical transmissibility. The difference in the gas recovery of the whole sector from the perfect case of x1 to the pessimistic case of x0.02, falls slightly to 5%.

Figure 132 also shows that region 1 is now contributing to the gas recovery with an increase up to 2.5% in the best cas scenario, while region 2 sees no real change to recovery. Conversely, the recovery of region 1, as the ratio of kv/kh is altered, does not follow the behaviour of region 2, or the whole sector. Rather than seeing a decrease in the recovery of region 1 as the kv/kh ratio drops, Figure 132 shows the opposite, that the presence of a hydraulic fracture and a high permeability zone increases recovery in the region as the vertical transmissibility falls.

The cross section of the reservoir sector cutting the wellbore along the x-axis displaying the pressure in the blocks around the well after 1186 days (T20), Figure 131 & Figure 132 confirm this. The pressure in region 1 when the model has a kv/kh ratio x0.02 is around 20bar lower than with the optimal case of kv/kh x1. As the ability of fluid to flow vertically to the hydraulic fracture in region 2 is hindered, the high permeability zone in region 1 allows more fluid to flow horizontally, and hence the increase in production in that region as the vertically transmissibility falls, Figure 127 & Figure 128. In Figure 132 which is the case of poor vertical transmissibility, it can be seen that directly below the well, the pressure is quite homogenous, while in Figure 132, a drop in pressure in the blocks direclty below implying that fluid is vacating those pores by flowing vertically against gravity in the direction of the hydraulic fracture. Figure 132 also shows that there is a greater fall in pressure, in region 2 where the hydraulic fracture is, further away horizontally from the wellbore when the vertical transmissibility is low, implying that more fluid is vacating the blocks and flowing horizontally into the wellbore. However as can be seen in Figure 127 & Figure 128 that this increase in horizontal production in region 2 is not enough to counter the loss of vertical recovery, as the production rate and cumulative total fall as the vertical transmissibility falls.

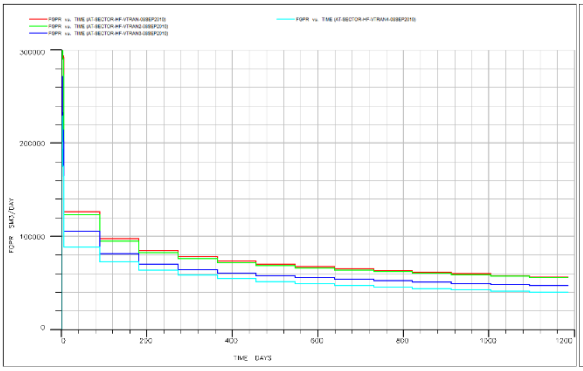

*Figure 124 sector gas production rates comparison of vertical well, with a hydraulic fracture, passing through a 2m high permeability layer with a $k_v/k_h$ ratio of 1 (red curve), 0.8 (green), 0.15 (blue) and 0.02 (cyan)*

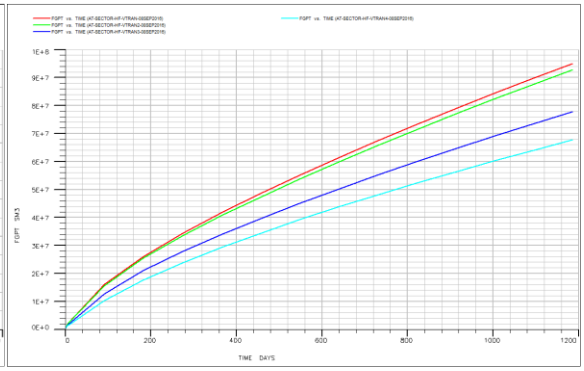

*Figure 125 sector cumulative gas production comparison of vertical well, with a hydraulic fracture, passing through a 2m high permeability layer with a $k_v/k_h$ ratio of 1 (red curve), 0.8 (green), 0.15 (blue) and 0.02 (cyan)*

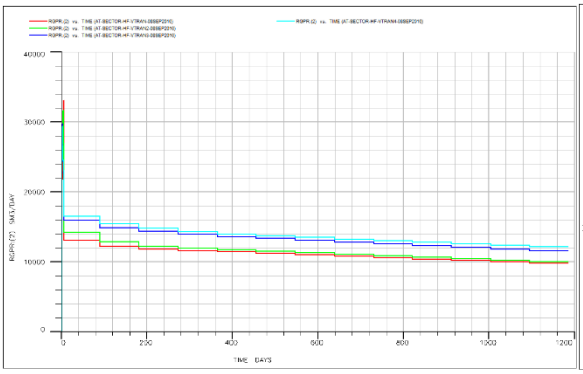

*Figure 126 gas production rates of region 1 comparison of vertical well, with a hydraulic fracture, passing through a 2m high permeability layer with a $k_v/k_h$ ratio of 1 (red curve), 0.8 (green), 0.15 (blue) and 0.02 (cyan)*

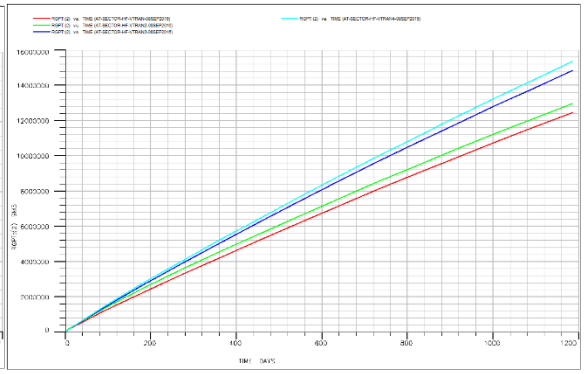

*Figure 127 sector cumulative gas production of region 1 comparison of vertical well, with a hydraulic fracture, passing through a 2m high permeability layer with a $k_v/k_h$ ratio of 1 (red curve), 0.8 (green), 0.15 (blue) and 0.02 (cyan)*

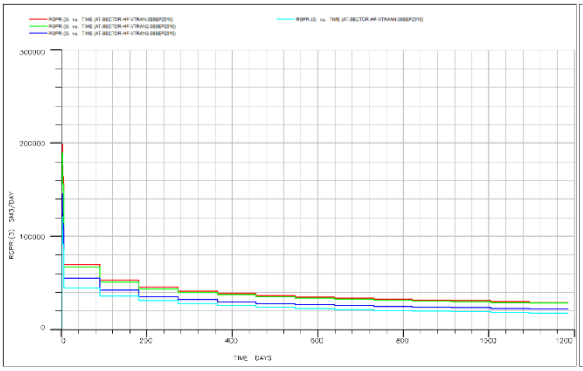

*Figure 128 gas production rates of region 2 comparison of vertical well, with a hydraulic fracture, passing through a 2m high permeability layer with a $k_v/k_h$ ratio of 1 (red curve), 0.8 (green), 0.15 (blue) and 0.02 (cyan)*

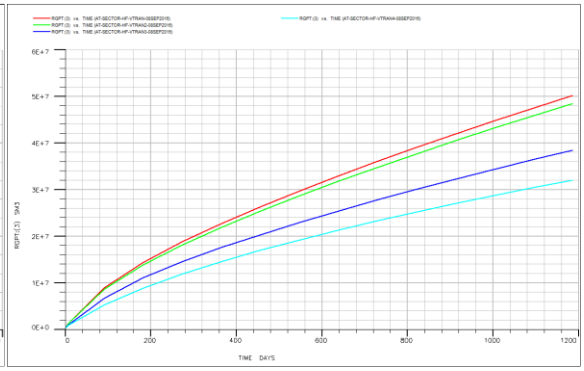

*Figure 129 sector cumulative gas production of region 2 comparison of vertical well, with a hydraulic fracture, passing through a 2m high permeability layer with a $k_v/k_h$ ratio of 1 (red curve), 0.8 (green), 0.15 (blue) and 0.02 (cyan)*

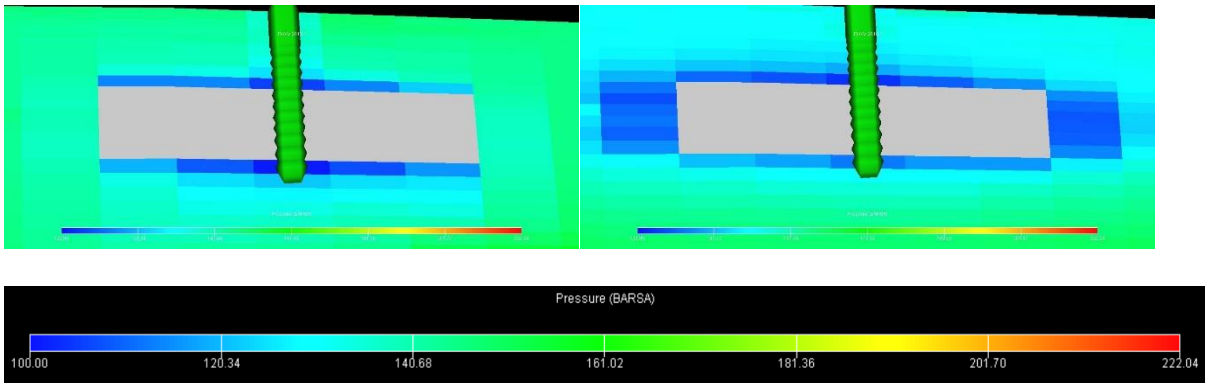


*Figure 130 Pressure distribution of $k_v/k_h$ ratio 1 at T20*

*Figure 131 Pressure distribution of $k_v/k_h$ ratio 0.02 at T20*

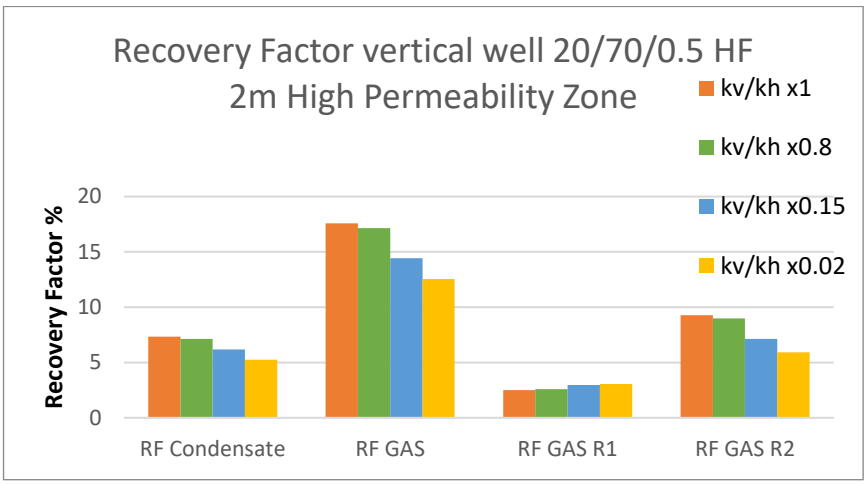


*Figure 132 Shallow vertical well with a hydraulic fracture passing through 2m high permeability zone recovery factor of the condensate (RF CONDENSATE), and gas from the sector (RF GAS), gas recovered from region 1 through the sector (RF GAS R1), and region 2 (RF GAS R1) comparison of $k_v/k_h$ ratios*

#### *5.3.2.3. 20/70/0.5m HF + 8m High Permeability Zone*

The size of the region of high permeability was increased by an additional 6m in its height (525x750x8m). This increase in turn, increases the recovery of the hydraulically fractured, uncased vertical well, which is quantified in Figure 141, showing an increase in the gas recovery from the sector, from 17.6, when the high permeability zone was 2m high, to 24.2%, in the best case scenario. Condensate recovery sees a small fall of 0.1%. The sensitivity of recovery to vertical transmissibility remains the same with a difference of 5%.

Figure 141 also shows an increase in gas recovery for region 1, from 2.5 to 9.9% in the optimal case of vertical transmissibility, surpassing recovery for region 2, which has seen a small drop of around 0.5%. Additionaly, region 1 still appears to follow the previously seen trend of increasing recovery with

decreasing vertical transmissibility, the sensitivity to this change is diminished to the point where it is almost negligible.

Figure 135 & Figure 136 are cross sections of the reservoir sector cutting the wellbore along the x-axis displaying the pressure in the blocks around the well after 1186 days (T20) for an optimal case of kv/kh x1 versus a pessimistic case of 0.02. The optimal case sees the greatest drop in pressure of around 90 bar in the blocks immediately above and below the hydraulic fracture. The pressure gradually increases, the deeper the block gets from the wellbore, to the value of region 1, where the high permeability zone is located, of around 120 bar. In the pessimistic case of x0.02 there is a clear distinction between the pressures above and below the hydraulic fracture. This bottom layer is largely homogenous registering a pressure value of ~160bar, while the upper layer where region 1 is located is ~120bar.

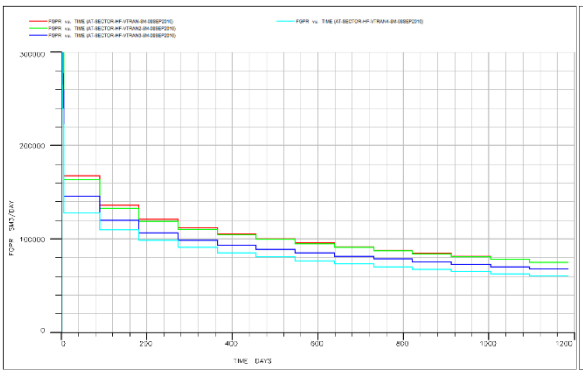

*Figure 133 sector gas production rates comparison of vertical well, with a hydraulic fracture, passing through an 8m high permeability layer with a $k_v/k_h$ ratio of 1 (red curve), 0.8 (green), 0.15 (blue) and 0.02 (cyan)*

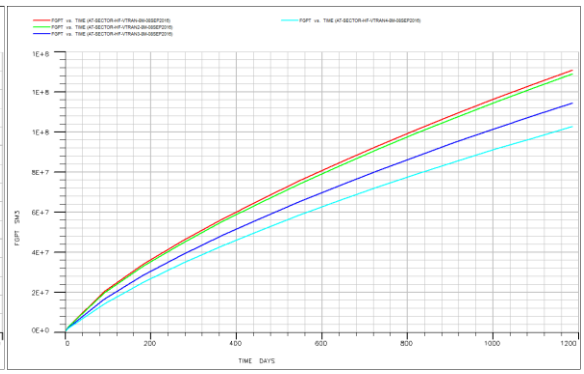

*Figure 134 sector cumulative gas production comparison of vertical well, with a hydraulic fracture, passing through an 8m high permeability layer with a $k_v/k_h$ ratio of 1 (red curve), 0.8 (green), 0.15 (blue) and 0.02 (cyan)*

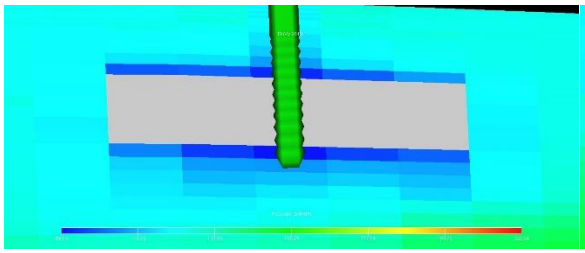

*Figure 135 Pressure distribution of $k_v/k_h$ ratio 1 at T20*

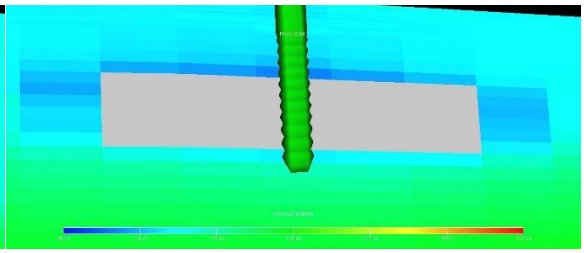

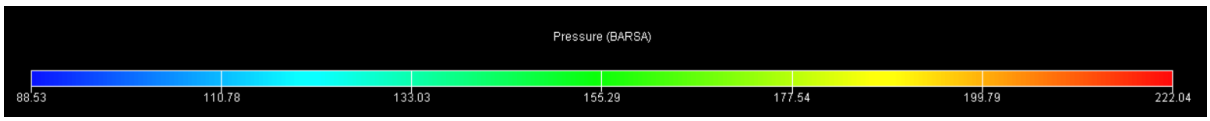


*Figure 136 Pressure distribution of $k_v/k_h$ ratio 0.02 at T20*

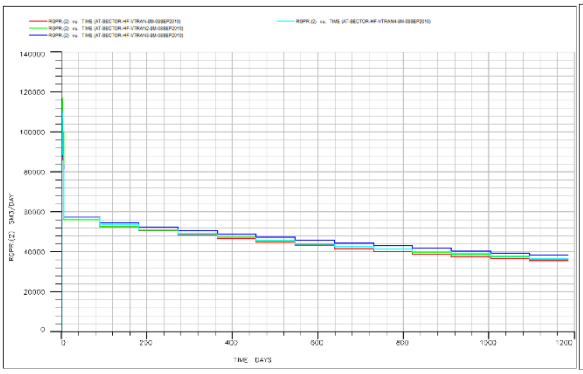

*Figure 137 gas production rates of region 1 comparison of vertical well, with a hydraulic fracture, passing through an 8m high permeability layer with a $k_v/k_h$ ratio of 1 (red curve), 0.8 (green), 0.15 (blue) and 0.02 (cyan)*

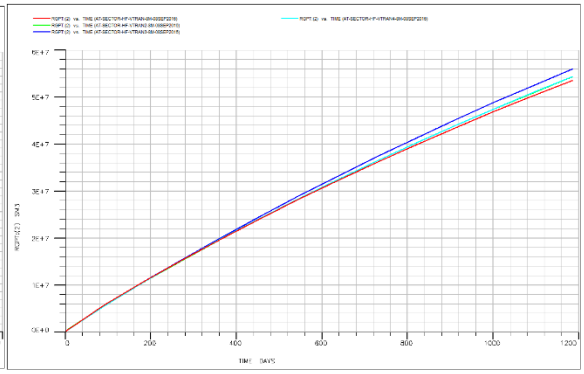

*Figure 138 sector cumulative gas production of region 1 comparison of vertical well, with a hydraulic fracture, passing through an 8m high permeability layer with a $k_v/k_h$ ratio of 1 (red curve), 0.8 (green), 0.15 (blue) and 0.02 (cyan)*

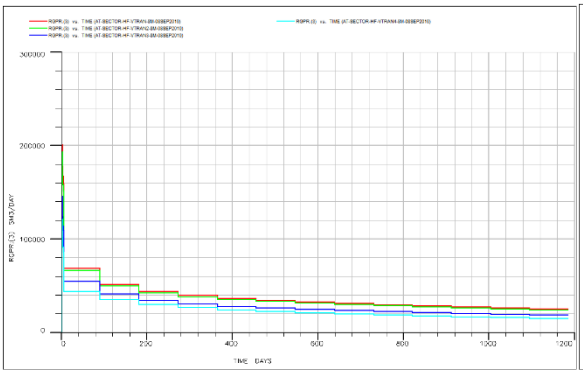

*Figure 139 gas production rates of region 2 comparison of vertical well, with a hydraulic fracture, passing through an 8m high permeability layer with a $k_v/k_h$ ratio of 1 (red curve), 0.8 (green), 0.15 (blue) and 0.02 (cyan)*

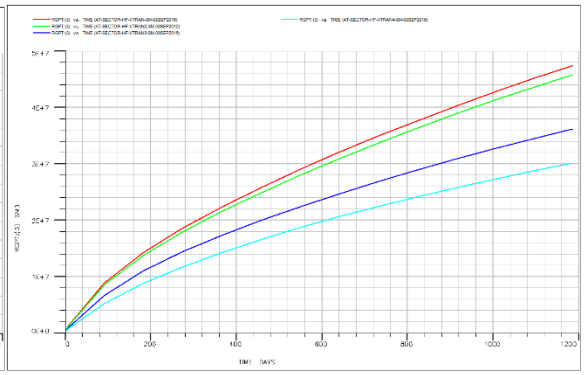

*Figure 140 cumulative gas production of region 2 comparison of vertical well, with a hydraulic fracture, passing through an 8m high permeability layer with a $k_v/k_h$ ratio of 1 (red curve), 0.8 (green), 0.15 (blue) and 0.02 (cyan)*

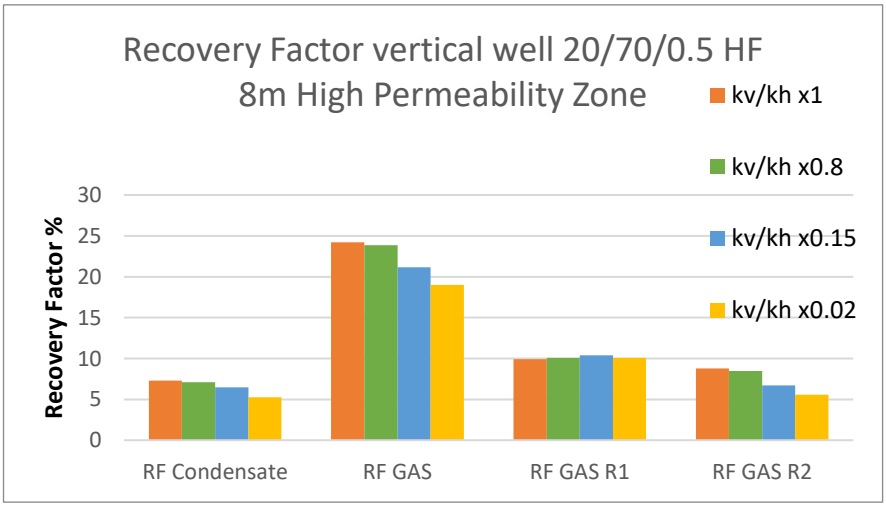


*Figure 141 Shallow vertical well with a hydraulic fracture passing through 8m high permeability zone recovery factor of the condensate (RF CONDENSATE), and gas from the sector (RF GAS), gas recovered from region 1 through the sector (RF GAS R1), and region 2 (RF GAS R1) comparison of $k_v/k_h$ ratios*

## 5.4. Impact of Fracture Conductivity

This part of the project assesses the effect altering the hydraulic fracture conductivity has on well productivity and total recovery.

The model consisted of a shallow vertical well cased above a hydraulic fracture of 20m height, 70m half-length, and 0.5m width, but with the conductivity modified. To avoid crossflow, the well was cased above the hydraulic fracture. So as not to complicate the model further by altering the geometry of sub-cells in the HF's path, the HF width remained constant and only the value of the permeability within the HF was altered using the Multiplier keyword in the GRID section of the model. Three cases were looked at:

| Case | Fracture Conductivity |
|---|---|
| 1 Optimistic | 1000 |
| 2 Realistic | 224 |
| 3 Pessimistic | 100 |

The principal observation from the following results is that changing the fracture conductivity does impact production, the higher the conductivity, the higher the recovery.

### 5.4.1. No high permeability region

The recovery was initially simulated without a region of high permeability in the model. The reservoir conditions are identical to those of the previous scenarios.

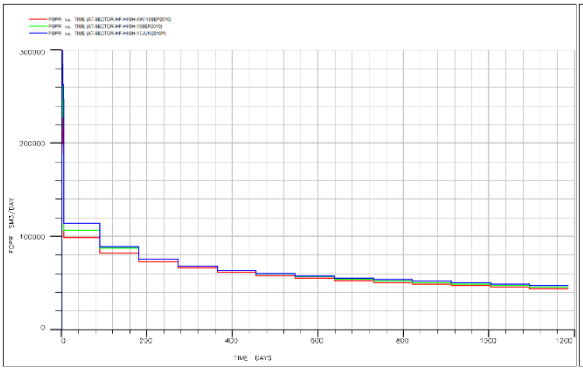

*Figure 142 sector gas production rates comparison of vertical well with a 20m high, 70m half-length, 0.5m wide hydraulic fracture, with a fracture conductivity of 1000 mD.m (blue curve), 224 mD.m (green), 100 mD.m (red)*

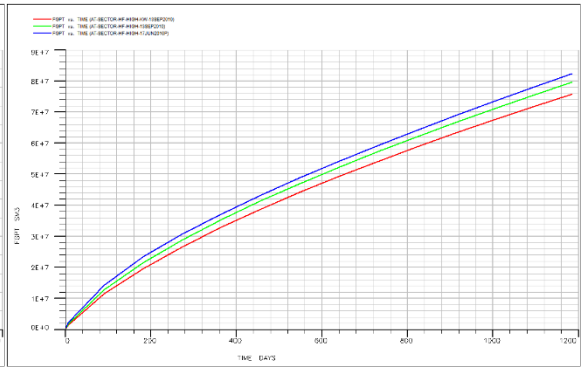

*Figure 143 sector cumulative gas production comparison of vertical well with a 20m high, 70m half-length, 0.5m wide hydraulic fracture, with a fracture conductivity of 1000 mD.m (blue curve), 224 mD.m (green), 100 mD.m (red)*

Figure 142 & Figure 143 show how the larger the fracture conductivity is, the more gas that is recovered; however, the difference is small and is only felt within the first 200 days, before their rates converge.

### 5.4.2. 2m high permeability region

A 2m high permeability zone was then added to the model to see the effect this would have on the three cases of HF conductivity.

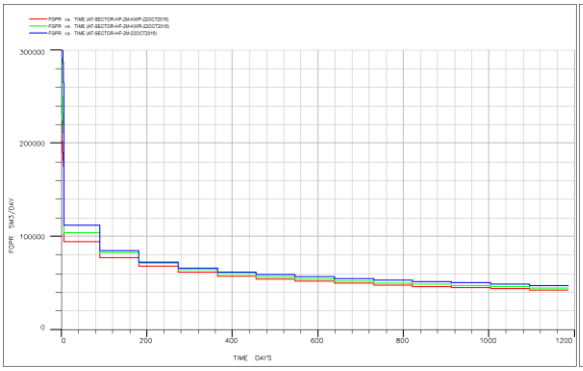

*Figure 144 sector gas production rates comparison of vertical well passing through a 2m high permeability layer, with a 20m high, 70m half-length, 0.5m wide hydraulic fracture, with a fracture conductivity of 1000 mD.m (blue curve), 224 mD.m (green), 100 mD.m (red)*

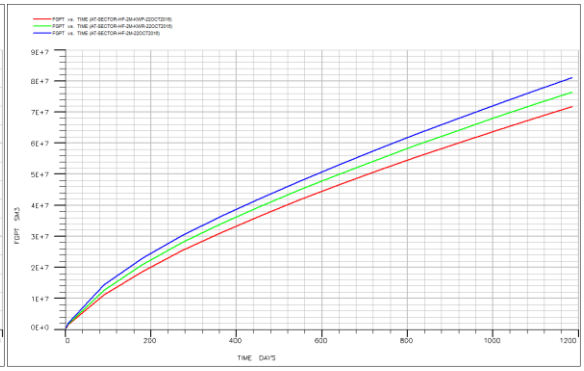

*Figure 145 sector cumulative gas production comparison of vertical well passing through a 2m high permeability layer, with a 20m high, 70m half-length, 0.5m wide hydraulic fracture, with a fracture conductivity of 1000 mD.m (blue curve), 224 mD.m (green), 100 mD.m (red)*

The addition of the high permeability zone maintains the same behaviour: the larger the fracture conductivity, the more gas recovered; however, the difference between gas production rates increases slightly, meaning that the amount recovered in Case 1 is larger than Case 2.

### 5.4.3. 8m high permeability region

An 8m high permeability zone was then added to the model to see the effect this would have on the three cases of HF conductivity

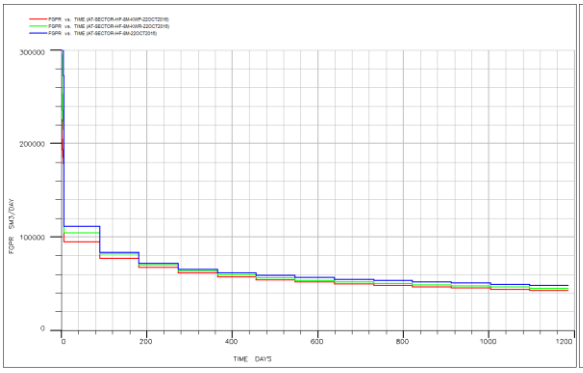

*Figure 146 sector gas production rates comparison of vertical well passing through a 8m high permeability layer, with a 20m high, 70m half-length, 0.5m wide hydraulic fracture, with a fracture conductivity of 1000 mD.m (blue curve), 224 mD.m (green), 100 mD.m (red)*

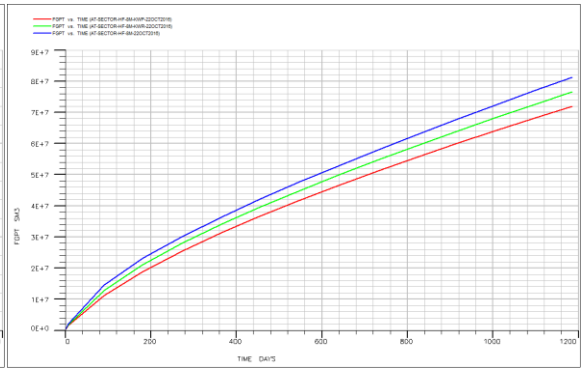

*Figure 147 sector cumulative gas production comparison of vertical well passing through a 8m high permeability layer, with a 20m high, 70m half-length, 0.5m wide hydraulic fracture, with a fracture conductivity of 1000 mD.m (blue curve), 224 mD.m (green), 100 mD.m (red)*

The increase in size of the high permeability zone maintains the same behaviour yet has no discernible differences compared to the cases with a smaller high permeability zone.

## 5.5. Hydraulic fracture height comparison

This part of the project assesses the effect hydraulic fracture height has on well productivity and total recovery.

The model consisted of a shallow uncased vertical well with a hydraulic fracture of half-length 70m, 0.5m width and fracture conductivity of 1000md.m, but with the height modified. Three cases were looked at:

| Case | HF height (m) |
|---|---|
| 1 | 20 |
| 2 | 40 |
| 3 | 80 |

The principal observation from the following results is that by increasing the height of the hydraulic fracture, the greater the value of production recovered.

### 5.5.1. No high permeability region

The model was simulated initially without a region of high permeability. The reservoir conditions are identical to those of the previous scenarios.

Figure 148 & Figure 149 show that the increase in size of the hydraulic fracture has the effect of substantially increasing the gas recovery of the whole sector.

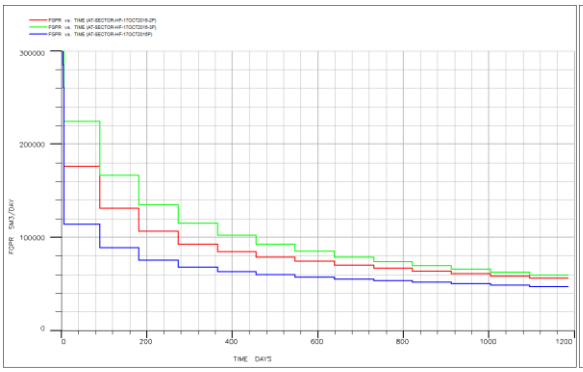

*Figure 148 sector cumulative gas production comparison of HF height 20m (blue curve), 40m (red), and 80m (green)*

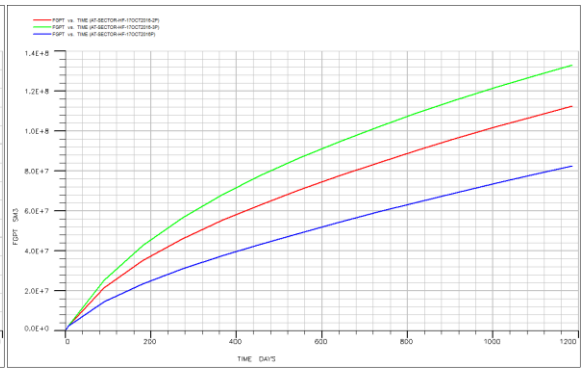

*Figure 149 sector cumulative gas production of HF height 20m (blue curve), 40m (red), and 80m (green)*

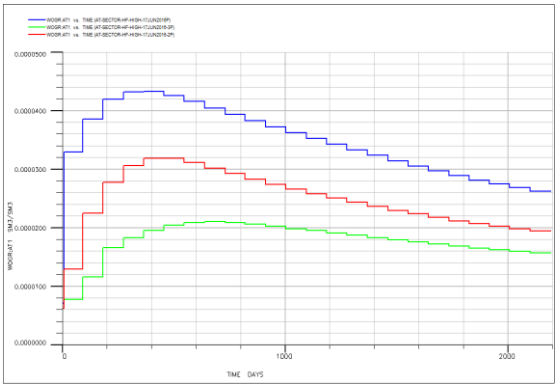

*Figure 150 CGR comparison of vertical well with HF 70m half-length with 20m height (blue curve), 40m (red) and 80m (green)*

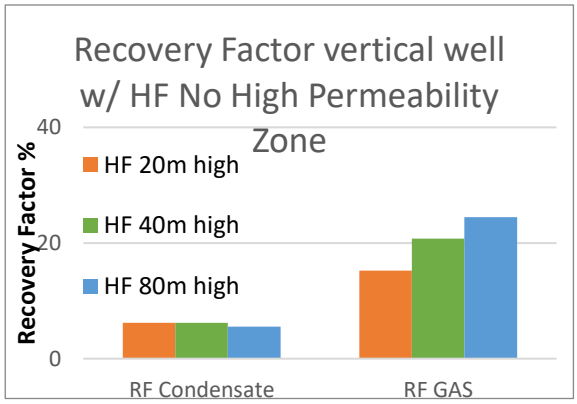


*Figure 151 Shallow vertical well with a 70m half-length HF recovery factor of the condensate (RF CONDENSATE), and gas from the sector (RF GAS) comparison of HF heights*

Figure 150 shows that as the hydraulic fracture height is increased, so the initial and max CGR values become smaller. There is also a small rate decrease in the fall from the max value with increasing HF height.

Figure 151 shows that increasing HF height results in the recovery factor of the gas increasing, however there is a small drop in the recovery factor of the condensate, suggesting that more condensate is dropping out from the gas in the reservoir.

### 5.5.2. 2m high permeability region

A 2m high permeability zone was then added to the model to see the effect this would have on the three cases of HF height.

Figure 152 & Figure 153 show that by having a high permeability zone, the increase in the gas recovery with the increase in size of the hydraulic fracture is not affected.

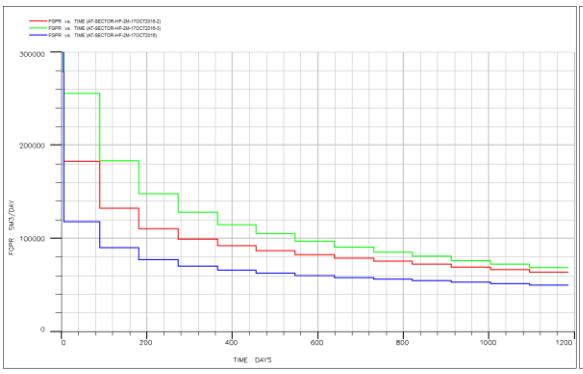


*Figure 152 sector cumulative gas production comparison of a vertical well passing through a 2m high permeability zone, comparing the HF height 20m (blue curve), 40m (red), and 80m (green)*

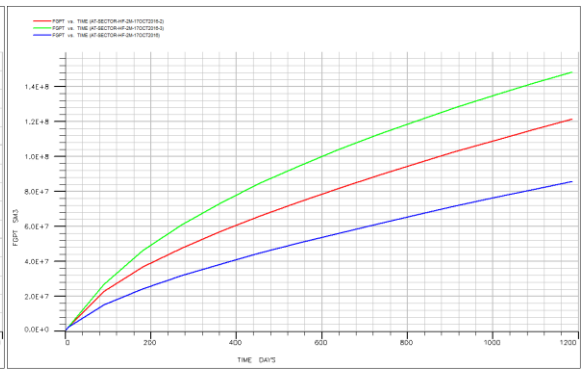


*Figure 153 sector cumulative gas production of a vertical well passing through a 2m high permeability zone, comparing the HF height 20m (blue curve), 40m (red), and 80m (green)*

Figure 154 shows that with the introduction of a high permeability layer (2m) there is an increase in the initial and max CGR values in all three cases. However, there is no alteration in the behaviour of the CGR over time.

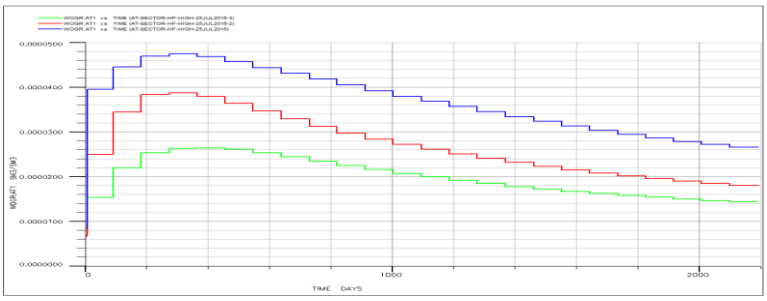


*Figure 154 CGR comparison of vertical well passing through a 2m high permeability layer with HF 70m half-length with 20m height (blue curve), 40m (red) and 80m (green)*

Figure 155 shows that despite the fact that case 3 now overlaps into region 1 by one block, the gas recovery increase remains constant with case 2, by 5%. However, case 2 is now producing more than case 1. The high permeability region has a small effect on the condensate recovery, increasing by 0.5% in all three cases, however, the trend of decreasing recovery with increasing HF height remains.

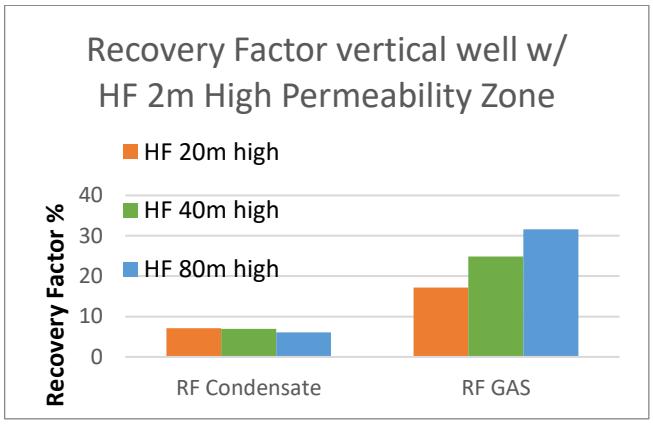


*Figure 155 Shallow vertical well with a 70m half-length HF passing through a 2m high permeability zone recovery factor of the condensate (RF CONDENSATE), and gas from the sector (RF GAS) comparison of HF heights*

### 5.5.3. 8m high permeability region

The high permeability zone size was then increased to 8m within the model to see the effect this would have on the three cases of HF height.

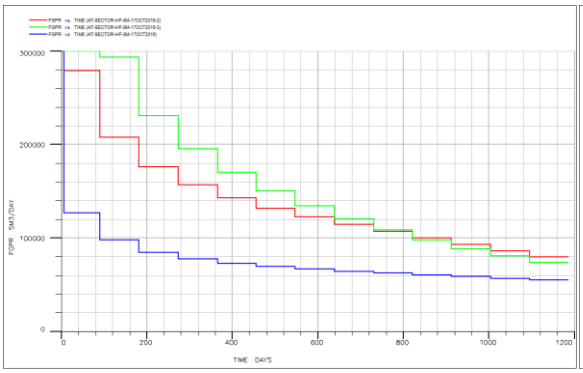

*Figure 156 sector cumulative gas production comparison of a vertical well passing through an 8m high permeability zone, comparing the HF height 20m (blue curve), 40m (red), and 80m (green)*

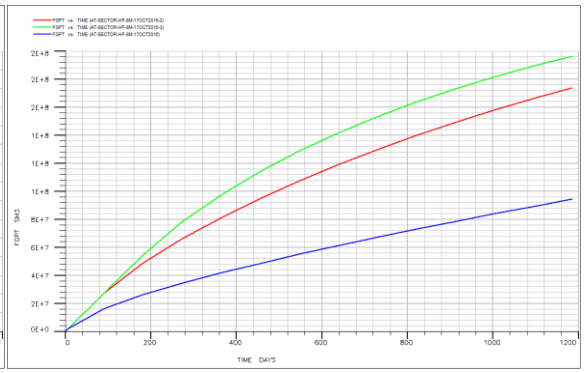

*Figure 157 sector cumulative gas production of a vertical well passing through an 8m high permeability zone, comparing the HF height 20m (blue curve), 40m (red), and 80m (green)*

Figure 156 & Figure 157 shows that the increase in size of the hydraulic fracture has the effect of substantially increasing the gas recovery to the point where in case 3 it can be seen that the flow rate of 300000 $sm^3$/day is maintained for around 80 days.

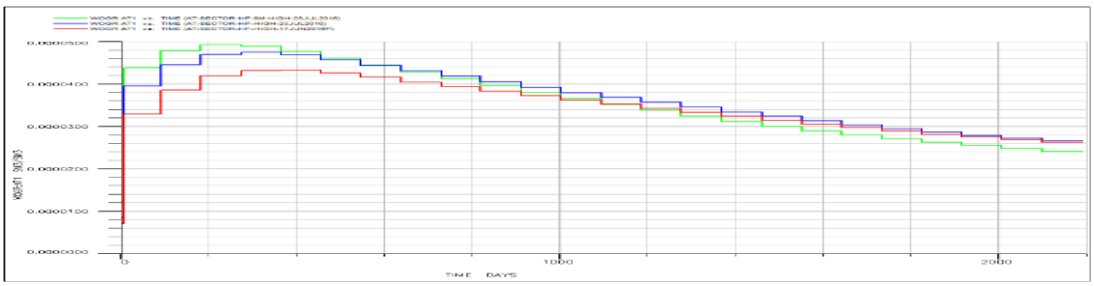

*Figure 158 CGR comparison of vertical well with HF 70m half-length with 20m height passing through 0m high permeability zone (red curve), 2m (blue) and 8m (green)*

Figure 158 shows how after 2200 days a 2m high permeability, green curve, zone reaches the same value as the case with no high permeability zone, red curve. However, the green curve for the 8m perm zone, while it has a greater max CGR value, falls below the CGR value of the other two.

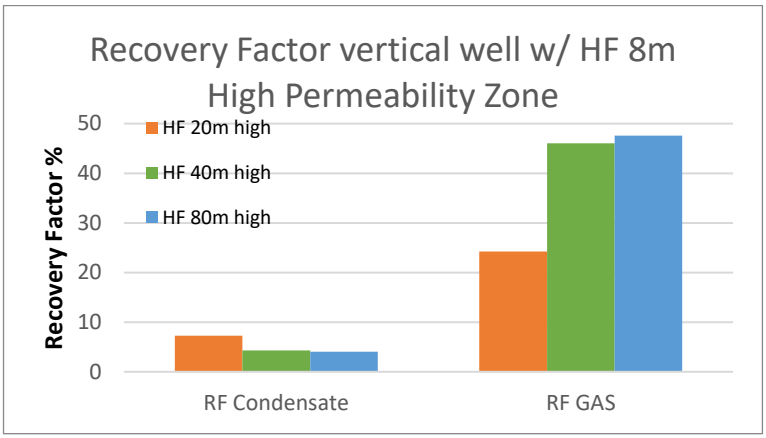


*Figure 159 Shallow vertical well with a 70m half-length HF passing through an 8m high permeability zone recovery factor of the condensate (RF CONDENSATE), and gas from the sector (RF GAS) comparison of HF heights*

Figure 159 shows that while the larger high permeability region has a minimal effect on the condensate recovery for case 1, there is a fall of more than 2% in the recovery of the other two HF heights, which in addition see negligible difference between them. The gas recovery for case 2 has massively increasded, almost doubling in comparison to case 1, while the difference in the recovery factor values for case 2 and 3 has been reduced to less than 1.5%.

## 5.6. Impact of Hydraulic fracture length

This part of the project assesses the effect increasing the hydraulic fracture length has on well productivity and total recovery.

The model consisted of a shallow vertical well with a hydraulic fracture of varying height, 0.5m width and fracture conductivity of 1000md.m, but with the half-length modified. Three cases were looked at:

| Case | HF half-length (m) |
|---|---|
| 1 | 70 |
| 2 | 100 |
| 3 | 140 |

The principal observation from the following results is that by increasing the half-length of the hydraulic fracture, the greater the value of production recovered.

### 5.6.1. No high permeability region

The model was simulated initially without a region of high permeability. The reservoir conditions are identical to those of the previous scenarios.

#### 5.6.1.1. 20m height HF

The hydraulic fracture height was set at 20m in the model, while the effect altering the fracture half-length has on recovery was recorded. The results of which show that the increase in length of the hydraulic fracture has the effect of substantially increasing the gas recovery of the whole sector.

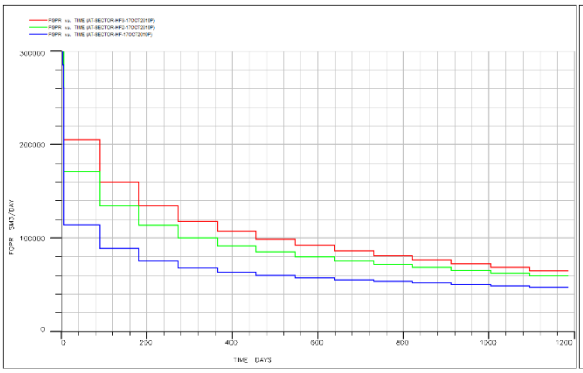

*Figure 160 sector cumulative gas production comparison of vertical with an 20m high 0.5m wide hydraulic fracture, with a 70m half-length (blue curve), 100m (green), 140m (red)*

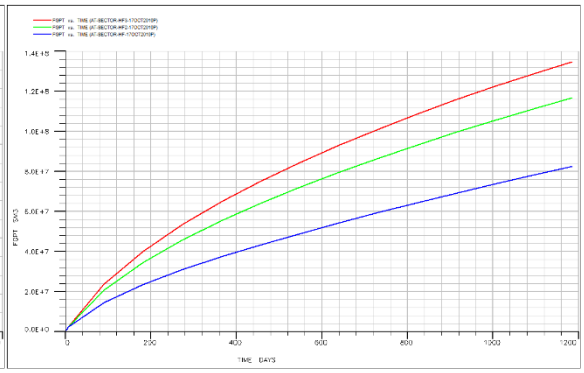

*Figure 161 sector cumulative gas production comparison of vertical well with an 20m high 0.5m wide hydraulic fracture, with a 70m half-length (blue curve), 100m (green), 140m (red)*

#### 5.6.1.2. 40m height HF

The hydraulic fracture height was set at 40m in the model. The increase in HF height maintains the same behaviour: the larger the fracture half-length, the more gas recovered. However, while it can be seen in Figure 162, that the gas production rate increases for all cases and Case 3 especially maintains the maximum set production rate of 300 000 $sm^3$/day for up to 80 days, there is a greater fall back to the same production rate of ~60 000 $sm^3$/day after 1200 days.

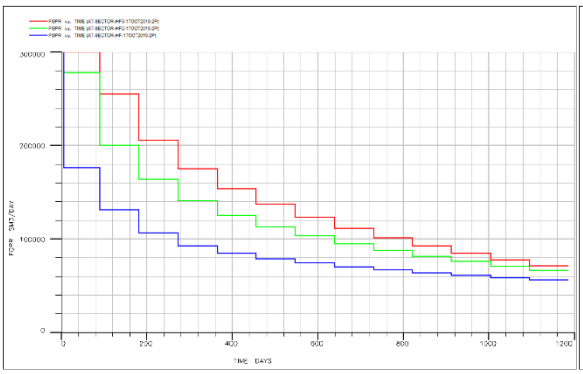

*Figure 162 sector cumulative gas production comparison of a vertical well with an 40m high 0.5m wide hydraulic fracture, with a 70m half-length (blue curve), 100m (green), 140m (red)*

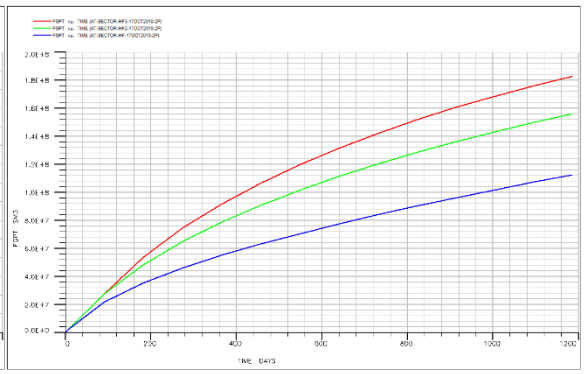

*Figure 163 sector cumulative gas production comparison of a vertical well with an 40m high 0.5m wide hydraulic fracture, with a 70m half-length (blue curve), 100m (green), 140m (red)*

#### 5.6.1.3. 80m height HF

The hydraulic fracture height was set at 80m in the model. The increase in HF height maintains the same behaviour: the larger the fracture half-length, the more gas recovered. Figure 164, shows that

while the gas production rate again falls to ~60 000 $sm^3$/day after 1200 days, the maximum set production rate of 300 000 $sm^3$/day is maintained for longer, 180 and 450 days for case 2 and 3 respectively.

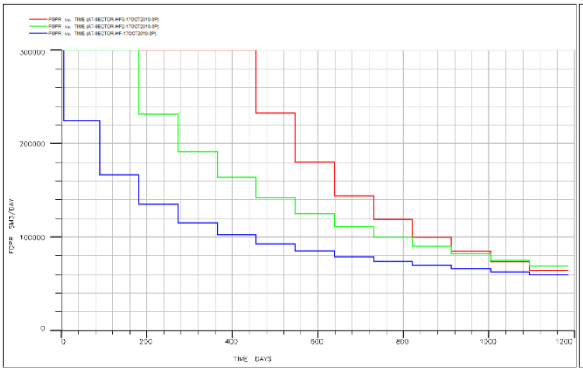

*Figure 164 sector cumulative gas production comparison of a vertical well with an 80m high 0.5m wide hydraulic fracture, with a 70m half-length (blue curve), 100m (green), 140m (red)*

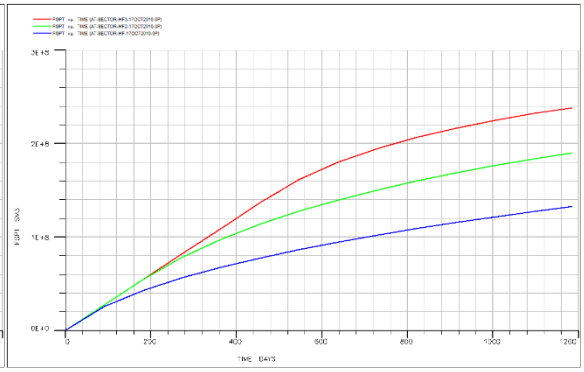

*Figure 165 sector cumulative gas production comparison of a vertical well with an 80m high 0.5m wide hydraulic fracture, with a 70m half-length (blue curve), 100m (green), 140m (red)*

### 5.6.2. 2m high permeability region

A 2m high permeability zone was then added to the model to see the effect this would have on the three cases of HF half-length.

#### *5.6.2.1. 20m height HF*

The addition of a high permeability zone makes no change to the previously noted behaviour of increased production, the greater the hydraulic fracture half-length. It also appears that the increase in amount recovered is very small compared to when there is no high permeability zone.

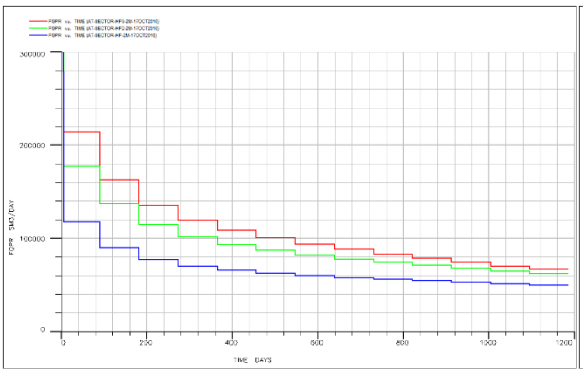

*Figure 166 sector cumulative gas production comparison of vertical well passing through a 2m high permeability zone with an 20m high 0.5m wide hydraulic fracture, with a 70m half-length (blue curve), 100m (green), 140m (red)*

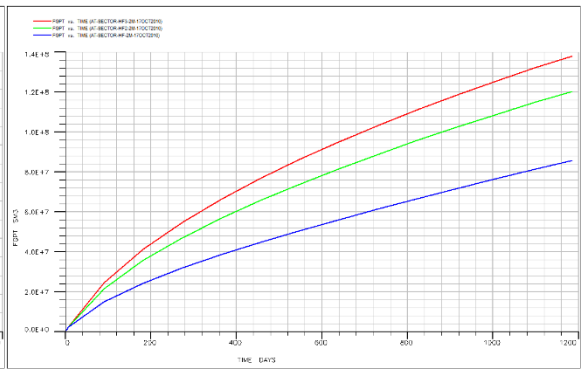

*Figure 167 sector cumulative gas production comparison of vertical well passing through a 2m high permeability zone with an 20m high 0.5m wide hydraulic fracture, with a 70m half-length (blue curve), 100m (green), 140m (red)*

#### 5.6.2.2. 40m height HF

Comparing Figure 162 with Figure 168, shows that the high permeability zone increases the recovery but only by a small margin, meaning that the uncertainty over the size of the high permeability zone will ultimately only have a small impact on recovery.

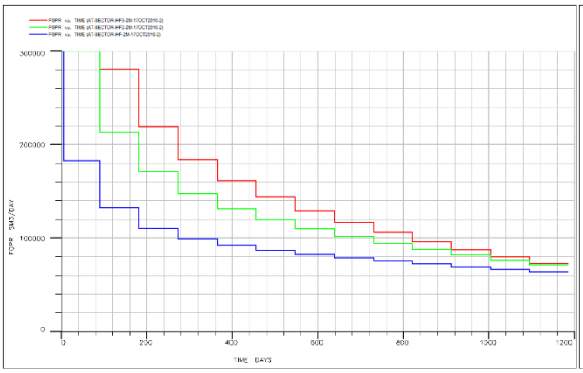

*Figure 168 sector cumulative gas production comparison of vertical well passing through a 2m high permeability zone with an 40m high 0.5m wide hydraulic fracture, with a 70m half-length (blue curve), 100m (green), 140m (red)*

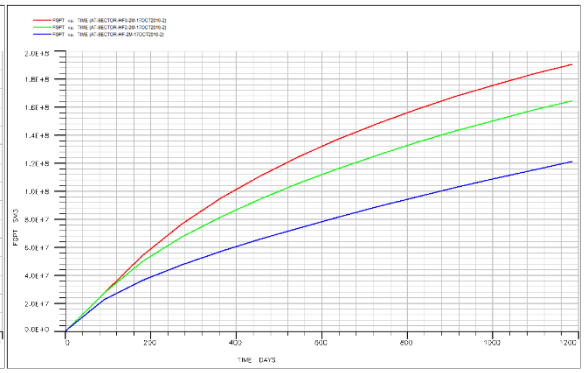

*Figure 169 sector cumulative gas production comparison of vertical well passing through a 2m high permeability zone with an 40m high 0.5m wide hydraulic fracture, with a 70m half-length (blue curve), 100m (green), 140m (red)*

#### 5.6.2.3. 80m height HF

Again, a small increase in recovery is registered but the behaviour of the gas production remains the same.

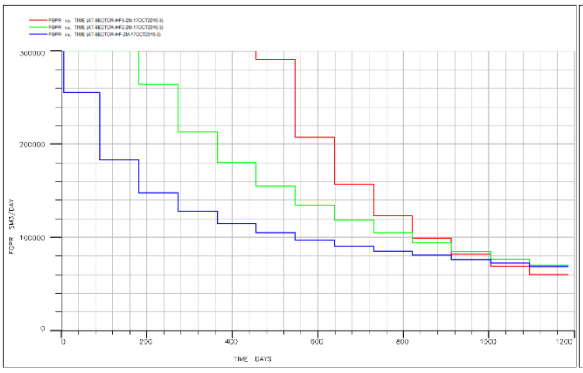

*Figure 170 sector cumulative gas production comparison of vertical well passing through a 2m high permeability zone with an 80m high 0.5m wide hydraulic fracture, with a 70m half-length (blue curve), 100m (green), 140m (red)*

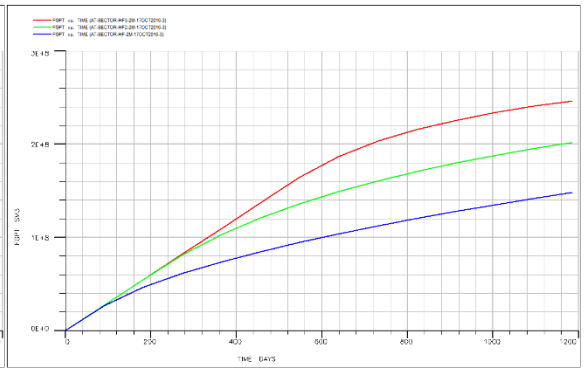

*Figure 171 sector cumulative gas production comparison of vertical well passing through a 2m high permeability zone with an 80m high 0.5m wide hydraulic fracture, with a 70m half-length (blue curve), 100m (green), 140m (red)*

## 5.7. Hydraulic Fracture Configuration Comparison

The graphs below are of the cumulative gas productions of all the HF variations. Figure 172 has no high perm zone and shows that the 140m long 80m high HF (orange curve) far exceeds all the other variations of HF in terms of total production. However, Figure 173 which has an 8m high perm zone, shows that the 140m long 80m high HF maintains the same production rate as before but for longer period, lasting an extra 100 days. This can be seen in more detail in Figure 175.

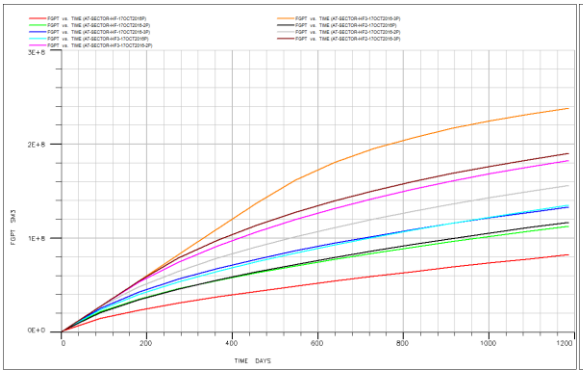

*Figure 172 sector cumulative gas production comparison of vertical well passing through no high permeability zone with HF configurations from 20m high 70m half-length (red curve) to 80m high 140m half-length (orange curve)*

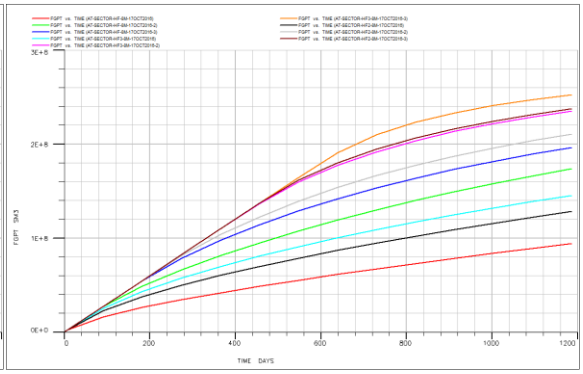

*Figure 173 sector cumulative gas production comparison of vertical well passing through an 8m high permeability zone with HF configurations from 20m high 70m half-length (red curve) to 80m high 140m half-length (orange curve)*

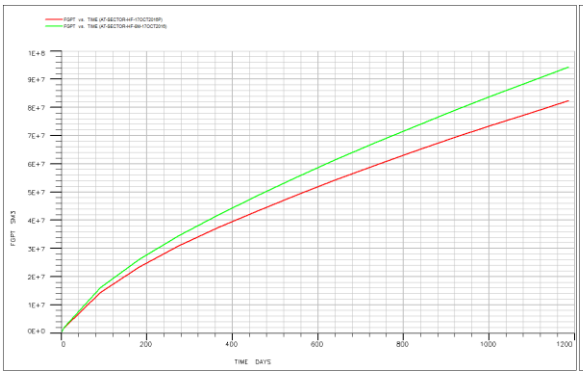

*Figure 174 cumulative gas production comparison of vertical well, with a 20m high 70m half-length hydraulic fracture, passing through no high permeability zone (red curve), and an 8m zone (green)*

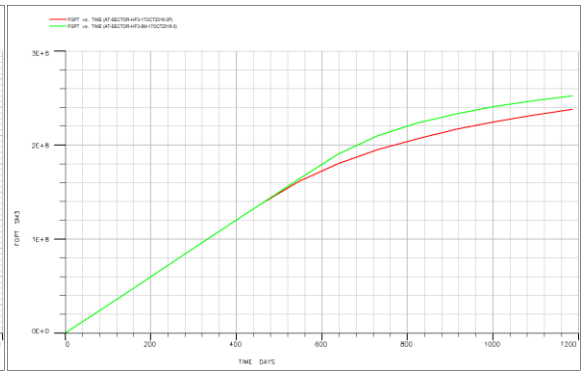

*Figure 175 cumulative gas production comparison of vertical well, with an 80m high 140m half-length hydraulic fracture, passing through no high permeability zone (red curve), and an 8m zone (green)*

The following is the ranking of each HF configuration's cumulative gas production total in descending order from lowest to highest after 1200 days of simulation

*Table 5 cumulative gas production total of hydraulic fracture scenarios ranked*

| Rank | No high permeability | 8m high permeability |
|---|---|---|
| 9 | 20/70/0.5 | 20/70/0.5 |
| 8 | 40/70/0.5 | 20/100/0.5 |
| 7 | 20/100/0.5 | 20/140/0.5 |
| 6 | 80/70/0.5 | 40/70/0.5 |
| 5 | 20/140/0.5 | 80/70/0.5 |
| 4 | 40/100/0.5 | 40/100/0.5 |
| 3 | 40/140/0.5 | 40/140/0.5 |
| 2 | 80/100/0.5 | 80/100/0.5 |
| 1 | 80/140/0.5 | 80/140/0.5 |

From Table 5, it can generally be inferred that without a high permeability zone present, the longer the hydraulic fracture half-length is, the more fluid that is recovered. However, when there is a high permeability zone present, the larger the HF height, the more fluid that is recovered.

## 5.8. Impact of Drilling Deeper

This part of the project compares the difference in recovery of drilling a deeper well to a depth of 1544m, and the shallow vertical well looked at thus far at a depth of 1505m.

The principal observation from the following results is that when hydraulically fractured, drilling deeper does not achieve a significant difference to recovery.

### 5.8.1. Not Hydraulically Fractured

#### *5.8.1.1. No high permeability zone*

The model was simulated initially without a region of high permeability. The reservoir conditions are identical to those of the previous scenarios.

When the reservoir is not hydraulically fractured, and is drilled to a depth of 1544m compared to a shallow well drilled to 1505m there is a noticeable increase in the production rate of the deep well (green curve).

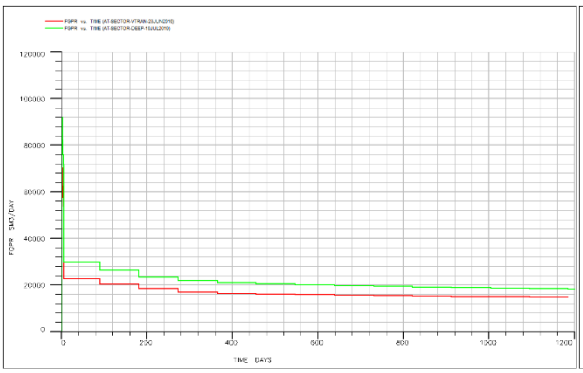

*Figure 176 sector gas production rates comparison of a shallow (red curve) and deep vertical well (green), with no HF*

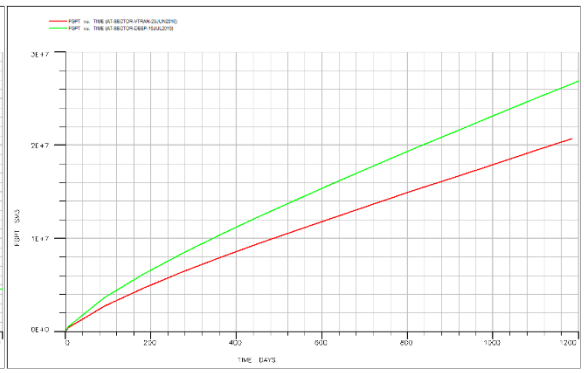

*Figure 177 sector cumulative gas production comparison of a shallow (red curve) and deep vertical well (green), with no HF*

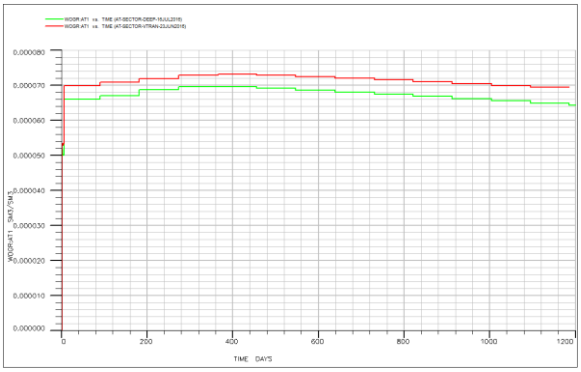

*Figure 178 CGR comparison of shallow vertical well (red curve), and a deep vertical well (green)*

Figure 178 shows that the shallow well (red curve) has a slightly higher condensate-gas ratio than the deep well and maintains that difference over a period of 1200 days; meaning that in the current conditions, the shallow well produces more condensate.

### 5.8.1.2. 2m high permeability zone

However, the introduction of a high permeability zone sees a reversal in terms of recovery. While production increases substantially for both, the shallow well now has the higher gas production rates, Figure 179, and hence the larger cumulative total, Figure 180, over the deep well.

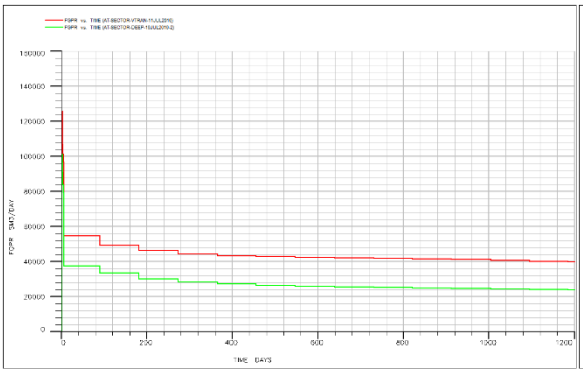

*Figure 179 sector gas production rates comparison of a shallow (red curve) and deep vertical well (green), passing through a 2m high permeability zone with no HF*

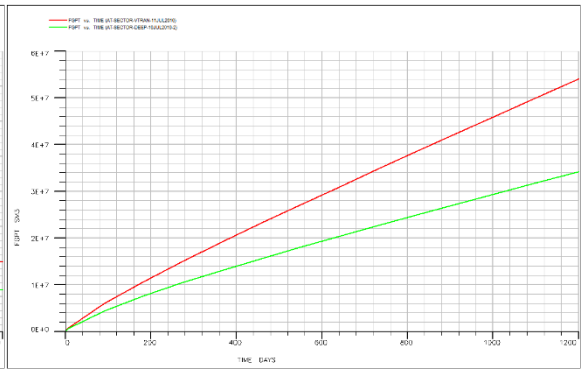

*Figure 180 sector cumulative gas production comparison of a shallow (red curve) and deep vertical well (green), passing through a 2m high permeability zone with no HF*

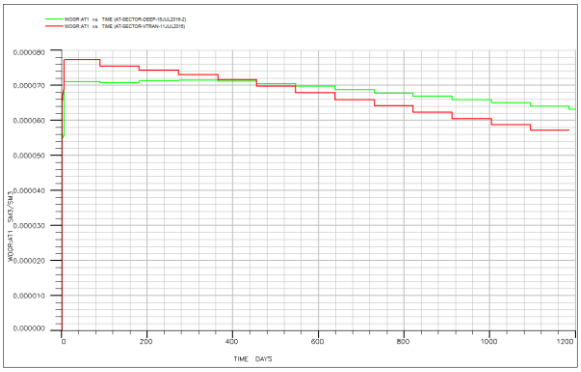

*Figure 181 CGR comparison of shallow vertical well (red curve), and a deep vertical well (green) passing through a 2m high permeability zone*

Figure 181 shows that the shallow well (red curve) initially has a higher condensate-gas ratio than the deep well, though it falls at a faster rate, and by 500 days, less condensate is being produced compared to the deep well.

#### *5.8.1.3. 8m high permeability zone*

This trend continues when the size of the high permeability zone is increased. Both wells see an increase in production, however the rate of recovery of the shallow well is much larger and hence the shallow well sees a greater increase.

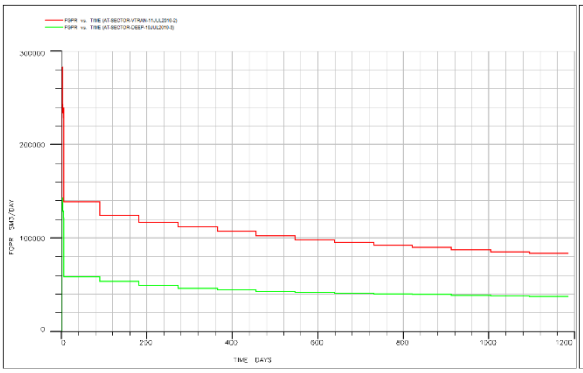

*Figure 182 sector gas production rates comparison of a shallow (red curve) and deep vertical well (green), passing through an 8m high permeability zone with no HF*

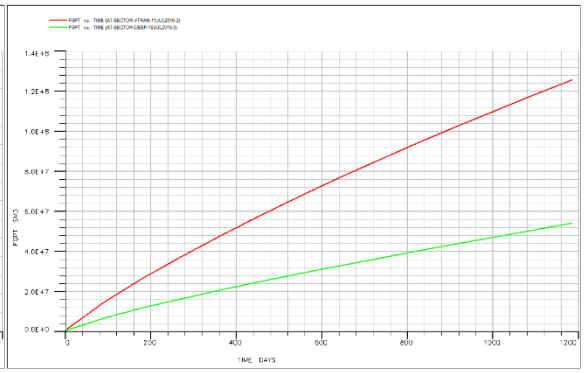

*Figure 183 sector cumulative gas production comparison of a shallow (red curve) and deep vertical well (green), passing through an 8m high permeability zone with no HF*

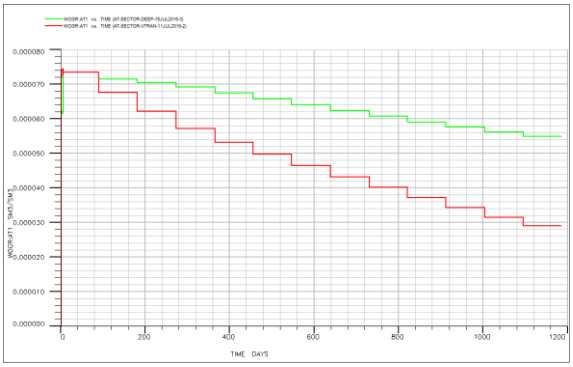

*Figure 184 CGR comparison of shallow vertical well (red curve), and a deep vertical well (green) passing through an 8m high permeability zone*

Figure 184 shows that the CGR for both wells now start out with the same value, therefore producing the same amount of condensate. However, after 100 days the CGR starts to fall at a much faster rate.

### 5.8.2. Hydraulically Fractured

#### *5.8.2.1. No high permeability zone*

There is no discernible difference in the production rate, as can be seen in Figure 185 & Figure 186, when the same wells are hydraulically fractured to dimensions of 20m height, 70m length, and 0.5m width but do not pass through a high permeability zone.

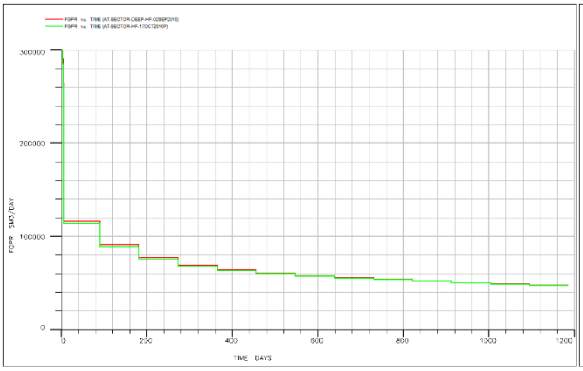

*Figure 185 sector gas production rates comparison of a shallow (red curve) and deep vertical well (green), with a 20/70/0.5*

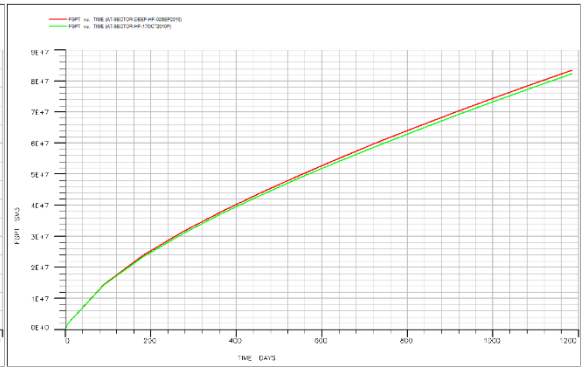

*Figure 186 sector cumulative gas production comparison of a shallow (red curve) and deep vertical well (green), with a 20/70/0.5*

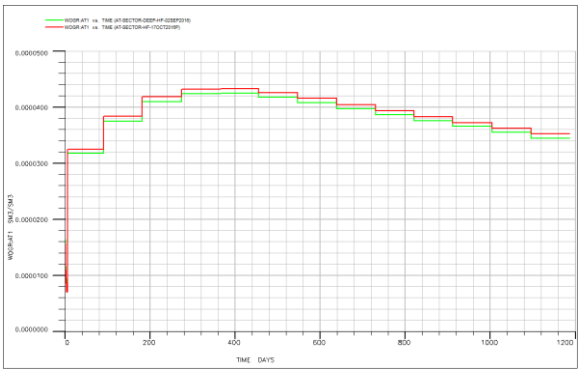

*Figure 187 CGR comparison of hydraulically fractured shallow vertical well (red curve), and a deep vertical well (green)*

Figure 187 shows that the CGR values and behaviour over 1200 days of the hydraulically fractured shallow and deep well are almost identical to one another.

### *5.8.2.2. 2m high permeability zone*

The introduction of a high permeability zone does not alter this dynamic, and only increases the recovery by a small amount.

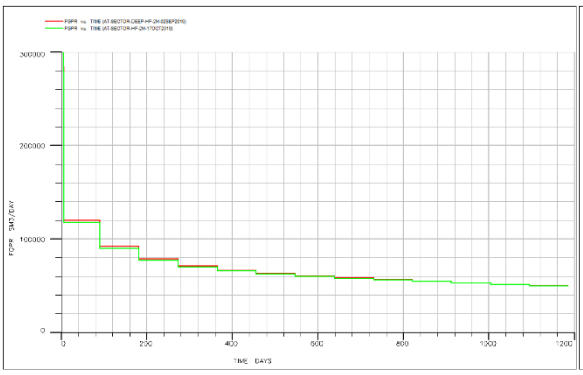

*Figure 188 sector gas production rates comparison of a shallow (red curve) and deep vertical well (green), passing through an 2m high permeability zone with a 20/70/0.5m HF*

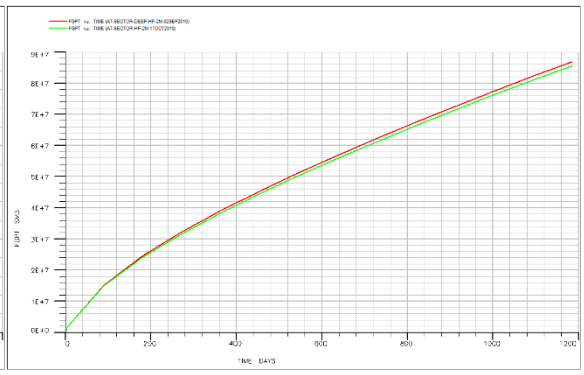

*Figure 189 sector cumulative gas production comparison of a shallow (red curve) and deep vertical well (green), passing through an 2m high permeability zone with a 20/70/0.5m HF*

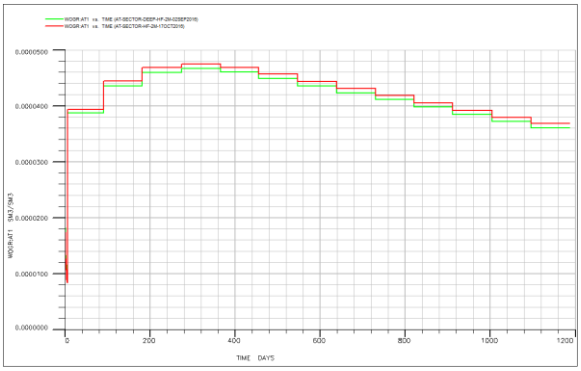

*Figure 190 CGR comparison of hydraulically fractured shallow vertical well (red curve), and a deep vertical well (green) passing through a 2m high permeability zone*

Figure 190 shows that the CGR values have increased slightly, meaning more condensate has been produced but the difference between the two wells remains the same.

### *5.8.2.3. 8m high permeability zone*

By increasing the size of the high permeability zone to 8m, the recovery increases slightly, but also results in the deep well producing slightly more than the shallow well, Figure 192. However, for all intents and purposes the difference between recovery of the two wells can be considered negligible.

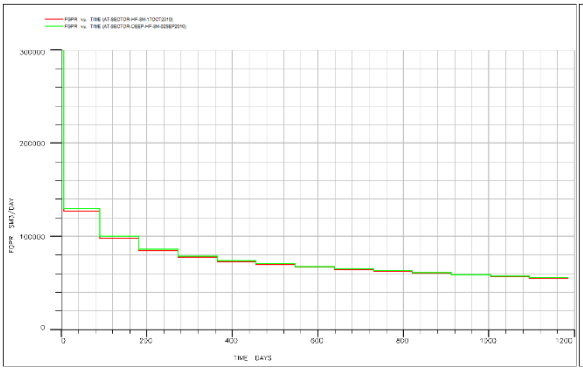

*Figure 191 sector gas production rates comparison of a shallow (red curve) and deep vertical well (green), passing through an 8m high permeability zone with a 20/70/0.5m HF*

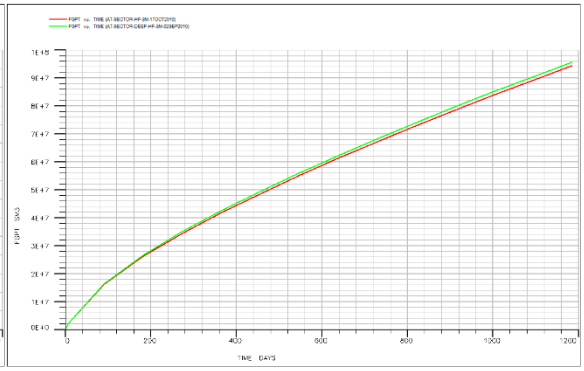

*Figure 192 sector cumulative gas production comparison of a shallow (red curve) and deep vertical well (green), passing through an 8m high permeability zone with a 20/70/0.5m HF*

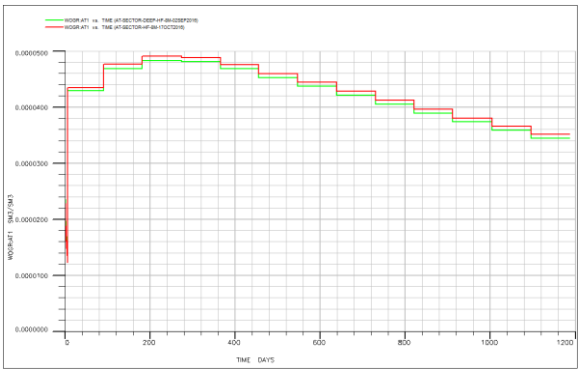

*Figure 193 CGR comparison of hydraulically fractured shallow vertical well (red curve), and a deep vertical well (green) passing through a 2m high permeability zone*

Figure 193 shows that the CGR values have increase more, meaning more condensate has been produced but the difference between the two wells remains almost indistinguishable.

Based on the current development plan, the formation will be hydraulically fractured, therefore drilling a deeper well cannot be justified as the production rate will remain roughly the same as a shallow well.

## 5.9. Horizontal Wells

Since the operating company is interested in the potential of horizontal wells, this study also evaluated the recovery potential of possible horizontal designs. At this stage the whole reservoir sector was analysed by removing the inactivation keywords in the Edit section of the model's data file. This left 177670 active cells

### 5.9.1. 1km Horizontal Well

The first well looked at was a 1km horizontal well passing through region 1 at a depth of around 1478m. Three cases were analysed: the well without HF, with 2 HF, and 4 HF, spaced out along the length of the well. The hydraulic fractures are 20m height, 70m half length, 0.5m width, and fracture conductivity of 1000mD.m. The reservoir conditions are identical to those of the previous scenarios.

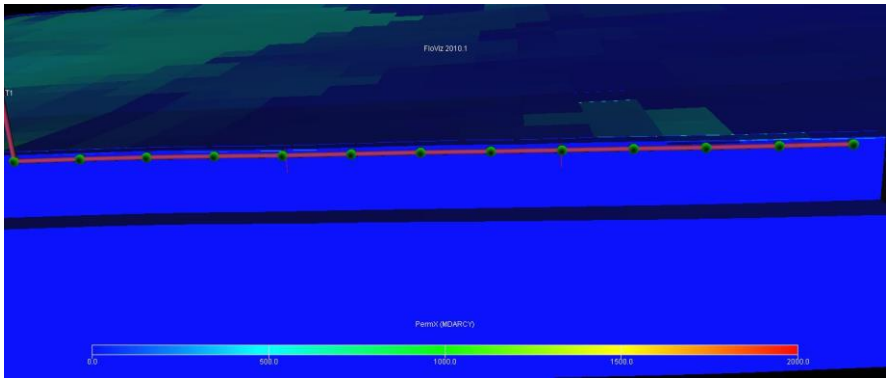


*Figure 194 1km horizontal well with 2 HF along length of well*

#### *5.9.1.1. No High Permeability Zone*

The model was initially simulated without a high permeability zone. The results from Figure 195 & Figure 196 show the impact HF have on the recovery. The gas production rate, and thus the cumulative total over 1200 days, of the horizontal well hydraulically fractured is much larger than when it is not. By increasing the number of HFs (blue curve), the recovery increase further, though not by the same rate.

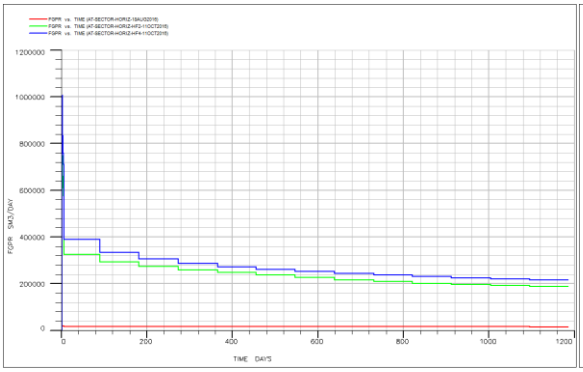


*Figure 195 sector gas production rates comparison of a 1km horizontal well passing through region 1 (red curve), with 2 HF (green curve) 4 HF (blue curve)*

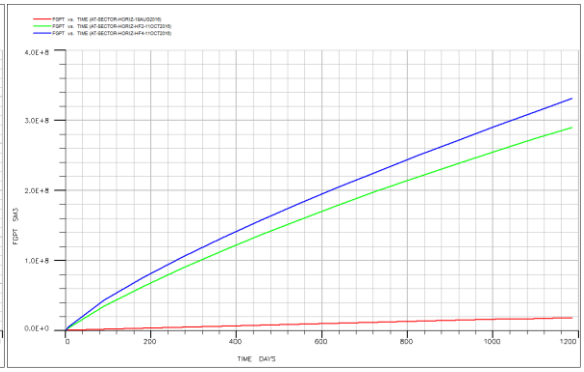


*Figure 196 sector cumulative gas production comparison of a 1km horizontal well passing through region 1 (red curve), with 2 HF (green curve) 4 HF (blue curve)*

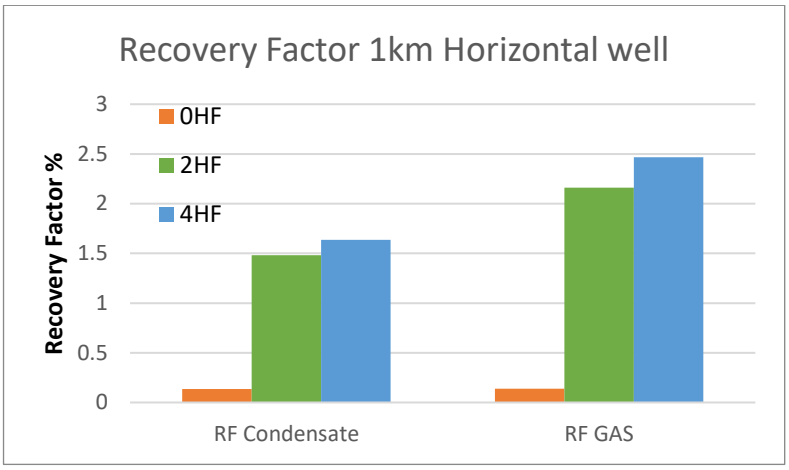


*Figure 197 1km horizontal well with and without HF recovery factor of the condensate (RF CONDENSATE), and gas from the sector (RF GAS)*

The recovery factor values from Figure 197 show that, even a horizontal well will require hydraulic fracturing, however at less than 2.5% the returns are still too low.

### *5.9.1.2. 8m High Permeability Zone*

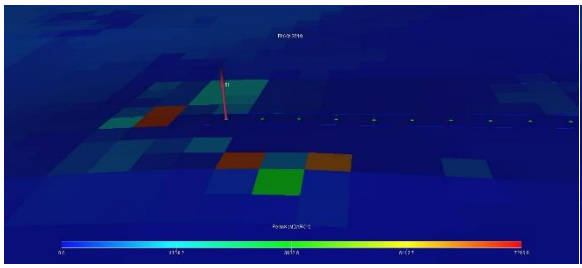

*Figure 198 Permeability distribution of a high permeability layer for a vertical well*

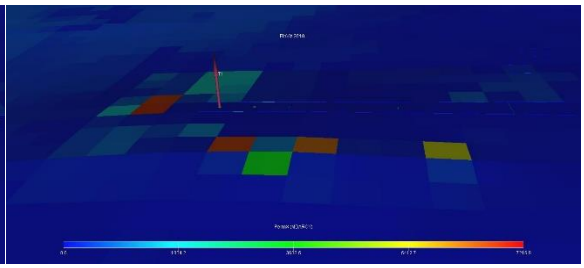

*Figure 199 Permeability distribution of a high permeability layer used for a horizontal well*

With the inclusion of a high permeability zone of 8m, the recovery increases by 100% and is seen to increase with the addition of hydraulic fractures. However, the difference between 2 and 4 hydraulic fractures in the Horizontal well is smaller as seen in Figure 202 compared to Figure 197 when there was no zone.

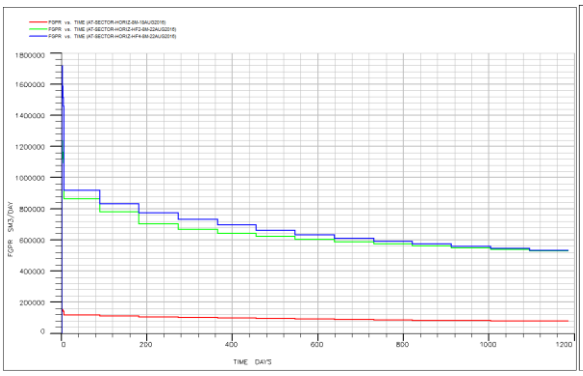

*Figure 200 sector gas production rates comparison of a 1km horizontal well passing through an 8m high permeability zone (red curve), with 2 HF (green curve) 4 HF (blue curve)*

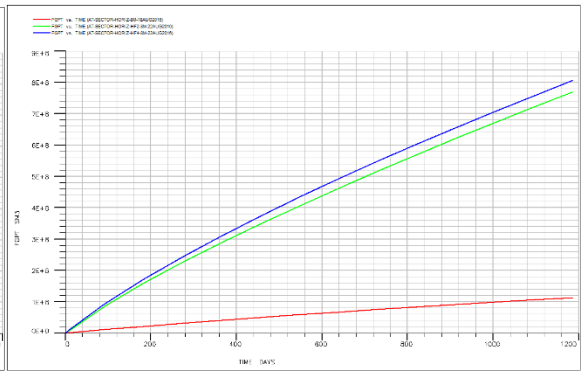

*Figure 201 sector cumulative gas production comparison of a 1km horizontal well passing through an 8m high permeability zone (red curve), with 2 HF (green curve) 4 HF (blue curve)*

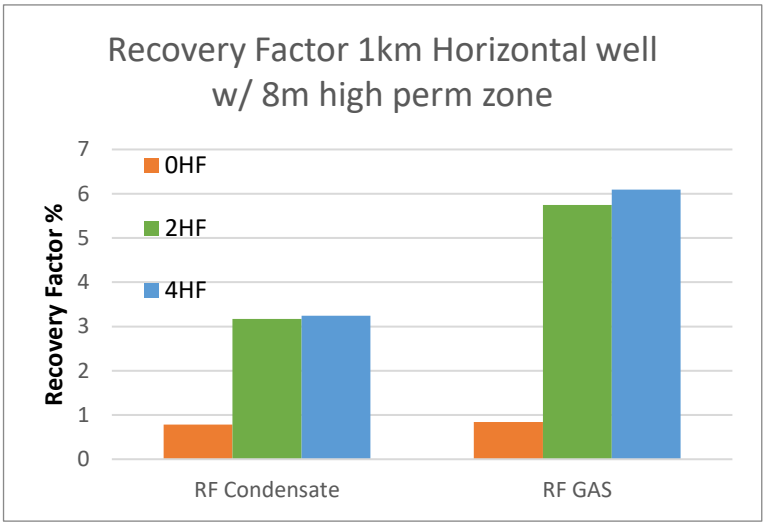


*Figure 202 1km horizontal well with and without HF passing through an 8m high permeability zone recovery factor of the condensate (RF CONDENSATE), and gas from the sector (RF GAS)*

### 5.9.2. 0.5km well

A shorter horizontal well of 0.5km, following the same path passing through region 1 at a depth of around 1478m, was simulated next. Two cases were analysed: the well without HF, and with 2 HF, spaced out along the length of the well. The hydraulic fractures are 20m height, 70m half length, 0.5m width, and fracture conductivity of 1000mD.m. The reservoir conditions remained unchanged.

#### *5.9.2.1. No High Permeability Zone*

The model was initially simulated without a high permeability zone.

The results from Figure 203, Figure 204 & Figure 205 show that there is a huge increase in the recovery from the well when HF are used, not only of the gas but the condensate as well.

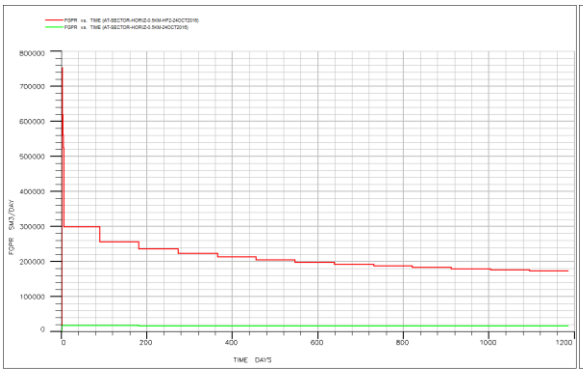

*Figure 203 sector gas production rates comparison of a 0.5km horizontal well passing through region 1 (green curve), with 2 HF (red curve)*

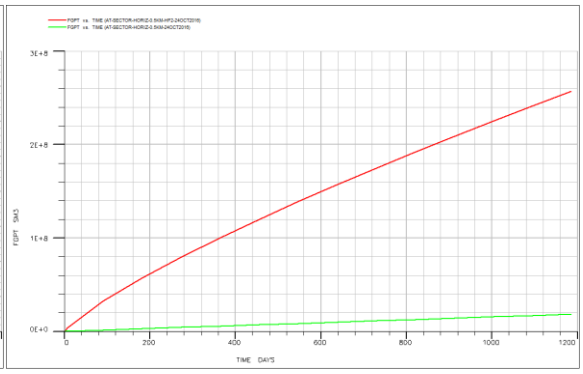

*Figure 204 sector cumulative gas production comparison of a 0.5km horizontal well passing through region 1 (green curve), with 2 HF (red curve)*

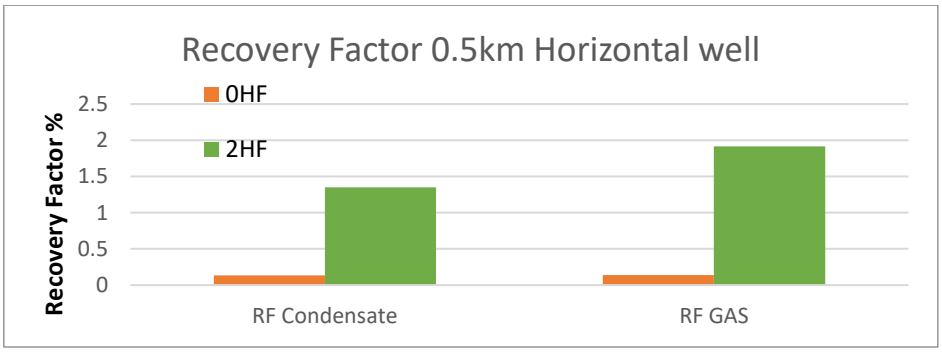


*Figure 205 0.5km horizontal well with and without HF recovery factor of the condensate (RF CONDENSATE), and gas from the sector (RF GAS)*

### *5.9.2.2. 8m High Permeability Zone*

The model was then simulated with an 8m high permeability zone in region 1.

With the inclusion of a high permeability zone, there is a significant relative increase in the recovery from 0.1 to 1%. When hydraulically fractured, the recovery factor registers an even greater increase, up to 5.7%.

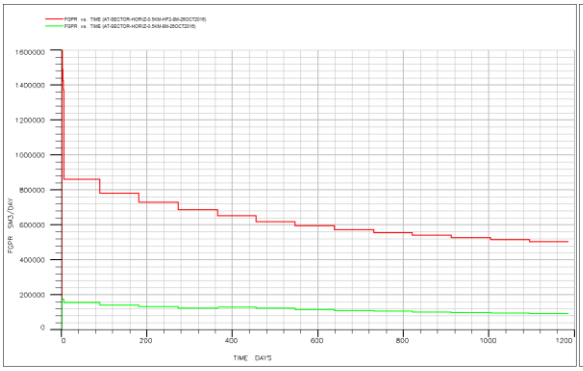

*Figure 206 sector gas production rates comparison of a 0.5km horizontal well passing through an 8m high permeability zone (green curve), with 2 HF (red curve)*

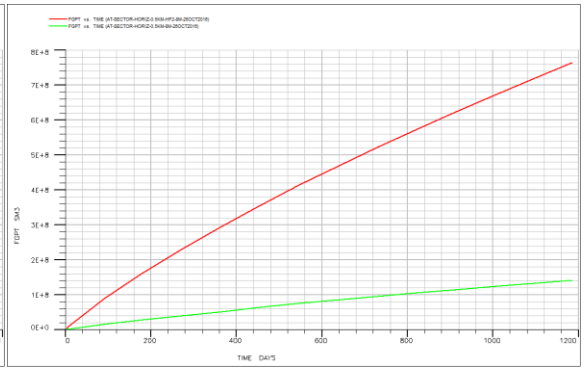

*Figure 207 sector cumulative gas production comparison of a 0.5km horizontal well passing through an 8m high permeability zone (green curve), with 2 HF (red curve)*

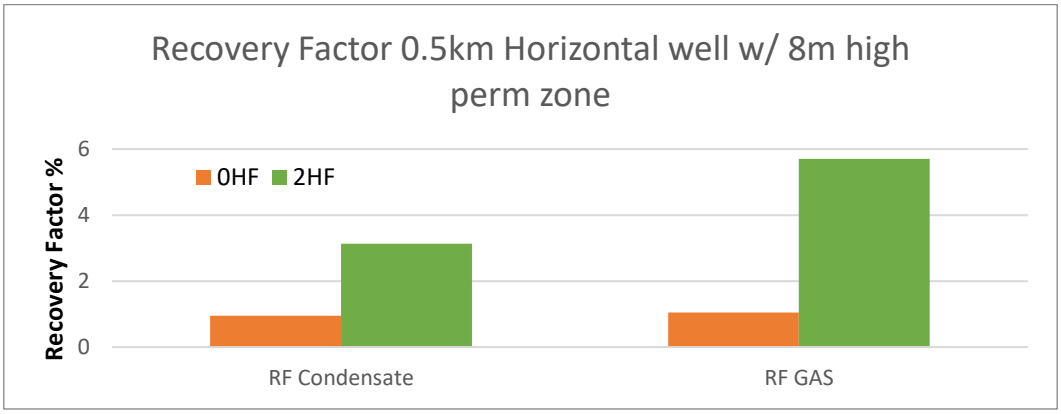


*Figure 208 0.5km horizontal well with and without HF passing through an 8m high permeability zone recovery factor of the condensate (RF CONDENSATE), and gas from the sector (RF GAS)*

### 5.9.3. 2km well

A horizontal well of 2km, following the same path passing through region 1 at a depth of around 1478m, was considered next. Two cases were analysed: the well without HF, and with 4 HF, spaced out along the length of the well. The hydraulic fractures are 20m height, 70m half length, 0.5m width, and fracture conductivity of 1000mD.m. The reservoir conditions remained unchanged.

#### *5.9.3.1. No High Permeability Zone*

The model was initially simulated without a high permeability zone.

The results from Figure 209, Figure 210, & Figure 211 follow the same behaviour as the other horizontal wells – a substantial increase in recovery when the well is hydraulically fractured. The difference is seen in the much larger recovery factor for the non-hydraulically fractured 2km well, 1%, when compared to the shorter horizontal wells, 0.1%.

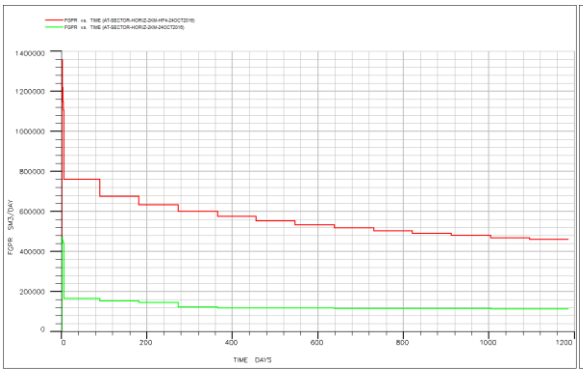

*Figure 209 sector gas production rates comparison of a 2km horizontal well passing through region 1 (green curve), with 4 HF (red curve)*

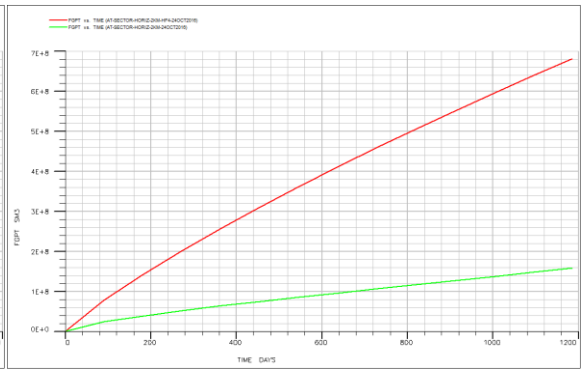

*Figure 210 sector cumulative gas production comparison of a 2km horizontal well passing through region 1 (green curve), with 4 HF (red curve)*

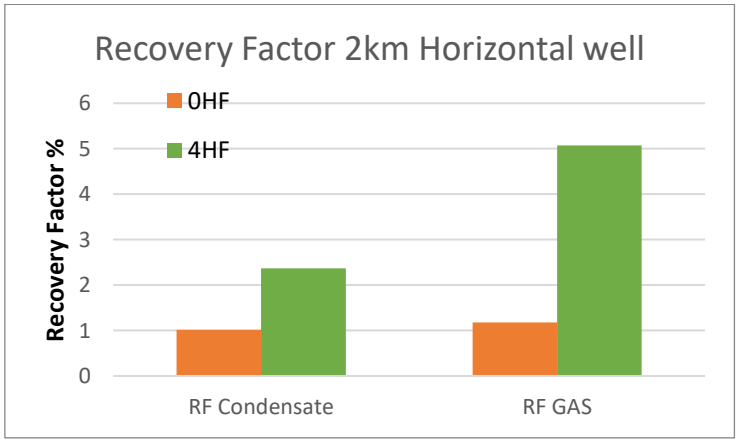


*Figure 211 2km horizontal well with and without HF recovery factor of the condensate (RF CONDENSATE), and gas from the sector (RF GAS)*

#### *5.9.3.2. 8m High Permeability Zone*

The model was then simulated with an 8m high permeability zone in region 1.

The inclusion of a high permeability zone, sees a more modest increase in recovery when compared to the other size horizontal wells. The non-hydraulically fractured well only sees a 100% increase to 2%, while the hydraulically fractured case, only increase by 2%.

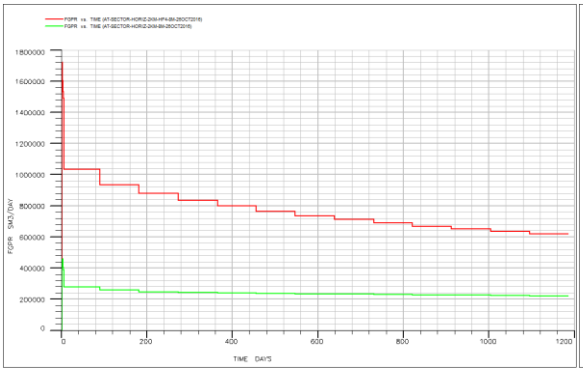

*Figure 212 sector gas production rates comparison of a 2km horizontal well passing through an 8m high permeability zone (green curve), with 4 HF (red curve)*

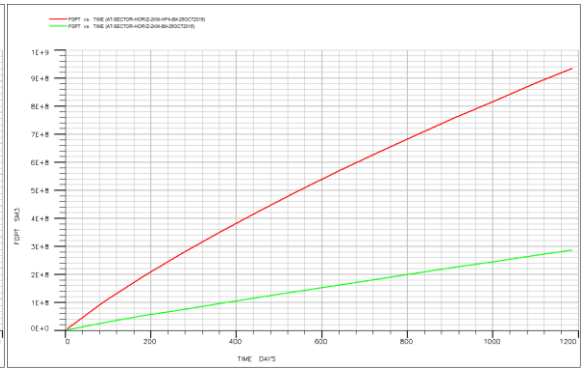

*Figure 213 sector cumulative gas production comparison of a 2km horizontal well passing through an 8m high permeability zone (green curve), with 4 HF (red curve)*

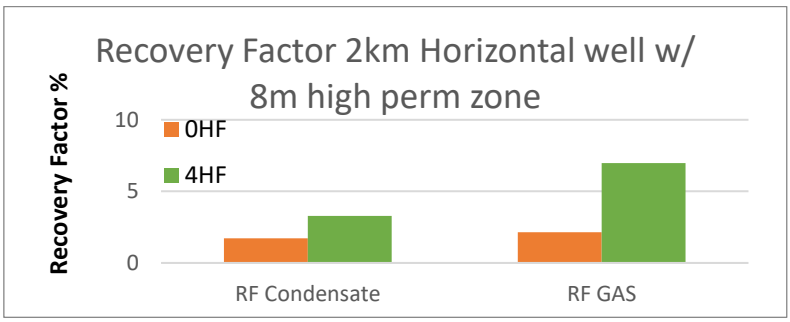


*Figure 214 2km horizontal well with and without HF passing through an 8m high permeability zone recovery factor of the condensate (RF CONDENSATE), and gas from the sector (RF GAS)*

### 5.9.4. Inclined well

A well was then drilled Horizontally inclined from the upper region (1463m) to the lower (1500m), and then hydraulically fractured with and without an 8m region of high permeability.

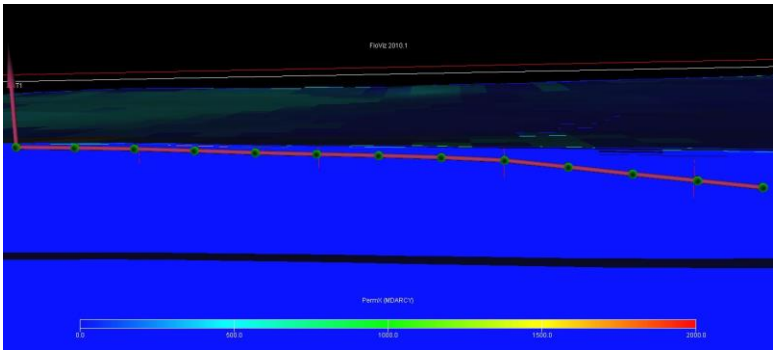

*Figure 215 1km inclined horizontal well with 4 HF along length of well*

#### *5.9.4.1. No High Permeability Zone*

The model was initially simulated without a high permeability zone.

The results from Figure 216, Figure 217, & Figure 218 show that there is a huge increase in the recovery from the well when HF are used, not only of the gas but the condensate as well. By doubling the number of HFs, the recovery increases further, though by a much smaller percent.

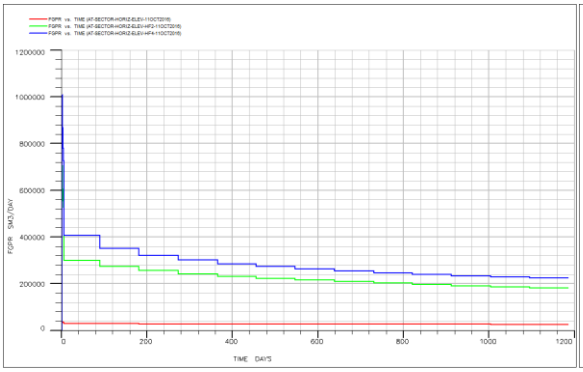

*Figure 216 sector gas production rates comparison of a 1km inclined horizontal well passing through the upper and lower regions of the reservoir (red curve), with 2 HF (green curve), and 4HF (blue)*

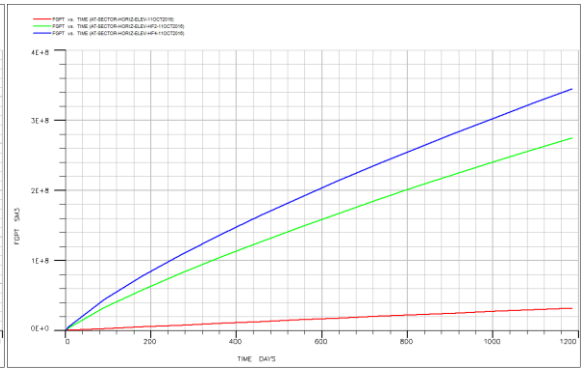

*Figure 217 sector cumulative gas production comparison of a 1km inclined horizontal well passing through the upper and lower regions of the reservoir (red curve), with 2 HF (green curve), and 4HF (blue)*

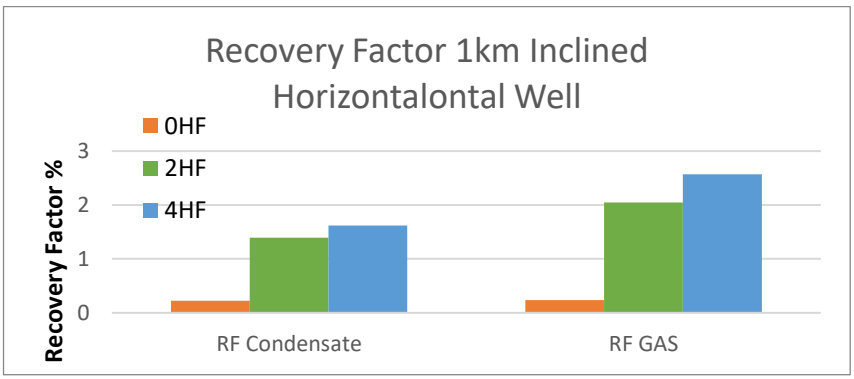


*Figure 218 1km inclined horizontal well with and without HF recovery factor of the condensate (RF CONDENSATE), and gas from the sector (RF GAS)*

### *5.9.4.2. 8m high permeability zone*

With the inclusion of a high permeability zone of 8m, the recovery increases by 100% and is seen to increase with the addition of hydraulic fractures. However, the difference between 2 and 4 hydraulic fractures in the Horizontal well is smaller as seen in Figure 221 compared to Figure 218 when there was no zone.

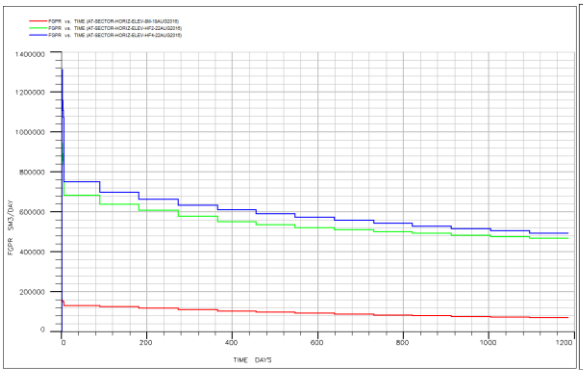

*Figure 219 sector gas production rates comparison of a 1km inclined horizontal well passing through an 8m high permeability zone and down to a lower zone of the reservoir (red curve), with 2 HF (green curve), and 4HF (blue)*

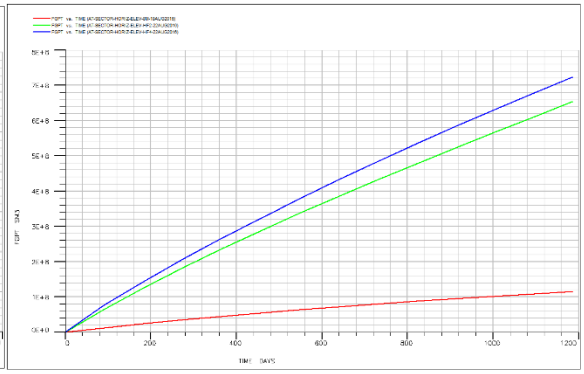

*Figure 220 sector cumulative gas production comparison of a 1km inclined horizontal well passing through an 8m high permeability zone and down to a lower zone of the reservoir (red curve), with 2 HF (green curve), and 4HF (blue)*

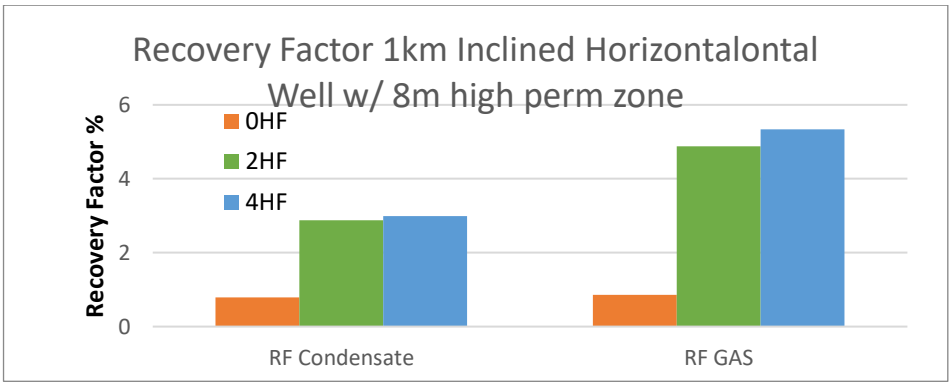


*Figure 221 1km inclined horizontal well with and without HF passing through an 8m high permeability zone recovery factor of the condensate (RF CONDENSATE), and gas from the sector (RF GAS)*

### 5.9.5. Vertical & Horizontal Well Comparison

The following is a comparison of the recovery of all the horizontal well scenarios versus a vertical well.

#### *5.9.5.1. No Hydraulic Fractures*

Figure 222 & Figure 223 are comparing the cases when there are no hydraulic fractures and no region of high permeability.

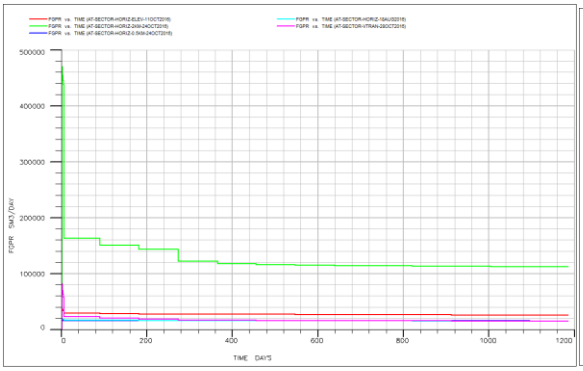

*Figure 222 sector gas production rates comparison of a shallow vertical well (purple curve) and horizontal wells of 0.5km length (blue curve), 1km (cyan curve), 2km (green), and a 1km inclined well (red)*

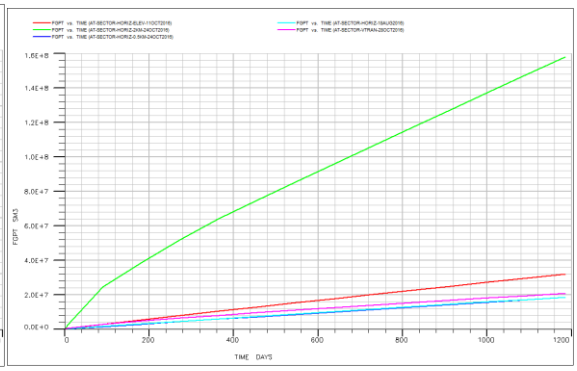

*Figure 223 sector cumulative gas production comparison of a shallow vertical well (purple curve) and horizontal wells of 0.5km length (blue curve), 1km (cyan curve), 2km (green), and a 1km inclined well (red)*

As can be seen there is a substantial difference between the gas production of the 2km horizontal well compared to the 1km inclined horizontal well. This is to be expected due to the increase in size of the well. However, third in terms of quantity produced is the vertical well, followed by the 1km and 0.5km wells passing through the upper zone only. The difference between the latter two is negligible.

#### 5.9.5.2. *Hydraulically fractured*

Figure 224 & Figure 225 are comparing the cases when hydraulic fractures are introduced but there is no region of high permeability.

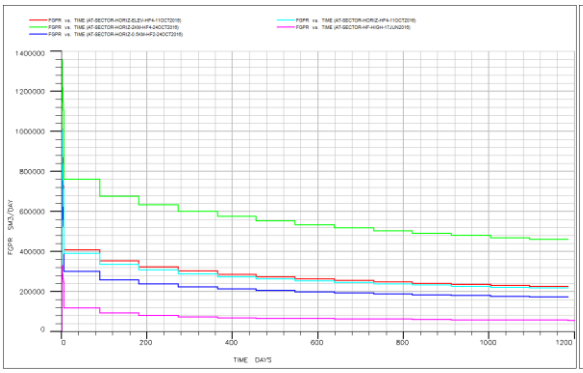

*Figure 224 sector gas production rates comparison of a shallow vertical well w/ 20/70/0.5m HF (purple curve) and horizontal wells of 0.5km length with 2HF (blue curve), 1km with 4HF (cyan curve), 2km with 4HF (green), and a 1km inclined well with 4HF (red)*

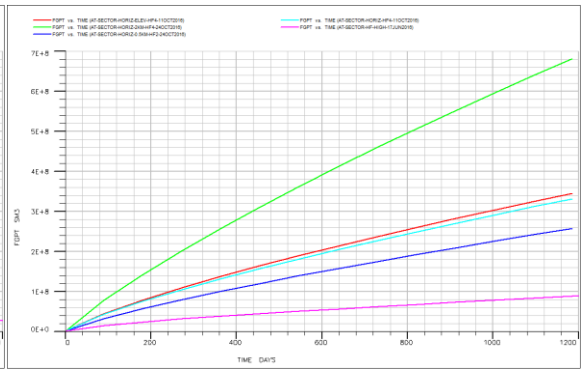

*Figure 225 sector cumulative gas production comparison of a shallow vertical well w/ 20/70/0.5m HF (purple curve) and horizontal wells of 0.5km length with 2HF (blue curve), 1km with 4HF (cyan curve), 2km with 4HF (green), and a 1km inclined well with 4HF (red)*

As can be seen, the substantial difference between the gas production of the 2km horizontal well compared to the other well remains. The 1km inclined horizontal well comes second, followed by the 1km well passing through only the upper region with little to separate them. Unlike when there was no hydraulic fracture, there is now a noticeable difference between the production of the 1km and 0.5km wells, the latter clearly producing less. All the horizontal wells, regardless of dimensions, when hydraulically fractured, produce much more gas than a vertical well.

## 5.10. Optimal Well Spacing

With the current development plan in mind, this next section looks at the optimal spacing between two wells. Three cases were looked at, where a second identical shallow vertical well with a hydraulic fracture of 20/70/0.5m was added to the model a set distance apart:

| Case | Well Spacing (km) |
|---|---|
| 1 | 0.5 |
| 2 | 1 |
| 3 | 2 |

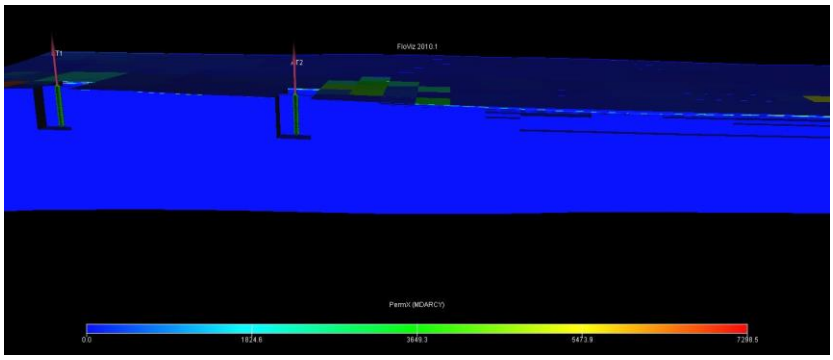


*Figure 226 Two shallow hydraulically fractured (20/70/0.5) vertical wells 0.5km apart*

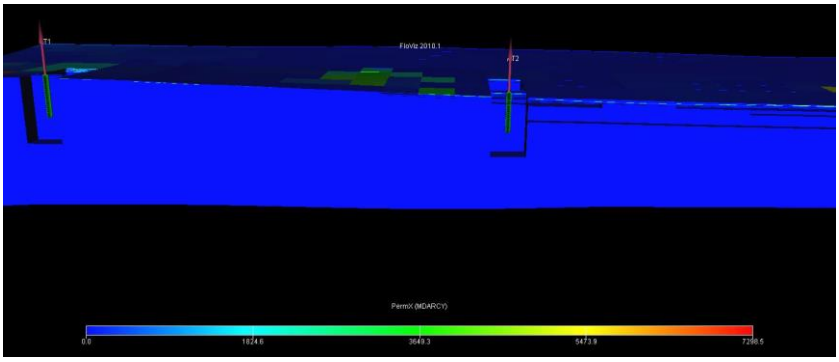


*Figure 227 Two shallow hydraulically fractured (20/70/0.5) vertical wells 1km apart*

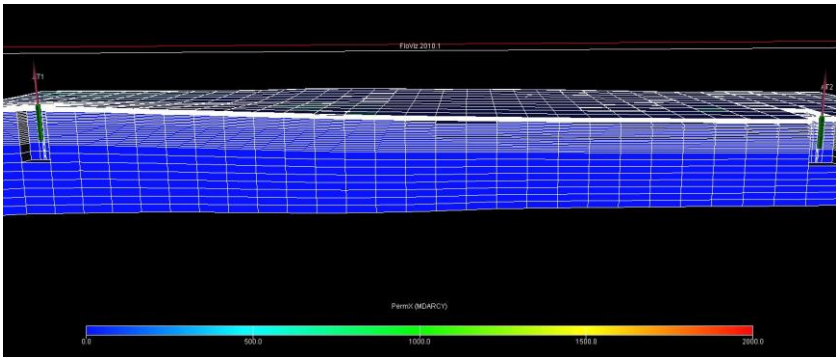


*Figure 228 Two shallow hydraulically fractured (20/70/0.5) vertical wells 2km apart*

### 5.10.1. No high permeability zone

The simulations were run initially with no high permeability zone. The results from Figure 229 & Figure 230 appear to indicate that the further apart the two wells are, the greater the recovery, which subscribes to the development plan of having wells 2km apart.

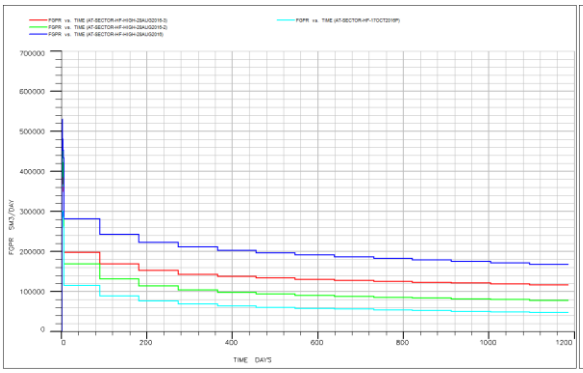

*Figure 229 sector gas production rates comparison of a shallow vertical well w/ 20/70/0.5m HF (cyan curve) against 2 identical wells spaced 0.5km apart (green curve), 1km (red), and 2km (blue)*

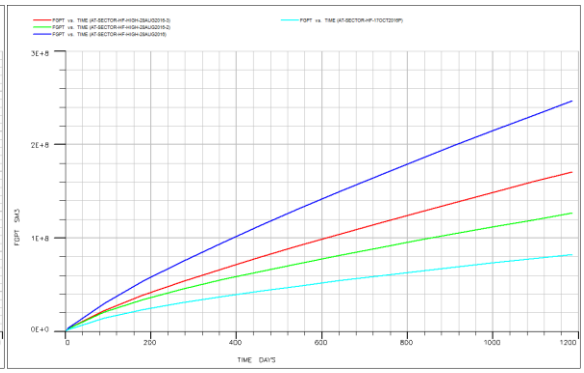

*Figure 230 sector cumulative gas production comparison of a shallow vertical well w/ 20/70/0.5m HF (cyan curve) against 2 identical wells spaced 0.5km apart (green curve), 1km (red), and 2km (blue)*

### 5.10.2. 8m high permeability zone

The models were then altered to include an 8m high permeability zone. With a high permeability zone present, there is a clearer picture of what the optimal well spacing is. Figure 231 & Figure 232 suggest that 1km is the optimal distance between 2 wells. 0.5km appears too short, as while it does show an increase in recovery compared to a single well, it is substantially less than the other two cases. On the other hand, 2km initially produces more than the 1km spacing, however it is not capable of sustaining its production rate and falls, to be overtaken by the 1km model after 350 days and continues to produce more.

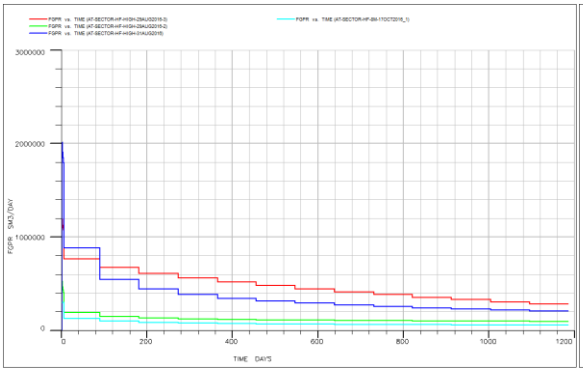

*Figure 231 sector gas production rates comparison of a shallow vertical well w/ 20/70/0.5m HF passing through an 8m high permeability zone (cyan curve) against 2 identical wells spaced 0.5km apart (green curve), 1km (red), and 2km (blue)*

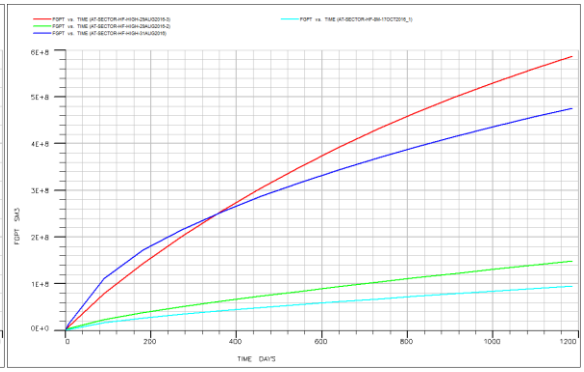

*Figure 232 sector cumulative gas production comparison of a shallow vertical well w/ 20/70/0.5m HF passing through an 8m high permeability zone (cyan curve) against 2 identical wells spaced 0.5km apart (green curve), 1km (red), and 2km (blue)*

## 6. Financial analysis

Financial analysis identifies the well types and hydraulic fracture designs that bring the greatest commercial value to the company. A particular design may yield better recovery or a longer plateau period than other configurations. However, it may not be the preferred option.

A financial model was created to calculate net present value (NPV) for possible well trajectories and hydraulic fracture designs. NPV allows ranking development options; the one with the greatest NPV is preferred since it provides greatest value to the company.

The base model for a shallow vertical well with no hydraulic fractures can be seen in Appendix B. Table 6 displays the parameters of the financial model:

*Table 6 Parameters of financial model*

| Financial parameters | Value | Unit |
|---|---|---|
| Discount rate | 6.00 | % annual |
| Tax rate | 34.00 | % taxable income |
| Price gas, year 1 (http://pubdocs.worldbank.org/en/104481475607967889/CMO-Pink-Sheet-October-2016.pdf) | 0.175 | USD/sm3 |
| Increase gas price | 4.00 | %/year |
| Price condensate, year 1 (http://pubdocs.worldbank.org/en/104481475607967889/CMO-Pink-Sheet-October-2016.pdf) | 290.54 | USD/sm3 |
| Increase price condensate | 4.00 | %/year |
| **Costs** (Source: PetroCeltic) | | |
| OPEX | 24.00 | % year production |
| Construction cost, short vertical well | 1.98 | USD million |
| Construction cost, deep vertical well | 2.97 | USD million |
| Construction cost, 500m horizontal well | 3.63 | USD million |
| Construction cost, 1000m horizontal well | 3.96 | USD million |
| Construction cost, 2000m horizontal well | 5.61 | USD million |
| Cost, 20m hydraulic fracture | 0.98 | USD million |
| Cost, 40m hydraulic fracture | 1.19 | USD million |
| Cost, 80m hydraulic fracture | 1.33 | USD million |
| **Assumptions** | | |
| 100% of finance provided by operating company (no debt) | | |
| Depreciation period of CAPEX | 10 | years |
| Tax relief on depreciation | 34 | % |

The price for gas and condensate were taken from the World Bank's Pink Sheet (http://pubdocs.worldbank.org/en/104481475607967889/CMO-Pink-Sheet-October-2016.pdf to be 4.21 USD/MMBTU and 46.19 USD/bbl for natural gas in Europe and Brent respectively. MMBTU cannot be directly converted to $sm^3$ therefore the energy content for the reservoir fluid had to be calculated in joules. The PVT report gave the composition values from a separator gas sample,

Table 7, which were used to calculate the volume of each component in $m^3$, by using the ideal gas equation pV = nRT. Standard conditions: p = $1.01x10^5$Pa; T = 288.75K. This was then used to calculate the volume fraction, which in turn was multiplied by the heating value (MJ/$sm^3$) for each component (http://www.enggcyclopedia.com/2011/09/heating-values-natural-gas), and then dividing the conversion value of BTU to joules by the sum to give the amount of energy per $sm^3$. This gives a gas price of 0.175 USD/$sm^3$.

The condensate price in the cash flow analysis of 46.19 USD/bbl equates to 290.54 USD/$sm^3$.

*Table 7 Seperator Gas Sample Composition*

| Component | MW (g/mol) | Separator Gas (mole %) |
|---|---|---|
| **N2** | 28.01 | 1.92 |
| **CO2** | 44.01 | 1.83 |
| **H2S** | 34.08 | 0.00 |
| **C1** | 16.04 | 81.14 |
| **C2** | 30.07 | 8.15 |
| **C3** | 44.10 | 4.29 |
| **i-C4** | 58.12 | 0.51 |
| **n-C4** | 58.12 | 1.25 |
| **i-C5** | 72.15 | 0.30 |
| **n-C5** | 72.15 | 0.32 |
| **C6** | 84.00 | 0.19 |
| **Mcyclo-C5** | 84.16 | 0.02 |
| **Benzene** | 78.11 | 0.00 |
| **Cyclo-C6** | 84.16 | 0.01 |
| **C7** | 96.00 | 0.05 |
| **Mcyclo-C6** | 98.19 | 0.01 |
| **Toluene** | 92.14 | 0.00 |
| **C8** | 107.00 | 0.01 |
| **C2-Benzene** | 106.17 | 0.00 |
| **m&p-Xylene** | 106.17 | 0.00 |
| **o-Xylene** | 106.17 | 0.00 |
| **C9** | 121.00 | 0.00 |
| **C10** | 134.00 | 0.00 |
| **C11** | 147.00 | 0.00 |
| **C12** | 161.00 | 0.00 |
| **C13** | 175.00 | 0.00 |
| **C14** | 190.00 | 0.00 |
| **C15+** | 206.00 | 0.00 |
| **MW** | | 20.43 |
| | | 100.00 |

The values of the gas and condensate recovered for every year up to 20, were used from each well trajectory and hydraulic fracture configuration scenario to calculate revenue from sales, assuming a

yearly 4% increase in price. Offsetting this are the costs. OPEX is calculated at 24% of yearly production, while the CAPEX, the values of which were provided by PetroCeltic, is the construction cost of each well type and hydraulic fracture configuration. The cost of surface plants have not been included in the CAPEX. The value of CAPEX was depreciated over a period of 10 years, and added to the income but only to calculate tax, as it is not considered part of the cash flow. The income is then taxed at 34%, from which the Present Value is calculated for each year and then summed using equation (5) to give the NPV. Due to the missing costs, the value attained cannot be considered the true NPV and is only being used for comparative reasons between the options.

None of the scenarios looked at included high permeability regions in their models.

Table 8 shows the difference between the Net Present Values (NPV) of all of the well type and hydraulic fracture scenarios:

*Table 8 NPV values of Well Type Scenarios*

| Well Type | NPV (USD) | Total Volume Gas Produced (sm3) |
|---|---|---|
| 2km Horizontal Well 4 HF | 142,247,067 | 2,071,570,000 |
| 1km Inclined Horizontal Well 4 HF | 89,931,484 | 1,260,630,000 |
| 1km Horizontal Well 4 HF | 85,809,024 | 1,204,470,000 |
| 0.5km Horizontal Well 2 HF | 77,581,606 | 1,058,640,00 |
| 1km Inclined Horizontal Well 2 HF | 76,466,993 | 1,055,450,000 |
| 1km Horizontal Well 2 HF | 75,662,019 | 1,044,450,000 |
| 2 Shallow Vertical Well w/ 20m high 70m length HF 2km Spacing | 57,589,368 | 834,528,000 |
| 2km Horizontal Well No HF | 53,664,448 | 752,813,000 |
| 2 Shallow Vertical Well w/ 20m high 70m length HF 1km Spacing | 43,431,770 | 643,020,000 |
| 2 Shallow Vertical Well w/ 20m high 70m length HF 0.5km Spacing | 27,651,596 | 418,880,000 |
| Shallow Vertical Well w/ 80m high 140m length HF | 25,797,066 | 358,746,000 |
| Shallow Vertical Well w/ 80m high 100m length HF | 23,333,303 | 331,374,000 |
| Shallow Vertical Well w/ 40m high 140m length HF | 22,942,551 | 325,802,000 |
| Shallow Vertical Well w/ 40m high 100m length HF | 21,103,718 | 304,529,000 |
| Shallow Vertical Well w/ 20m high 140m length HF | 19,684,743 | 285,434,000 |
| Shallow Vertical Well w/ 80m high 70m length HF | 19,438,421 | 285,973,000 |
| Shallow Vertical Well w/ 20m high 100m length HF | 18,305,046 | 268,797,000 |
| Shallow Vertical Well w/ 40m high 70m length HF | 18,007,423 | 267,017,000 |
| Shallow Vertical Well w/ 20m high 70m length HF | 14,943,874 | 226,652,000 |
| Deep Vertical Well w/ HF | 14,665,262 | 230,146,000 |
| Inclined Horizontal Well No HF | 10,278,185 | 163,831,000 |
| Deep Vertical Well no HF | 6,267,754 | 109,257,000 |
| Shallow Vertical Well no HF | 5,751,002 | 92,724,600 |
| 0.5km Horizontal Well No HF | 5,329,054 | 101,034,000 |
| 1km Horizontal Well No HF | 3,892,750 | 86,280,000 |

A 2km horizontal well along the upper region, with four hydraulic fractures spaced out along the length of the well, gives the greatest NPV. The bar graph of the cash flow of each well trajectory and hydraulic fracture design option, Appendix C, shows how the net cash flow of the hydraulically fractured 2km horizontal well (grey bar), increases with each year, over the 10-year period, as opposed to all the other cases which decrease. This is because the well manages to maintain maximum production (300,000 $sm^3$/day) for over 10 years, and with the estimated yearly gas price increase, results in the increasing values of Net Cash Flow.

# 7. Conclusion

The main objective of this project was to determine the optimal well trajectory and hydraulic fracture design for a low-quality gas-condensate reservoir to sustain high production rates that maximise recovery.

The simulation results reveal that a shallow vertical well cannot produce commercial quantities of gas and is also seen to be insensitive to change in the vertical transmissibility, unless a high permeability zone is present.

A hydraulic fracture gives a notable boost in recovery from the well, which in turn increases depending on the size of the high permeability zone. For example, a shallow uncased vertical well, hydraulically fractured (20m height, 70m half length, 0.5m width, and fracture conductivity of 1000mD.m), passing through a 2m high permeability zone sees an increase in the recovery factor from 10, for an unfractured well, to 17.6%. With a HF, the recovery is very sensitive to the $k_v/k_h$ ratio. A poor ratio results in a lower recovery factor as less fluid can flow vertically.

This answers the secondary question of whether pressures should be recorded to establish $k_v/k_h$ -which should only be required to select the most appropriate well design. From the shallow vertical wells, the recovery factor has a difference of 5% between the best and worst case scenarios. However, as the difference of the total amount of gas recovered between the two well types with the highest NPV values is so large, 2,300,750,000 to 1,261,200,000 $sm^3$, the reduction in recovery would not alter the order with which the well types are chosen by NPV. Therefore, a pressure build up test is not required to record pressures and hence determine the $k_v/k_h$.

Altering the fracture conductivity does impact on the recovery, but not enough to warrant concern over the uncertainty, even with the presence of high permeability zone.

There is an increase in recovery when the hydraulic fracture penetrates the high permeability zone, as can be seen when a shallow uncased vertical well, hydraulically fracturing (20m height, 70m half length, 0.5m width, and fracture conductivity of 1000mD.m) an 8m high permeability zone, registers a 70M $sm^3$ increase in production over 1200 days compared to a well where the hydraulic fracture only penetrates the low permeability zone.

Increasing the height of the hydraulic fracture, also sees a significant increase in the recovery, which gets larger still with the increasing size of the high permeability zone. The same effect is seen when the HF's half-length is altered. To the point where it can be concluded that the longer the hydraulic fracture half length, the higher the recovery, especially when there is no high permeability zone. It should be noted however that when there is a high permeability zone present, it is the HF height which has the greater influence on recovery.

Despite, the initial assumptions, drilling deeper does not have the desired effect of increasing production. An increase is registered when there is no HF, which has already been determined to be

necessary, and depending on the size of the high permeability zone, more condensate is produced. For example, with an 8m high permeability zone, a shallow well's CGR falls 0.000025 below that of a deep well. The addition of a hydraulic fracture sees virtually no difference in the recovery, nor the CGR, of a deep well to that of a shallow well.

While the impact of condensate deposition in the formation should always be considered, the evaluation of the conditions here found that it is not an immediate issue as the formation of condensate, once the reservoir pressures falls below the dewpoint, reduces the gas permeability (and hence the gas productivity) by a maximum of 5% - a value considered insignificant.

Due to their extra coverage, simulation predicts that drilling horizontally will see greatly increased production values and this is the case when the wells are hydraulically fractured, with substantial returns being made compared to a vertical well.

When considering drilling more than one well, and there is no high permeability zone, the further away two wells are, in this case the max distance is 2km, the higher the recovery will be. However, when there is a high permeability zone the optimal distance between wells is seen to be 1km. This is an unexpected outcome: generally, the more homogeneous and poor quality the formation, the wider the spacing required to maximise recovery.

From the financial model, the most lucrative system, based on its NPV, is a hydraulically fractured 2km horizontal well, assuming there is no high permeability zone and an optimal $k_v/k_h$ ratio of 1. Though based on the increased recovery factors of the well options when there is an 8m high permeability zone present, the extra revenue brought about from production sales would still not be enough to change the outcome reached. Therefore, the ideal system for this reservoir, based on the cases tested, is a hydraulically fractured 2km horizontal well.

## 8. Further work

Normally, lean gas injection could be looked at to see if it aids recovery, which would result in switching to using a compositional model. However, this is not necessary with this reservoir as the condensate loss is low.

It would be valuable evaluating separate wells each producing from the high and low permeability zones, instead of production from both zones simultaneously.

The production rate limit could be altered, changing the plateau length, to see the effect this would have on the recovery of the different well types.

More work needed in optimising hydraulic fracture dimensions for the given reservoir conditions.

## References


Berman, K., Knight, J., & Case, J. (2013). *Financial Intelligence, Revised Edition: A Manager's Guide to Knowing What the Numbers Really Mean.* Boston: Harvard Business Publishing.

Bickel, J. E., & Bratvold, R. B. (2007). *Decision-Making in the Oil and Gas Industry--From Blissful Ignorance to Uncertainty-Induced Confusion.* Society of Petroleum Engineers. doi:10.2118/109610-MS

Blasingame, T. A. (n.d.). *PVT Concepts (Reservoir Fluids).* Retrieved from Texas A&M University: http://www.pe.tamu.edu/blasingame/data/z_zCourse_Archive/P324_06A/P324_06A_w_Lessons/PDF_P324_06A_(for_class)_Lec_Mod1_02b_Phase_Behavior_(Orientation).pdf

Dake, L. P. (1991). *Fundamentals of reservoir engineering* (12th ed.). Amsterdam: Elsevier.

Economides, M. J., & Martin, T. (2007). *Modern Fracturing.* Houston: Energy Tribune Publishing Inc.

English, K. L., Redfern, J., Corcoran, D. V., English, J. M., & Cherif, R. Y. (2016, April). Constraining burial history and petroleum charge in exhumed basins: New insights from the Illizi Basin, Algeria. *AAPG Bulletin, 100*(4), 623–655.

Firoozabadi, A., & Ramey, H. J. (1988). *Surface Tension Of Water-Hydrocarbon Systems At Reservoir Conditions.* Petroleum Society of Canada. doi:10.2118/88-03-03

Gallo, A. (2014, November 19). *A Refresher on Net Present Value*. Retrieved from Harvard Business Review: https://hbr.org/2014/11/a-refresher-on-net-present-value

Glover, P. W. (2000). *Petrophysics MSc Course Notes.* Retrieved from University of Leeds: http://homepages.see.leeds.ac.uk/~earpwjg/PG_EN/CD%20Contents/GGL-66565%20Petrophysics%20English/Chapter%204.PDF

*Heating Values of Natural Gas*. (2011, September 30). Retrieved from Enggcyclopedia: http://www.enggcyclopedia.com/2011/09/heating-values-natural-gas/

Henderson, G. D., Danesh, A., Tehrani, D. H., Al-Shaidi, S., & Peden, J. M. (1998). *Measurement and Correlation of Gas Condensate Relative Permeability by the Steady-State Method.* Society of Petroleum Engineers. doi:10.2118/30770-PA

Honarpour, M., Nagarajan, N., & Sampath, K. (2006). Rock/Fluid Characterization and their Integration-Implications on Reservoir Management. *JPT*, 120-130.

L. Fan, B. H. (2005). Understanding gas-condensate reservoirs. *Oilfield Review*, 14-27.

McCain, W. D. (1990). *The Properties of Petroleum Fluids.* Tulsa: PennWell Books.

McGuire, W. J., & Sikora, V. J. (1960). *The Effect of Vertical Fractures on Well Productivity.* Society of Petroleum Engineers. doi:10.2118/1618-G

Moffatt, B., Fawcett, M., Maurera, J., & Bruzco, A. (2013). Reservoir Fluid Chacterisation from Test on Tight Formations. *EAGE Annual Conference and Exhibition.* London: SPE 164887.

Novosad, Z. (1996). Composition and phase changes in Testing and Producing Retrograde gas wells. *Gas Technology Conference.* Calgary: SPE 35645.

Panien, M. P. (2010). Fractured Reservoir Characterisation: A Fully Integrated Study, From Borehole Imagery, Cores and Seismic Data to Production Logs - Example of an Algerian Gas Field (Sbaa Basin, SW Algeria).

Pedersen, K. S., & Christensen, P. L. (2007). *Phase Behavior of Petroleum Reservoir Fluids.* Boca Raton: CRC Press.

Prats, M. (1961). *Effect of Vertical Fractures on Reservoir Behavior-Incompressible Fluid Case.* Society of Petroleum Engineers. doi:10.2118/1575-G

Shi, C. (2009). *FLOW BEHAVIOR OF GAS-CONDENSATE WELLS.* Stanford: STANFORD UNIVERSITY.

SPE. (2015). *Formation damage from condensate banking*. Retrieved from Petrowiki: http://petrowiki.org/Formation_damage_from_condensate_banking

Steve Cuddy, G. A. (1993). A simple, convincing model for calculating water saturations in southern north sea gas fields. *Annual Logging Symposium.* Calgary: The Society of Petrophysicists and Well Log Analysts .

Whitson, C. H., & Brulé, M. R. (2000). *Phase Behavior* (Vol. 20). Richardson, Texas: SPE.

Whitson, C. H., Fevang, Ø., & Yang, T. (1999). *Gas Condensate PVT – What's Really Important and Why?* London.

# Appendix A Stratigraphic Column

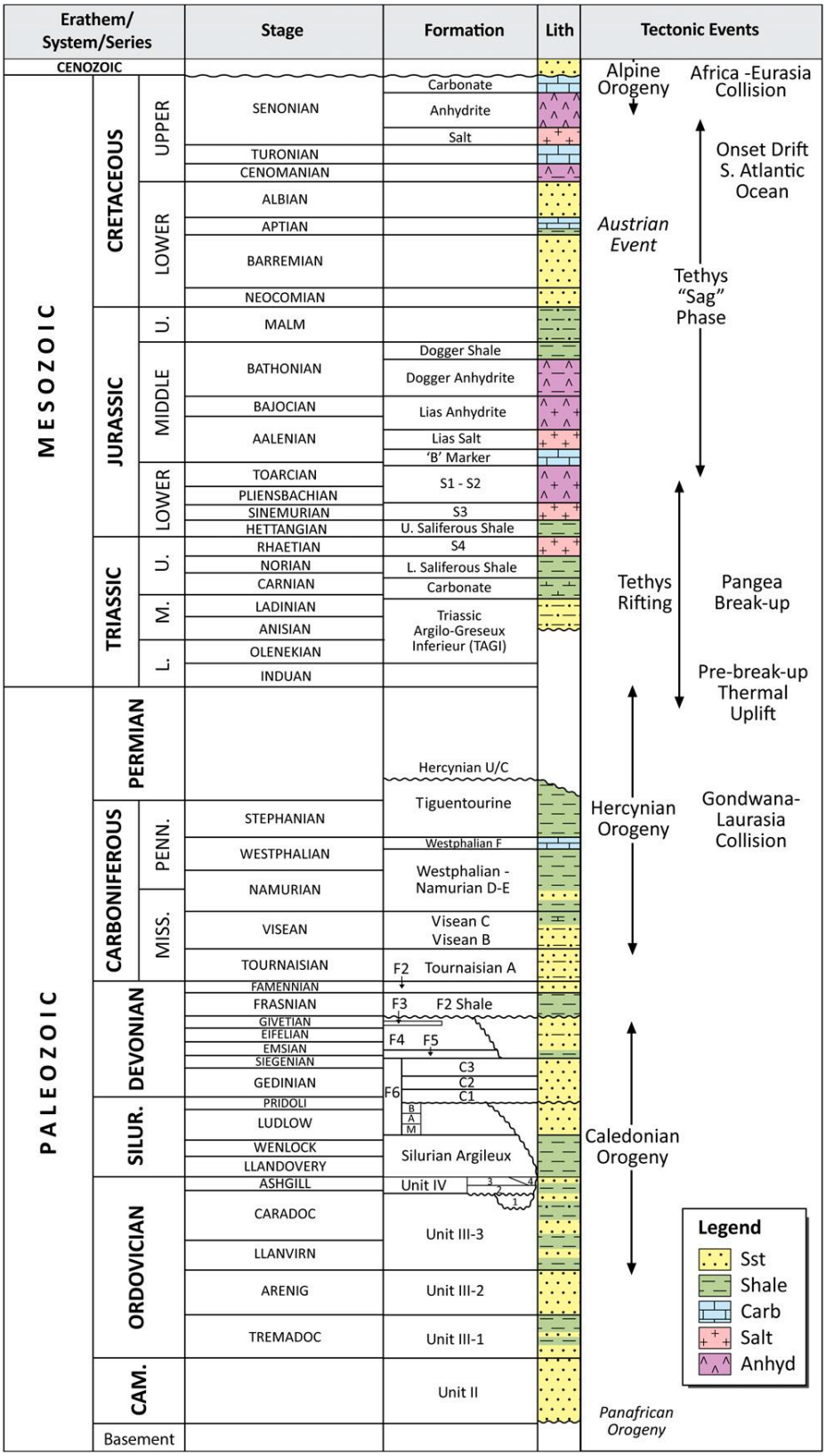

## Appendix B Financial model

| **Cash flow analysis** | | | | | |
|---|---|---|---|---|---|
| **Year** | | **0** | **1** | **2** | **3** |
| **Predictions** | **Unit** | | | | |
| Cumulative Volume gas produced | sm3 | | 8018510.00 | 13849100.00 | 19361300.00 |
| Volume gas produced | sm3 | | 8018510.00 | 5830590.00 | 5512200.00 |
| Cumulative Volume Condensate produced | sm3 | | 584.68 | 996.08 | 1352.32 |
| Volume condensate produced | sm3 | | 584.68 | 411.40 | 356.24 |
| **Revenues from gas sales** | USD | | **1400675.09** | **1059228.29** | **1041442.69** |
| **Revenues from condensate sales** | USD | | **169871.48** | **124305.68** | **111947.40** |
| **Costs** | | | | | |
| CAPEX well construction + HF costs | USD | 1980000.00 | 0.00 | 0.00 | 0.00 |
| Depreciation | USD | 0.00 | 198000.00 | 198000.00 | 198000.00 |
| OPEX | USD | | 376931.18 | 284048.15 | 276813.62 |
| **Income Before Tax** | USD | -1980000.00 | 995615.40 | 701485.82 | 678576.47 |
| **Tax** | USD | 0.00 | 338509.23 | 238505.18 | 230716.00 |
| **Income after tax** | USD | -1980000.00 | 657106.16 | 462980.64 | 447860.47 |
| Depreciation | USD | 0.00 | 198000.00 | 198000.00 | 198000.00 |
| **Net CASH FLOW** | USD | -1980000.00 | 855106.16 | 660980.64 | 645860.47 |
| Present Value of CASH FLOW | USD | -1980000.00 | 806703.93 | 588270.42 | 542276.90 |
| **NET PRESENT VALUE** | USD | **5751002.05** | | | |

## Appendix C Net Cash Flow bar graph

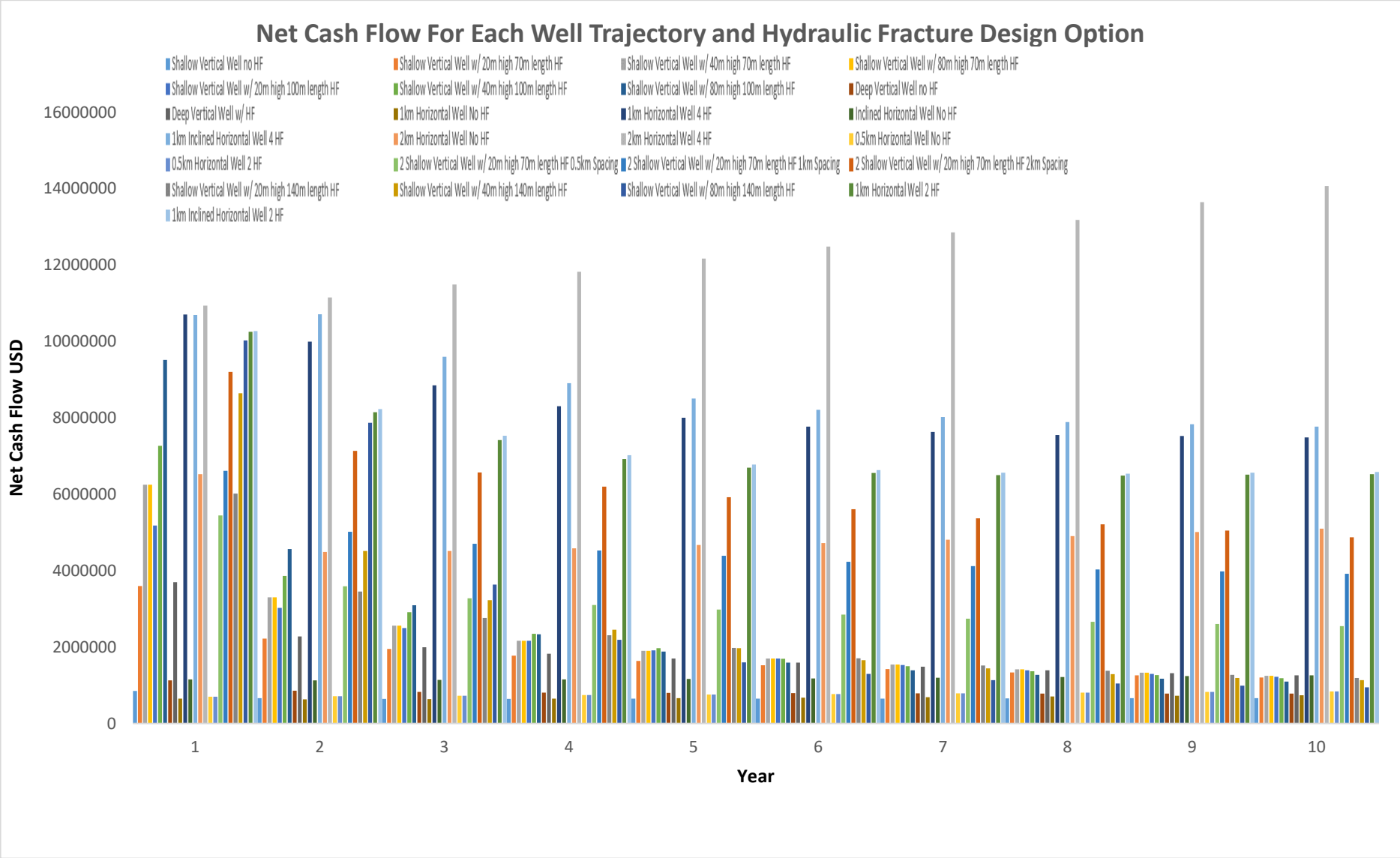

## Appendix D Saturation Tables

| SGFN | | | SWFN | | |
|---|---|---|---|---|---|
| -- Petrofacies 1 | | | | | |
| $S_g$ | $k_{rg}$ | $p_c$ | $S_w$ | $k_{rw}$ | $p_{cgw}$ |
| 0.000 | 0.000 | 0.000 | 1.000 | 1.000 | 0.000 |
| 0.050 | 0.050 | 0.000 | 0.950 | 0.950 | 0.000 |
| 0.100 | 0.100 | 0.000 | 0.900 | 0.900 | 0.000 |
| 0.150 | 0.150 | 0.000 | 0.850 | 0.850 | 0.000 |
| 0.200 | 0.200 | 0.000 | 0.800 | 0.800 | 0.000 |
| 0.250 | 0.250 | 0.000 | 0.750 | 0.750 | 0.000 |
| 0.300 | 0.300 | 0.000 | 0.700 | 0.700 | 0.000 |
| 0.350 | 0.350 | 0.000 | 0.650 | 0.650 | 0.000 |
| 0.400 | 0.400 | 0.000 | 0.600 | 0.600 | 0.000 |
| 0.450 | 0.450 | 0.000 | 0.550 | 0.550 | 0.000 |
| 0.500 | 0.500 | 0.000 | 0.500 | 0.500 | 0.000 |
| 0.550 | 0.550 | 0.000 | 0.450 | 0.450 | 0.000 |
| 0.600 | 0.600 | 0.000 | 0.400 | 0.400 | 0.000 |
| 0.650 | 0.650 | 0.000 | 0.350 | 0.350 | 0.000 |
| 0.700 | 0.700 | 0.000 | 0.300 | 0.300 | 0.000 |
| 0.750 | 0.750 | 0.000 | 0.250 | 0.250 | 0.000 |
| 0.800 | 0.800 | 0.000 | 0.200 | 0.200 | 0.000 |
| 0.850 | 0.850 | 0.000 | 0.150 | 0.150 | 0.000 |
| 0.900 | 0.900 | 0.000 | 0.100 | 0.100 | 0.000 |
| 0.950 | 0.950 | 0.000 | 0.050 | 0.050 | 0.000 |
| 1.000 | 1.000 | 0.000 | 0.000 | 0.000 | 0.000 |
| -- Petrofacies 2 | | | | | |
| $S_g$ | $k_{rg}$ | $p_c$ | $S_w$ | $k_{rw}$ | $p_{cgw}$ |
| 0.000 | 0.000 | 0.000 | 1.000 | 1.000 | 0.000 |
| 0.000 | 0.000 | 0.020 | 1.000 | 1.000 | 0.020 |
| 0.000 | 0.000 | 0.034 | 1.000 | 1.000 | 0.034 |
| 0.050 | 0.000 | 0.039 | 0.950 | 0.774 | 0.039 |
| 0.100 | 0.000 | 0.045 | 0.900 | 0.590 | 0.045 |
| 0.150 | 0.000 | 0.052 | 0.850 | 0.444 | 0.052 |
| 0.200 | 0.000 | 0.060 | 0.800 | 0.328 | 0.060 |
| 0.250 | 0.000 | 0.071 | 0.750 | 0.237 | 0.071 |
| 0.300 | 0.000 | 0.084 | 0.700 | 0.168 | 0.084 |
| 0.350 | 0.001 | 0.101 | 0.650 | 0.116 | 0.101 |
| 0.400 | 0.002 | 0.123 | 0.600 | 0.078 | 0.123 |
| 0.450 | 0.004 | 0.152 | 0.550 | 0.050 | 0.152 |
| 0.500 | 0.008 | 0.190 | 0.500 | 0.031 | 0.190 |
| 0.550 | 0.015 | 0.244 | 0.450 | 0.018 | 0.244 |
| 0.600 | 0.028 | 0.320 | 0.400 | 0.010 | 0.320 |
| 0.650 | 0.049 | 0.433 | 0.350 | 0.005 | 0.433 |
| 0.700 | 0.082 | 0.608 | 0.300 | 0.002 | 0.608 |
| 0.750 | 0.133 | 0.894 | 0.250 | 0.001 | 0.894 |
| 0.800 | 0.210 | 1.400 | 0.200 | 0.000 | 1.400 |
| 0.850 | 0.321 | 2.391 | 0.150 | 0.000 | 2.391 |
| 0.900 | 0.478 | 4.641 | 0.100 | 0.000 | 4.641 |
| 0.950 | 0.698 | 11.112 | 0.050 | 0.000 | 11.112 |
| 1.000 | 1.000 | 40.000 | 0.000 | 0.000 | 40.000 |

| Petrofacies 3 | | | | | |
|---|---|---|---|---|---|
| $S_g$ | $k_{rg}$ | $p_c$ | $S_w$ | $k_{rw}$ | $p_{cgw}$ |
| 0.000 | 0.000 | 0.000 | 1.000 | 1.000 | 0.000 |
| 0.000 | 0.000 | 2.000 | 1.000 | 1.000 | 2.000 |
| 0.040 | 0.000 | 3.465 | 0.960 | 0.885 | 3.465 |
| 0.080 | 0.000 | 3.589 | 0.920 | 0.779 | 3.589 |
| 0.120 | 0.000 | 3.721 | 0.880 | 0.681 | 3.721 |
| 0.160 | 0.000 | 3.863 | 0.840 | 0.593 | 3.863 |
| 0.200 | 0.000 | 4.014 | 0.800 | 0.512 | 4.014 |
| 0.240 | 0.000 | 4.177 | 0.760 | 0.439 | 4.177 |
| 0.280 | 0.001 | 4.352 | 0.720 | 0.373 | 4.352 |
| 0.320 | 0.002 | 4.541 | 0.680 | 0.314 | 4.541 |
| 0.360 | 0.004 | 4.746 | 0.640 | 0.262 | 4.746 |
| 0.400 | 0.006 | 4.967 | 0.600 | 0.216 | 4.967 |
| 0.440 | 0.011 | 5.209 | 0.560 | 0.176 | 5.209 |
| 0.480 | 0.018 | 5.472 | 0.520 | 0.141 | 5.472 |
| 0.520 | 0.027 | 5.761 | 0.480 | 0.111 | 5.761 |
| 0.560 | 0.041 | 6.079 | 0.440 | 0.085 | 6.079 |
| 0.600 | 0.060 | 6.431 | 0.400 | 0.064 | 6.431 |
| 0.640 | 0.086 | 6.821 | 0.360 | 0.047 | 6.821 |
| 0.680 | 0.120 | 7.257 | 0.320 | 0.033 | 7.257 |
| 0.720 | 0.164 | 7.746 | 0.280 | 0.022 | 7.746 |
| 0.760 | 0.221 | 8.298 | 0.240 | 0.014 | 8.298 |
| 0.800 | 0.293 | 8.927 | 0.200 | 0.008 | 8.927 |
| 0.840 | 0.383 | 9.648 | 0.160 | 0.004 | 9.648 |
| 0.880 | 0.495 | 10.483 | 0.120 | 0.002 | 10.483 |
| 0.920 | 0.632 | 11.459 | 0.080 | 0.001 | 11.459 |
| 0.960 | 0.799 | 12.614 | 0.040 | 0.000 | 12.614 |
| 0.990 | 0.946 | 13.628 | 0.010 | 0.000 | 13.628 |
| 1.000 | 1.000 | 20.000 | 0.000 | 0.000 | 20.000 |
| -- Petrofacies 4 | | | | | |
| $S_g$ | $k_{rg}$ | $p_c$ | $S_w$ | $k_{rw}$ | $p_{cgw}$ |
| 0.000 | 0.000 | 0.000 | 1.000 | 1.000 | 0.000 |
| 0.000 | 0.000 | 4.000 | 1.000 | 1.000 | 4.000 |
| 0.010 | 0.000 | 8.540 | 0.990 | 0.978 | 8.540 |
| 0.020 | 0.000 | 8.569 | 0.980 | 0.957 | 8.569 |
| 0.030 | 0.000 | 8.597 | 0.970 | 0.935 | 8.597 |
| 0.050 | 0.000 | 8.655 | 0.950 | 0.893 | 8.655 |
| 0.070 | 0.000 | 8.713 | 0.930 | 0.852 | 8.713 |
| 0.090 | 0.000 | 8.772 | 0.910 | 0.813 | 8.772 |
| 0.110 | 0.000 | 8.831 | 0.890 | 0.774 | 8.831 |
| 0.150 | 0.001 | 8.952 | 0.850 | 0.699 | 8.952 |
| 0.190 | 0.001 | 9.074 | 0.810 | 0.629 | 9.074 |
| 0.230 | 0.003 | 9.199 | 0.770 | 0.563 | 9.199 |
| 0.270 | 0.005 | 9.326 | 0.730 | 0.500 | 9.326 |
| 0.310 | 0.009 | 9.456 | 0.690 | 0.442 | 9.456 |
| 0.350 | 0.015 | 9.588 | 0.650 | 0.388 | 9.588 |
| 0.390 | 0.023 | 9.723 | 0.610 | 0.337 | 9.723 |
| 0.430 | 0.034 | 9.861 | 0.570 | 0.290 | 9.861 |
| 0.470 | 0.049 | 10.001 | 0.53 | 0.247404 | 10.00095 |
| 0.510 | 0.068 | 10.144 | 0.49 | 0.208176 | 10.14407 |

| | | | | | |
|---|---|---|---|---|---|
| 0.550 | 0.092 | 10.290 | 0.45 | 0.172611 | 10.29013 |
| 0.590 | 0.121 | 10.439 | 0.41 | 0.140645 | 10.43921 |
| 0.630 | 0.158 | 10.591 | 0.37 | 0.112213 | 10.59141 |
| 0.670 | 0.202 | 10.747 | 0.33 | 0.087243 | 10.74683 |
| 0.710 | 0.254 | 10.906 | 0.29 | 0.065656 | 10.90558 |
| 0.750 | 0.316 | 11.068 | 0.25 | 0.047366 | 11.06776 |
| 0.790 | 0.390 | 11.233 | 0.21 | 0.032276 | 11.23348 |
| 0.830 | 0.475 | 11.403 | 0.17 | 0.020276 | 11.40287 |
| 0.870 | 0.573 | 11.576 | 0.13 | 0.011238 | 11.57604 |
| 0.890 | 0.627 | 11.664 | 0.11 | 0.007782 | 11.66408 |
| 0.910 | 0.686 | 11.753 | 0.09 | 0.005004 | 11.75312 |
| 0.930 | 0.748 | 11.843 | 0.07 | 0.002879 | 11.84317 |
| 0.950 | 0.815 | 11.934 | 0.05 | 0.001373 | 11.93425 |
| 0.970 | 0.885 | 12.026 | 0.03 | 0.000446 | 12.02638 |
| 0.975 | 0.904 | 12.050 | 0.025 | 0.000299 | 12.04958 |
| 0.980 | 0.922 | 12.073 | 0.02 | 0.000183 | 12.07284 |
| 0.985 | 0.941 | 12.096 | 0.015 | 9.71E-05 | 12.09617 |
| 0.990 | 0.961 | 12.120 | 0.01 | 3.98E-05 | 12.11957 |
| 0.995 | 0.980 | 12.143 | 0.005 | 8.66E-06 | 12.14304 |
| 1.000 | 1.000 | 20.000 | 0 | 0 | 20 |

| **SOF3** | | |
|---|---|---|
| **$S_o$** | **$k_{ro}$** | **$p_c$** |
| 0.000 | 0.000 | 0.000 |
| 0.200 | 0.200 | 0.200 |
| 1.000 | 1.000 | 1.000 |
| **$S_o$** | **$k_{ro}$** | **$p_c$** |
| 0.000 | 0.000 | 0.000 |
| 0.200 | 0.200 | 0.200 |
| 1.000 | 1.000 | 1.000 |
| **$S_o$** | **$k_{ro}$** | **$p_c$** |
| 0.000 | 0.000 | 0.000 |
| 0.200 | 0.200 | 0.200 |
| 1.000 | 1.000 | 1.000 |
| **$S_o$** | **$k_{ro}$** | **$p_c$** |
| 0.000 | 0.000 | 0.000 |
| 0.200 | 0.200 | 0.200 |
| 1.000 | 1.000 | 1.000 |

## Appendix E Data File

```
GRID

OPERATE

 PERMX 1 82 1 61 1 53 'MINLIM' PERMX 0.0001 /

 WORK1 1 82 1 61 1 53 'LOGE'   PERMX /

/

MULTIPLY

PERMX  10  28 34 25 34 2 18 /

PERMY  10  28 34 25 34 2 18 /

PERMZ  10  28 34 25 34 2 18 /

PORO  0.7  28 34 25 34 2 18 /

/

CARFIN

LGRAT1 31 31 27 31 1 47 7 15 47 /

HXFIN

25        10        2.5       0.5       2.5       10        25 /

BOX

4 4 6 10 30 35 /

PORO

30*0.4 /

PERMX

30*2000 /

COPY

PERMX PERMY /

PERMX PERMZ /

/

ENDBOX

ENDFIN
```

```
EDIT

MULTIPLY

 PORV 0 1 82 1 24 1 53 /

 PORV 0 1 82 35 61  1 53 /

 PORV 0 1 25 1 61 1 53 /

 PORV 0 36 82 1 61 1 53 /

/

PROPS

OPERATE

SWL 1 82 1 61 1 53 'MULTA'  WORK1 -0.0300 0.2029 /

SWL   1 82 1 61 1 53 'MINLIM' SWL 0.06 /

-- SGL = smallest gas sat

SGL   1 82 1 61 1 53 'MULTA'  WORK1 -0.0365 0.3446 /

SGL 1 82 1 61 1 53 'MAXLIM' SGL 0.44 /

/

-- max SW = 1- SGL

OPERATE

SWU 1 82 1 61 1 53 'MULTA' SGL -1.0 1.0 /

/

-- max Sg = 1- Swc

OPERATE

SGU 1 82 1 61 1 53 'MULTA' SWL -1.0 1.0 /

/

COPY

SWL SWCR /

SGL SGCR /

/

SOWCR
```

```
 265106*0.2
/
OPERATE
SOGCR 1 82 1 61 1 53 'MULTA' WORK1 0 0.15 /
/
-- KRG = krg (Swc)
OPERATE
WORK1 1 82 1 61 1 53 'LOGE'   PERMX /
KRG   1 82 1 61 1 53 'MULTA'  WORK1 0.0385 0.3933 /
/
KRO
265106*0.7
/
-- krw (Sg res) = KRW
OPERATE
KRW   1 82 1 61 1 53 'MULTP'  PERMX 0.0497 0.4138 /
/
REGIONS
BOX
28 34 25 34 2 18 /
FIPNUM
1190*1
/
ENDBOX
BOX
28 34 25 34 20 33 /
FIPNUM
980*2
```

```
/
ENDBOX
SCHEDULE
WELSPECL
 AT1  GROUP  LGRAT1 4 8  1454.2 GAS 1* STD 6* /
/
COMPDATL
--                                        Skin
 AT1 LGRAT1 4 8 1  36 'OPEN'  1* 1*  0.1143    1*  0  1* Z 1* /
/
WDFAC
AT1 4E-6 /
/
WCONPROD
    AT1    OPEN    GRAT   2*    300000    2*    40     /
/
DATES
02 JAN 2020 /
03 JAN 2020 /
04 JAN 2020 /
05 JAN 2020 /
06 JAN 2020 /
07 JAN 2020 /
08 JAN 2020 /
01 APR 2020     /
01 JUL 2020     /
01 OCT 2020     /
01 JAN 2021     /
```

```
01 APR 2021     /

01 JUL 2021     /

01 OCT 2021     /

01 JAN 2022     /

01 APR 2022     /

01 JUL 2022     /

01 OCT 2022     /

01 JAN 2023     /

01 APR 2023     /

/

END
```